공학박사 학위논문

Substrate channeling and promoter engineering for the production of 2,3-butanediol and cellulosic ethanol in *Saccharomyces cerevisiae*

Saccharomyces cerevisiae **에서 2,3-부탄다이올과 섬유소 유래 에탄올 생산을 위한 기질 채널링 및 프로모터의 개발**

2015 년 8 월

서울대학교 대학원

화학생물공학부

김 수 진

Substrate channeling and promoter engineering for the production of 2,3-butanediol and cellulosic ethanol in *Saccharomyces cerevisiae*

지도교수 한 지 숙

이 논문을 공학박사 학위논문으로 제출함

2015 년 8 월

서울대학교 대학원

화학생물공학부

김 수 진

김수진의 공학박사 학위논문을 인준함

2015 년 8 월

위 원 장 유 영제 (인)

부위원장 한 지 숙 (인)

위 원 정 병 기 (인)

위 원 박 태 현 (인)

위 원 오 민 규 (인)

Substrate channeling and promoter engineering for the production of 2,3-butanediol and cellulosic ethanol in *Saccharomyces cerevisiae*

by

Sujin Kim

Advisor : Professor Ji-Sook Hahn, Ph.D.

Submitted in Partial Fulfillment of the Requirements

for the Degree of Doctor of Philosophy

in Seoul National University

August, 2015

School of Chemical and Biological Engineering

Graduate School

Seoul National University

ABSTRACT

Substrate channeling and promoter engineering for the production of 2,3-butanediol and cellulosic ethanol in *Saccharomyces cerevisiae*

Sujin Kim
School of Chemical and Biological Engineering
The Graduate School
Seoul National University

Saccharomyces cerevisiae is a well-studied eukaryotic model system with great potential as microbial cell factories for the production of fuels and chemicals. In this dissertation, several strategies were developed and applied to produce cellulosic ethanol and 2,3-butanediol in *S. cerevisiae*.

Firstly, a cellulolytic yeast consortium for consolidated bioprocessing (CBP) was developed based on the surface display of cellulosome structure, mimicking *Clostridium thermocellum*. The assembly of cellulosome is mediated through high-affinity interaction between cohesin domains in structural scaffoldin and dockerin

domains in enzymes. The cellulosome activity and ethanol production of a yeast consortium were optimized by controlling the combination ratio among the four yeast strains capable of either displaying a scaffoldin (mini CipA) or secreting one of the three types of cellulases. As a result, a mixture of cells with the optimized mini CipA:CelA:CBHII:BGLI ratio of 2:3:3:0.53 produced 1.80 g/L ethanol after 94 h, indicating about 20% increase compared with a consortium composed of an equal amount of each cell type (1.48 g/L).

Secondly, substrate channeling modules were designed based on high affinity interaction between cohesin and dockerin domains. Substrate channeling is a process of transferring an intermediate from one enzyme to the next enzyme without diffusion into the bulk phase, thereby leading to an enhanced reaction rate. Synthetic scaffolds containing two, three, or seven cohesin domains were constructed, and the assembly of dockerin-tagged proteins onto the scaffolds was confirmed by pull-down assay and bimolecular fluorescent complementation (BiFC) assay. This system was applied to produce 2,3-butanediol by using dockerin-tagged AlsS, AlsD, and Bdh1 enzymes, resulting in a gradual increase in 2,3-butanediol production depending on the number of cohesin domains in the scaffold.

Thirdly, the effect of substrate channeling was further investigated at a metabolic branch point, focusing on pyruvate metabolism in *S. cerevisiae*. The cohesin-dockerin interaction was applied to recruit pyruvate-converting enzymes to a pyruvate kinase (Pyk1), which catalyzes the conversion of phosphoenolpyruvate to pyruvate. As a platform strain for pyruvate channeling, PYK1-Coh-Myc strain

was constructed, and the assembly of dockerin-tagged enzymes to cohesin-tagged Pyk1 was confirmed by co-immunoprecipitation. In the case of both lactate production and 2,3-butanediol production, pyruvate flux toward the target products was significantly enhanced, coinciding with a decrease in ethanol production.

Fourthly, promoters inducible by aromatic amino acids were constructed based on the binding sites of Aro80 transcription factor. A dynamic range of tryptophan-inducible promoter strengths can be obtained by modulating the number of Aro80 binding sites, plasmid copy numbers, and tryptophan concentrations. The synthetic U_4C_{ARO9} promoter, which is composed of four repeats of Aro80 binding half site (CCG) and *ARO9* core promoter element, was applied to express AlsS and AlsD for acetoin production, resulting in a gradual increase in acetoin titers depending on tryptophan concentrations. Furthermore, it has been demonstrated that γ-aminobutyrate (GABA)-inducible *UGA4* promoter can also be used in metabolic engineering as a dose-dependent inducible promoter.

Lastly, 2,3-butanediol production in *S. cerevisiae* was improved stepwise by eliminating byproduct formation and redox rebalancing. By introducing heterologous 2,3-butanediol biosynthetic pathway and deleting competing pathways producing ethanol and glycerol, metabolic flux was successfully redirected to 2,3-butanediol. In addition, the resulting redox cofactor imbalance was restored by overexpressing water-forming NADH oxidase (NoxE) from *Lactococcus lactis*. In a flask fed-batch fermentation with optimized conditions, the engineered strain (*adh1-5Δgpd1Δgpd2Δ*) overexpressing AlsS, AlsD, Bdh1, and

NoxE from a single multigene-expression vector, produced 72.9 g/L 2,3-butanediol with the highest yield (0.41 g/g glucose) and productivity (1.43 g/(L·h)) ever reported in *S. cerevisiae*.

Keywords : Metabolic engineering, Substrate channeling,
Promoter engineering, 2,3-Butanediol, Cellulosic ethanol,
Saccharomyces cerevisiae

Student Number **:** 2009-20983

CONTENTS

LIST OF FIGURES

LIST OF TABLES

LIST OF ABBREVIATIONS

ADH	alcohol dehydrogenase
BiFC	bimolecular fluorescence complementation
CBM	cellulose-binding module
CBP	consolidated bioprocessing
Coh	cohesin
co-IP	co-immunoprecipitation
DHAP	dihydroxyacetone phosphate
DNS	dinitrosalicylic acid
Doc	dockerin
EDTA	ehylenediaminetetraacetic acid
EGFP	enhanced green fluorescent protein
G3P	glycerol-3-phosphate
GABA	γ-aminobutyric acid
GAP	glyceraldehyde-3-phosphate
GC	gas chromatography
GOI	gene of interest
GRAS	generally recognized as safe
GST	glutathione S-transferase
His	histidine
HPLC	high performance liquid chromatography
IB	immunoblotting
MEK	methyl ethyl ketone
Leu	leucine
OD	optical density

PAGE	polyacrylamide gel electrophoresis
PASC	phosphoric acid swollen cellulose
PBS	phosphate-buffered saline
PCR	polymerase chain reaction
PDC	pyruvate decarboxylase
Phe	phenylalanine
PMSF	phenylmethylsulfonyl fluoride
*p*NPG	*p*-nitrophenyl-β-D-glucopyranoside
PPP	pentose phosphate pathway
qRT-PCR	quantitative reverse transcription PCR
RBS	ribosome binding sites
RFU	relative fluorescence units
RI	refractive index
SC	synthetic complete
SD	synthetic defined
SD-CAA	synthetic dextrose casamino acids
SDS	sodium dodecyl sulfate
SG-CAA	synthetic galactose casamino acids
SHF	separate hydrolysis and fermentation
SSCF	simultaneous saccharification and co-fermentation
SSF	simultaneous saccharification and fermentation
Trp	tryptophan
Tyr	tyrosine
UAS	upstream activation sequence
Ura	uracil
YP	yeast extract-peptone

Chapter 1.

Research background and objective

In recent decades, metabolic engineering of microbial cells has received a great attention for the production of chemicals, fuels, and pharmaceuticals, as an attractive alternative to chemical synthesis [1, 2]. To achieve high titer and yield of production, both amplification of the metabolic pathway toward desired compound and inhibition of the competing pathways are usually required. To this end, various strategies, including modulation of gene copy number, promoter strength, or ribosome binding sites (RBS), have been used [3-5].

Saccharomyces cerevisiae is one of the most intensively studied eukaryotic model organisms and economically important industrial microorganisms. As a platform organism for metabolic engineering, it has several advantages; well-characterized genetics and physiology, availability of abundant genetic tools, ease of genetic manipulation, high tolerance to alcohols and harsh industrial conditions, and generally regarded as safe status [6].

The first objective of this study was to develop a novel cellulolytic yeast consortium for efficient cellulosic ethanol production. Cellulosic biomass is considered as a promising alternative to fossil fuels, but its recalcitrant nature and high cost of cellulase are the major obstacles to utilize this material. Consolidated bioprocessing (CBP), combining cellulase production, saccharification, and fermentation into one step, has been proposed as the most efficient way to reduce the production cost of cellulosic bioethanol. However, since no natural microorganism possesses the ability of both cellulose utilization and ethanol production desired for CBP, it is necessary to develop metabolically engineered

microorganisms for cellulosic ethanol production.

The second objective of this study was to develop substrate channeling modules and verify its feasibility as a tool for metabolic engineering. Substrate channeling is considered as a powerful strategy for increasing metabolite production by facilitating direct transfer of an intermediate from one enzyme to the next enzyme, while protecting the intermediate from competing reaction pathways or unstable environment.

The third objective of this study was to construct tryptophan-inducible promoter and GABA-inducible promoter and verify their feasibility as a tool for metabolic engineering. Controlling the expression of genes in metabolic pathways or in regulatory networks is an essential component in metabolic engineering and synthetic biology. Although gene expression can be regulated at multiple points, promoter-driven transcriptional initiation is a key regulatory step in determining gene expression levels and timing. Successful pathway engineering requires diverse range of constitutive and inducible promoters, which allow sophisticated transcriptional regulation of each gene participating in the pathway. While numerous efforts have been made to isolate native promoters or to develop synthetic promoters suitable for genetic engineering, the number of inducible promoters is still limited for pathway engineering in *S. cerevisiae*.

The last objective of this study was to develop recombinant *S. cerevisiae* for the efficient production of 2,3-butanediol. 2,3-Butanediol is a promising valuable chemical that can be used in various areas, especially as a platform chemical and a

liquid fuel. Although a number of microorganisms can produce 2,3-butanediol from pyruvate in a mixed acid fermentation, the most of them have been considered unsuitable for industrial-scale fermentation because of the potential pathogenicity of these native producers. Especially, the 2,3-butanediol produced by these bacteria is restricted in the applications for food additives and cosmetics. Therefore, it is necessary to develop a safe and efficient microorganisms as 2,3-butanediol-producer.

The objectives of this study are summarized as follows.

- To develop a novel cellulolytic yeast consortium for efficient cellulosic ethanol production
- To construct substrate channeling modules and verify its feasibility as a tool for metabolic engineering
- To develop promoters inducible by aromatic amino acids and γ-aminobutyrate for metabolic engineering applications
- To develop recombinant *S. cerevisiae* for the efficient production of 2,3-butanediol

Chapter 2.

Literature review

2.1. Metabolic engineeirng

2.1.1. Overview of metabolic engineering

Metabolic engineering is generally defined as the use of genetic engineering to modify the metabolism of an organism [3, 7]. It can involve the optimization of existing biochemical pathways or the introduction of pathway components with the goal of high-yield production of specific metabolites such as chemicals, fuels, and pharmaceuticals. Fortunately, in the past decade there has been enormous progress in the development of advanced new tools, including genome sequencing, bioinformatics, metabolomics, and systems biology, that have greatly accelerated the capabilities of metabolic engineering [1].

The traditional procedure of metabolic engineering, called metabolic engineering cycle, consists of genetic manipulations, analysis of the consequences, and design of further modifications [7, 8]. As a strategy for genetic manipulations, both amplification of the metabolic pathway toward desired compound and inhibition of the competing pathways are generally employed to achieve high titer and yield of production. To this end, various tools, including modulation of gene copy number, promoter strength, or ribosome binding sites (RBS), have been used [3-5]. Recently, conditional knockout/down systems were also successfully applied to metabolic engineering [9, 10]. In order to examine the performance of the engineered strain, fermentation and downstream processing are performed. Based on the data and information obtained, further metabolic engineering is carried out.

This metabolic engineering cycle is also repeated until a strain showing a desired phenotype is obtained, such as yield, rate, and titer [8].

2.1.2. Metabolic engineering in *S. cerevisiae*

As the metabolic engineering approach relies on the genetic modification of microorganisms, this field was initially applied to model organisms such as *Escherichia coli* and *S. cerevisiae*, which also made them the platform organisms for the first biotechnological production processes through metabolic engineering.

Both of these organisms have the advantage of being very well-characterized and genetically tractable, with multiple tools available for their genetic manipulation [11]. Compared to *E. coli*, *S. cerevisiae* possesses several additional advantages; (i) a larger cell size thus enabling an easier separation; (ii) a lower growth temperature; (iii) industrial robustness such as its ability to grow anaerobic condition and high tolerance to low pH, high osmotic pressure, and alcohols; and (iv) a lack of potential phage contamination [6]. Furthermore, yeast mating allows for improved cellular engineering and can lead to diploids with robust growth and increased adaptation [12]. Taken together, above-mentioned advantageous characters support the industrial use of *S. cerevisiae* for the production of chemical and fuel.

The central carbon metabolism in *S. cerevisiae* is depicted in Figure 2.1. Immediately after transport into the cell, glucose is phosphorylated by hexokinase (*GLK1*, *HXK1*, and *HXK2*) to glucose 6-phosphate and then isomerized to fructose-

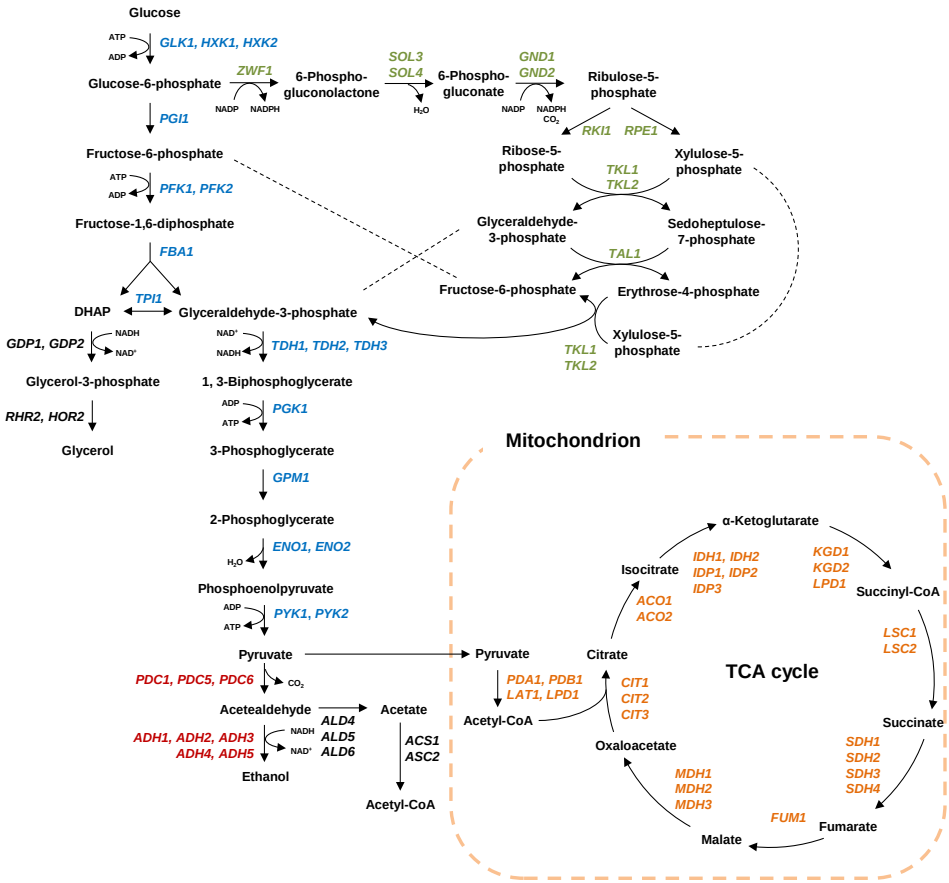

Figure 2.1 Central carbon metabolism in *S. cerevisiae*

Glycolysis (blue), pentose phosphate pathway (PPP, green), TCA cycle (orange), and ethanol fermentation (red) are described.

6-phosphate by phosphoglucose isomerase (*PGI1*). Fructose-6-phosphate is further phosphorylated to fructose-1,6-bisphosphate by phosphofructokinase (*PFK1* and *PFK2*), which is subject to regulation by several metabolites. The subsequently acting enzymes are fructose-bisphosphate aldolase (*FBA1*), triosephosphate isomerase (*TPI1*), glyceraldehyde-3-phosphate dehydrogenase (*TDH1*, *TDH2*, and *TDH3*), phosphoglycerate kinase (*PGK1*), phosphoglycerate mutase (*GPM1*), enolase (*ENO1* and *ENO2*) and pyruvate kinase (*PYK1* and *PYK2*) [13]. Although the glycolytic pathway is common to all yeast species, there are differences in the carbon flux regulation at the level of the pentose phosphate pathway (PPP). In *S. cerevisiae*, the carbon flux through pentose phosphate pathway is relatively low and it is known that PPP plays a role for NADPH production but not for biomass production or catabolic reactions [14].

Pyruvate can be converted to acetyl-CoA by mitochondrial multienzyme complex pyruvate dehydrogenase (PDH) or cytosolic pathway called by the PDH-bypass pathway, which requires the activity of pyruvate decarboxylase (PDC), acetaldehyde dehydrogenase (ALD), and acetyl-CoA synthetase (*ACS1* and *ASC2*) [15]. Although *S. cerevisiae* has a strong tendency towards ethanol fermentation and a tight flux regulation toward acetyl-CoA, acetyl-CoA is an essential precursor in the biosynthesis of amino acids, fatty acids, sterols, and polyketides [16, 17]. Since cytosolic acetyl-CoA is separated from the other pools in contrast to bacterial acetyl-CoA synthesis and the machinery to export the mitochondrial acetyl-CoA to the cytosol is deficient, the further metabolism of acetic acid through acetyl-CoA

synthetase is the only source of cytosolic acetyl-CoA in *S. cerevisiae* [18].

A number of studies have attempted to produce a range of chemicals by using metabolically engineered *S. cerevisiae* [11, 19, 20]. Several recent studies are summarized in Table 2.1.

2.1.3. Substrate channeling

Substrate channeling (or metabolite channeling) refers to the process in which the intermediate from one enzyme is directly transferred to the next enzyme without diffusion into the bulk phase [21]. In addition to enhanced reaction rates, substrate channeling has several potential benefits including; (i) prevention of the loss of intermediates to competing pathways or diffusion [22, 23]; (ii) reduction of the accumulation of toxic intermediates [24]; (iii) protection of unstable intermediates from solvent [25, 26]; and (iv) circumvention of unfavorable equilibria and kinetics associated with metabolite concentrations in bulk phase [27].

The mechanisms for substrate channeling can be generally divided into two categories [25]. One is a direct transfer mechanism (known as direct channeling or perfect channeling) that the intermediate is funneled from first enzyme to second enzyme by means of a protein tunnel that connects the active sites of these two enzymes. For example, tryptophan synthase, an $\alpha_2\beta_2$ complex, has a largely hydrophobic, protected tunnel that connects active sites, thus preventing the active indole intermediate from diffusing away [28]. The other mechanism is referred to as a proximity mechanism (known as proximity channeling or leaky channeling)

Table 2.1 Production of variety of chemicals in *S. cerevisiae*

Chemical	Discription	Titer	References
n-Butanol	BY4742; overexpression of thiolase *ERG10* (*S. cerevisiae*), 3-hydroxybutyryl-CoA dehydrogenase *hbd* (*Clostridium beijerinckii*), crotonase *crt* (*C. beijerinckii*), crotonyl-CoA reductase *ccr* (*Streptomyces collinus*), and aldehyde/alcohol dehydrogenase *adhE2* (*C. beijerinckii*)	2.5 mg/L	[29]
Isobutanol	BY4741; overexpression of acetolactate synthase *ILV2* (*S. cerevisiae*), ketol-acid reductoisomerase *ILV5* (*S. cerevisiae*), dehydroxyacid dehydratase *ILV3* (*S. cerevisiae*), α-ketoacid decarboxylase *ARO10* (*S. cerevisiae*, mitochondria-targeted), and alcohol dehydrogenase *ADH7* (*Lactococcus lactis*, mitochondria-targeted)	635 mg/L	[30]
3-Methyl-1-butanol	CEN.PK2-1C; deletion of aldehyde dehydrogenase *ALD6* and branched-chain amino acid aminotransferases *BAT1*; overexpression of *ILV2*, *ILV3*, *ILV5*, *ARO10*, alcohol dehydrogenase *ADH2*, a constitutively active form of Leu3 transcription factor *LEU3Δ601*, and a feedback-resistant mutant $LEU4^{D578Y}$ (all overexpressed genes from *S. cerevisaie*)	757 mg/L	[31]

Table 2.1 Production of variety of chemicals in *S. cerevisiae* (Continued)

Chemical	Discription	Titer	References
Lactic acid	CEN.PK2–1D; deletion of pyruvate decarboxylase *PDC1*, overexpression of L-lactate cytochrome-c oxidoreductase *CYB2*, glycerol-3-phosphate dehydrogenase *GPD1*, and external NADH dehydrogenase *NDE1* and *NDE2*; total five copy integration of lactate dehydrogenase *ldh* (*Pelodiscus sinensis*)	117 g/L	[32]
Succinic acid	TAM (*pdc1Δ pdc5 Δ pdc6Δ*, evloved pdc-deficient strain); deletion of *GPD1* and fumarase *FUM1*; overexpression of pyruvate carboxylase *PYC2* (*S.cerevisiae*), cytosolic retargeted *MDH3* (*S. cerevisiae*), fumarate reductase *FRD1* (*S.cerevisiae*), and fumarase *fumC* (*E.coli*)	13 g/L	[33]
3-hydroxypropionic acid	CEN.PK 113-11C; deletion of cytosolic malate synthase *MLS1*;overexpression of alcohol dehydrogenase *ADH2* (*S. cerevisiae*), aldehyde dehydrogenase *ALD6* (*S .cerevisiae*), modified acetyl-CoA synthetase *acs* (*Salmonella enterica*), acetyl-CoA carboxylase *ACC1* (*S. cerevisiae*), malonyl-CoA reductase *mcr* (*Chloroflexus aurantiacus*),and non-phosphorylating glyceraldehyde-3-phosphate dehydrogenase *gapN* (*Streptococcus mutans*)	436 mg/L	[34]

Table 2.1 Production of variety of chemicals in *S. cerevisiae* (Continued)

Chemical	Discription	Titer	References
Muconic acid	BY4741; deletion of 3-deoxy-D-arabino-heptulosonate-7-phosphate synthase ARO3 and glucose-6-phosphate dehydrogenase *ZWF1*; replacement of *ARO4* with a feedback-resistant mutant ARO4^{K229L}; overexpression of protocatechuic acid decarboxylase ECL_01944 (*Enterobacter cloacae*, codon-optimized), 3-dehydroshikimate dehydratase pa5_5120 (*P. anserina, codon-optimized), catechol 1,2-dioxygenase HQD2* (*Candida albicans*, codon-optimized), and transketolase *TKL1* (*S. cerevisiae*)	141 mg/L	[35]
Lycopene	Diploid prototrophic strain, BY4741/BY4742; overexpression of *tHMG1*(*S. cerevisiae*), *CrtYB11M* (*Xanthophyllomyces dendrorhous*), phytoene desaturase *CrtI* (*X. dendrorhous*), geranylgeranyl diphosphate synthase *CrtE03M* (*X. dendrorhous*)	1.61 g/L	[36]

near enough to each other to process cascade reactions. In this mechanism, the intermediate is processed by next enzyme before it can escape by diffusion, even in the absence of an actual channel.

Inspired by natural metabolic systems, several efforts have been focused on the spatial organization of metabolic enzymes to accelerate intermediate processing [28, 37]. These approaches, including fusion protein, scaffold-based enzyme complex, and localization to subcellular compartment or organelle, lead to substrate channeling effect in proximity mechanism. Expression of a fusion protein of 4-coumaroyl-CoA ligase and stilbene synthase in yeast resulted in up to 15-fold increased resveratrol production compared to co-expression of these enzymes [38]. Synthetic protein scaffold was applied to the heterologous mevalonate pathway in *E. coli*, resulting in a 77-fold increase in mevalonate titer with the optimized scaffold architecture [24]. In addition to protein scaffold, RNA- and DNA-based scaffold system have been constructed and used to produce various target products [39, 40]. The strategy of compartmentalization of metabolic pathways to organelle, especially mitochondria using N-terminal targeting sequence, has been also successfully applied to the production of isobutanol, itaconic acid, and acetoin in *S. cerevisiae*, *Aspergillus niger*, and *Candida glabrata*, respectively [30, 41, 42].

2.1.4. Promoter engineering

Controlling the expression of genes in metabolic pathways or in regulatory networks is an essential component in metabolic engineering and synthetic biology [2, 43]. Although gene expression can be regulated at multiple points, promoter-driven transcriptional initiation is a key regulatory step in determining gene expression levels and timing [44]. Successful pathway engineering requires diverse range of constitutive and inducible promoters, which allow sophisticated transcriptional regulation of each gene participating in the pathway [44, 45]. Therefore, numerous efforts have been made to isolate native promoters [46, 47] or to develop synthetic promoters suitable for genetic engineering [44, 48-50].

A promoter can be defined as a nucleotide sequence to which that RNA polymerase binds and initiates transcription. A typical promoter structure in *E. coli* includes two consensus sequences, the -10 consensus sequence (TATAAT motif) and the -35 consensus sequence (TTGACA motif). In addition, the distance between the -10 and -35 motif is also highly conserved to length of 17 base pairs (bp) [51]. Whereas, promoters in *S. cerevisiae* are less similar to each other and only about 20% of genes contain a TATA box [52]. Generally, eukaryotic promoters can be divided into two regions, a core element and an upstream enhancer element [44]. As the minimal promoter region required for transcription initiation, core promoter element plays an important role to determine transcriptional direction and start site. The upstream enhancer element is related to transcriptional frequency or promoter strength.

Promoter engineering has been an important tool for modulation of gene expression at the transcriptional level, in both basic and applied biological research. To date, several strategies, including mutagenesis through error-prone PCR, saturation mutagenesis of nucleotide spacer regions, hybrid promoter engineering and direct modification of transcription factor binding sites, are developed for promoter engineering.

Promoter strength can be altered by random mutagenesis through error-prone PCR method, mutating DNA sequence around or within transcription factor binding site on target promoter. In this manner, promoter library with a wide range of strength can be obtained. Also, the advantage of this approach is relatively easy to generate or improve specific promoters. Saturation mutagenesis of nucleotide spacer regions focuses on retaining consensus regions of the promoter regions by mutating only variable regions. This strategy has been successfully applied to yeast promoter for synthetic library construction [53].

Recently, hybrid promoter engineering have been conducted by using several well-known upstream activation sequence and endogenous core promoter in *S. cerevisiae* [54]. Synthetic hybrid promoters contain a core promoter region fused to a single UAS or multiple tandem UAS repeats that modulate promoter strength. These UAS regions recruit transcription factors to increase the transcriptional activity of the core promoter. Thus, the UAS and core promoter regions perform as modular synthetic parts that can be combined to produce various types of UAS-core promoters. In this concept, the strength of hybrid promoter can be elevated by

either utilizing a stronger core promoter or by increasing the number of UAS repeats for the binding of transcription factor. For example, synthetic hybrid galactose-inducible promoters showed a nearly 50-fold range of expression levels and additionally increased the transcriptional capacity of the original *GAL1* promoter by about 20% [54]. This approach demonstrates that endogenous promoters in yeast can be enhanced simply through the addition of upstream activation elements to original core promoters.

2.2. Cellulosic ethanol production in microorganisms

2.2.1. Cellulosic biomass

Cellulosic biomass is the most abundant and inexpensive material that can be used as a feedstock for the production of renewable fuels and chemicals. Cellulosic materials consist of mainly three different types of polymers, including cellulose (35-55%), hemicellulose (20-40%), and lignin (10-25%), and the proportion of these components depends on the material source (Table 2.2) [55-59]. Lignin and hemicellulose have cross-linked structure with each other, which wraps around the cellulose. Cellulose is a polysaccharide consisting of a linear chain of several hundred to ten thousand β-1,4-linked glucose units. Cellulose has crystalline properties, which make it harder for enzymes and chemicals to access cellulose. Hemicellulose is a polysaccharide that is derived from several sugars, which consists of glucose, xylose, mannose, galactose, and arabinose. Depending on the

composition and the linkage pattern of the hemicellulose, it can be divided into arabinoxylan, galactomannan, and xyloglucan, which differs in the composition ratio depending on the type of biomass (Fig 2.2) [60]. Because of its branched and amorphous nature, hemicellulose can be more readily hydrolyzed compared to cellulose. Lignin is a cross-linked macromolecule consisting of phenylpropanoid units bound by ether and carbon-carbon bonds. The major phenolic components of lignin are *p*-coumaryl alcohol, coniferyl alcohol, and sinapyl alcohol.

To completely degrade cellulose to fermentable glucose, the cooperative actions of at least three types of cellulases, endoglucanase, exoglucanase, and β-glucosidase, are required. Endoglucanase randomly breaks the β-1,4-glycosidic bonds within amorphous regions in crystalline cellulose. Exoglucanase (also known as cellobiohydrolase) further hydrolyzes the cellulose chains from their reducing or non-reducing ends, releasing cellodextrins, mainly cellobiose, which are finally converted to glucose by β-glucosidase [61, 62]. Compared to cellulose, hemicellulose has more complex structure, thus their degradation requires multiple enzymes, including α-glucoronisidase, acetyl xylan exterase, and ferulic acid esterase as well as endoxylanase, exoxylanase, and β-xylosidase (Fig 2.2) [60].

Processing of cellulosic biomass to ethanol includes four major unit operations: pretreatment, hydrolysis, fermentation, and distillation [61]. Due tothe recalcitrant nature of cellulosic materials, pretreatment is generally required as the first step for biological conversion (Fig. 2.3). Enzymatic hydrolysis and fermentation steps can be categorized depending on the degree of process

Table 2.2 The composition of common agricultural residues and wastes

Lignocellulosic materials	Cellulose (%)	Hemicellulose (%)	Lignin (%)
Hardwoods stems	40–55	24–40	18–25
Softwood stems	45–50	25–35	25–35
Nut shells	25–30	25–30	30–40
Corn cobs	45	35	15
Grasses	25–40	35–50	10–30
Paper	85–99	0	0–15
Wheat straw	30	50	15
Sorted refuse	60	20	20
Leaves	15–20	80–85	0
Cotton seed hairs	80–95	5–20	0
Newspaper	40–55	25–40	18–30
Waste papers from chemical pulps	60–70	10–20	5–10
Primary wastewater solids	8–15	*NA	24–29
Swine waste	6.0	28	*NA
Solid cattle manure	1.6–4.7	1.4–3.3	2.7–5.7
Coastal Bermuda grass	25	35.7	6.4
Switch grass	45	31.4	12.0

*NA : not available
Sources ; [55-59]

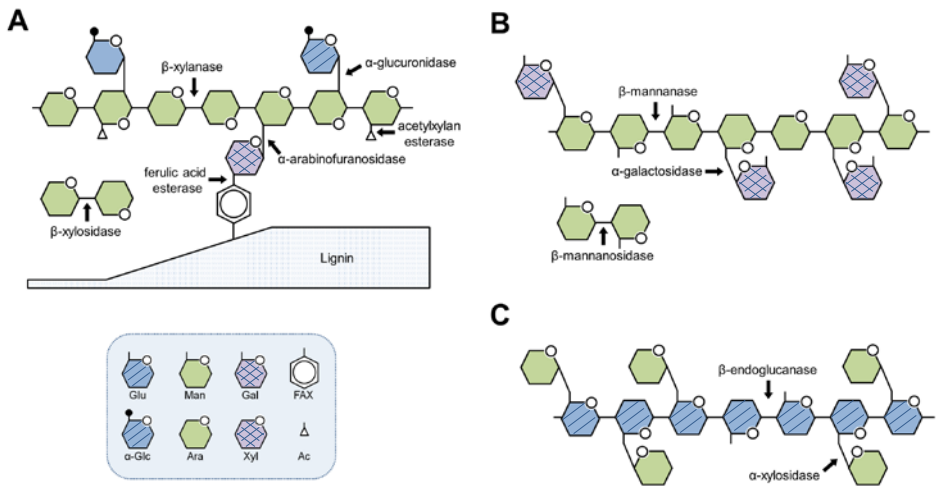

Figure 2.2 Structure of hemicellulose and hydrolase enzymes

A protruding line from the cyclic hexagon indicates the CH_2OH group. Hydrolase enzymes and the bonds targeted for cleavage in the polysaccharide structures are indicated by arrows. Arabinoxylan (A), galactomannan (B), and xyloglucan (C) [60].

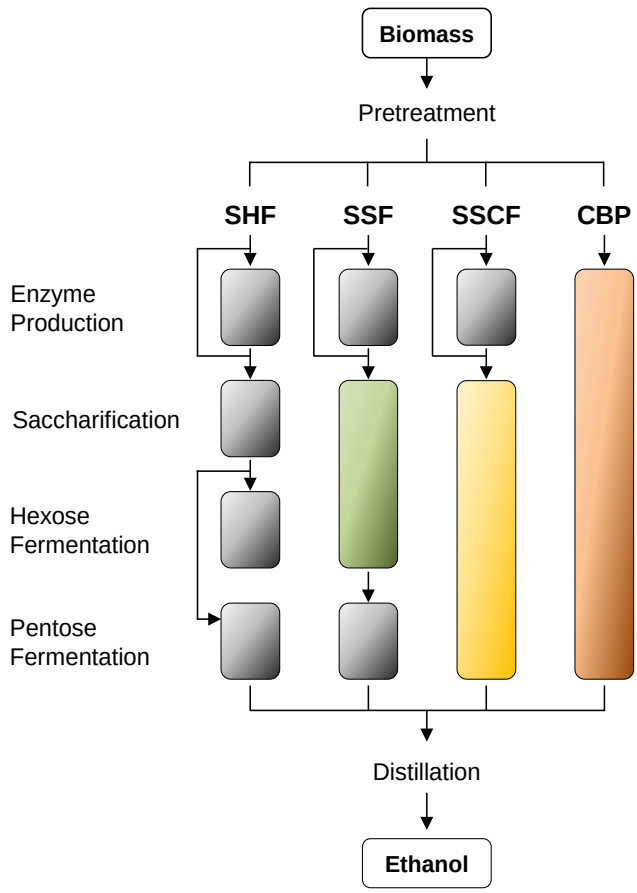

Figure 2.3 Schematic representation of process for ethanol production

Separate hydrolysis and fermentation (SHF), simultaneous saccharification and fermentation (SSF), simultaneous saccharification and co-fermentation (SSCF), and consolidated bioprocessing (CBP) [61].

integration. In these steps, four biologically mediated events can be required: (i) cellulase production, (ii) hydrolysis of cellulose and other insoluble polysaccharides, (iii) fermentation of cellulose-derived sugars, and (iv) fermentation of hemicellulose-derived sugars [61]. As shown in Figure 2.3, separate hydrolysis and fermentation (SHF) involves four discrete process steps. Simultaneous saccharification and fermentation (SSF) consolidates hydrolysis and fermentation of cellulose-derived sugars into one process step, with cellulase production and fermentation of hemicellulose-derived sugars occurring in two additional discrete process steps. Simultaneous saccharification and co-fermentation (SSCF) involves two process steps: cellulase production and a second step in which cellulose hydrolysis and fermentation of both cellulose and hemicellulose-derived sugars occurs. In consolidated bioprocessing (CBP), enzyme production, cellulose hydrolysis, and fermentation of products of both cellulose and hemicellulose hydrolysis are accomplished in a single process step.

2.2.2. Cellulosic bioethanol production in *S. cerevisiae*

Although no natural microorganism possesses the ability of both cellulose utilization and ethanol production desired for CBP, several microorganisms exhibit some of the desirable properties. These microorganisms can broadly be divided into two groups: (i) native cellulolytic microorganisms that possess capabilities of cellulase hydrolysis, but into which the ability to produce ethanol needs to be engineered, and (ii) recombinant cellulolytic microorganisms that naturally possess

the ability to produce ethanol with high yields, but into which cellulase hydrolysis systems need to be engineered [60, 61, 63]. Among microorganism belong to the second group, *S. cerevisiae* has been considered as one of the most promising candidates for CBP strain. With highly efficient ethanol production system, *S. cerevisiae* has a long commercial history in the traditional ethanol production. In addition, there are several beneficial characteristics, including resistance to low pH, high temperature, and various inhibitors [11, 64-66]. Accordingly, the major requirement for *S. cerevisiae* as CBP yeast would be sufficient expression of extracellular saccharification enzymes. It has been reported that heterologous cellulases were successfully secreted from *S. cerevisiae*, resulting in direct ethanol fermentation from cellulosic substrates. For example, *S. cerevisiae* expressing four individual cellobiohydrolases, including CBHI amd CBHII from *Trichoderma reesei*, CbhB from *A. niger*, and cbh1-4 from *Phanerochaete chrysosporium*, produced ethanol from several model cellulose [67]. When endoglucanase EGI from *T. reesei* and β-glucosidase BGL1 from *Saccharomycopsis fibuligera* were co-secreted, 1.0 g/L of ethanol was obtained from 10 g/L of phosphoric acid swollen cellulose (PASC) [68].

Apart from secreting cellulases from *S. cerevisiae*, several attempts have also been made to display cellulases on the yeast surface. In a previous report, direct ethanol production from PASC was achieved when the endoglucanse EGII and exoglucanase CBHII from *T. reesei* and β-glucosidase BGL1 from *A. aculeatus* were co-displayed on the yeast cell surface [69]. Remarkably, cellulase-displaying

system more efficiently produced ethanol from PASC compared to cellulase-secreting system [70]. Recently, some efforts have also been made for CBP by imitating the cellulosome structure [71-74]. Zhao group reported the first successful assembly of tri-functional minicellulosomes on the surface of *S. cerevisiae* [71]. In their concept, three cellulases and a scaffoldin, containing a single type of cohesin and dockerin pair form *C. thermocellum*, were co-expressed in a single strain, allowing a random assembly of the enzymes to the scaffoldin. On the other hand, Chen group constructed site-specific minicellulosomes using a scaffoldin carrying three divergent cohesin domains originated from three different strains, which allows site-specific binding of three enzymes, each tagged with the matching dockerin domain [73]. In addition, they introduced a consortium concept by expressing each cellulosome component, three cellulases and one scaffoldin, separately, and optimized the cellulolytic and ethanol production performance by adjusting the ratio of different populations in the consortium. Previous studies on cellulosic ethanol production in *S. cerevisiae* are summarized in Table 2.3.

Table 2.3 Cellulosic ethanol production in recombinant *S. cerevisiae*

Cellulase expression system	Substrate	Discription (Expressed cellulases)	Ethanol (g/L)	References
Secretion	PASC (10 g/L)	EGI from *T. reesei* and *bgl* from *Saccharomycopsis fibuligera*	1.0	[67]
	PASC (10 g/L)	EGII and CBHII from *T. reesei* and BGL1from *A. aculeatus*	1.6	[70]
	Avicel (8% (w/v))	*cdt-1* (cellodextrin transporter) and *gh1-1* (β-glucosidase) from *N. crassa*	27.0	[75]
Surface display	PASC (10 g/L)	EGII and CBHII from *T. reesei* and BGL1from *A. aculeatus*	2.9	[69]
	PASC (10 g/L)	EGII and CBHII from *T. reesei* and BGL1from *A. aculeatus*	2.1	[70]
	PASC (20 g/L)	EGII and CBHII from *T. reesei* and BGL1from *A. aculeatus*	7.6	[76]
	PASC (20 g/L)	EGII and CBHII from *T. reesei*, BGL1 from *A. aculeatus*, and AoelpI (expansin-like protein) from *A. oryzae*	3.4	[77]
	Cellobiose (5 g/L)	*bgl1* from *S. fibuligera*	2.3	[78]
	Cellulose (10 g/L)	EG1 (*cel7B*) from *T. reesei* and *cel3A* (β-glucosidase) from *S. fibuligera*	1.0	[67]
	PASC (10 g/L)	EGII and CBHII from *T. reesei*, BGL1from *A. aculeatus*, and *cdt-1* from *N. crassa*	4.3	[79]
Minicellulosome	PASC (10 g/L)	celCCA (endoglucanase), celCCE (cellobiohydrolase), and Ccel_2454 (β-glucosidase) from *C. cellulyticum* Displaying two individual scaffolds	1.1	[74]

PASC : phosphoric acid swollen cellulose

Table 2.3 Cellulosic ethanol production in recombinant *S. cerevisiae* (*Continued*)

Cellulase expression system	Substrate	Discription (Expressed cellulases)	Ethanol (g/L)	References
Minicellulosome	Avicel (10g/L)	celCCA, celCCE, and Ccel_2454 from *C. cellulyticum* Displaying two individual scaffolds	1.4	[74]
	PASC (10 g/L)	CelA (endoglucanase) from *C. thermocellum*, CBHII from *T. reesei*, and BGLI from *T. aurantiacus* Displaying a scaffoldin (Scaf-stf) containing three cohesin domains	1.3	[80]
	PASC (10 g/L)	*C. thermocellum* endoglucanase, *C. cellulolyticum* exoglucanase, *T. reesei* CBHII, *T. aurantiacus* BGLI Displaying a scaffoldin (Scaf-stf) containing three cohesin domains	1.9	[73]
	PASC (10 g/L)	EGII and CBHII from *T. reesei* and BGL1from *A. aculeatus* Displaying a scaffoldin (mini CipA) containing three cohesin domains	1.8	[71]
	PASC (10 g/L)	CelA from *C. thermocellum*, CBHII from *T. reesei*, and BGLI from *A. aculeatus* Displaying a scaffoldin (mini CipA) containing three cohesin domains	1.8	This study (Chapter 4)

PASC : phosphoric acid swollen cellulose

2.3. 2,3-Butanediol production in microorganisms

2.3.1. 2,3-Butanediol

2,3-Butanediol (butane-2,3-diol in IUPAC name), also known as 2,3-butylene glycol, dimethylene glycol, or 2,3-dihydroxybutane, is a colorless and odorless liquid with the molecular formula $C_4H_{10}O_2$. It has a high boiling point of 177-182˚C and a low freezing point of -60˚C. There are three stereoisomers of 2,3-butanediol: (2*S*,3*S*)-butanediol, meso-2,3-butanediol, and (2*R*,3*R*)-butanediol (Fig. 2.4).

2,3-Butanediol is a promising valuable chemical that can be used in various areas, especially as a platform chemical and a liquid fuel. Because 2,3-butanediol has a heating value of 27.2 kJ/g, which is similar to other liquid fuels such as ethanol and methanol (29.1 kJ/g and 22.1 kJ/g, respectively), it is considered to be an effective liquid fuel. Also, the low freezing point of (2*R*,3*R*)-butanediol, as mentioned above, makes it interesting for the use as an antifreeze agent. In addition, as a chiral compound for asymmetric synthesis, (2*S*,3*S*)- and (2*R*,3*R*)-butanediol can be used in pharmaceutical and fine chemical industries.

2,3-Butanediol can be dehydrated to methyl ethyl ketone (MEK, also known as 2-butanone) which can be used as an effective fuel additive and industrial organic solvent for gums, resins, and lacquers. 1,3-Butadiene, which is a building block of synthetic rubber, can also be obtained from further dehydration of 2,3-butanediol. The dehydrogenation of 2,3-butanediol gives two high-value

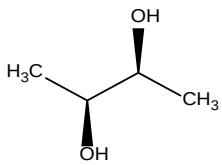

(2*S*,3*S*)-butanediol
L-(+)-; Dextrorotatory form

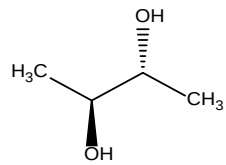

meso-2,3-butanediol
Optically inactive form

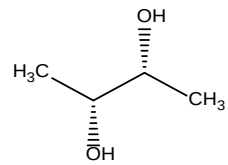

(2*R*,3*R*)-butanediol
D-(-)-; Levorotatory form

Figure 2.4 Stereoisomers of 2,3-butanediol

compounds, acetoin (also known as 3-hydroxybutanone) and diacetyl (also known as butanedion). As flavoring compounds with buttery aroma, both acetoin and diacetyl can be used in dairy products, cosmetics, and pharmaceuticals. Furthermore, tetramethyl compound and diester compound can also be prepared from 2,3-butanediol by ketalization with acetone and esterification, respectively.

2.3.2. 2,3-Butanediol production in bacteria

A number of microorganisms can produce 2,3-butanediol from pyruvate in a mixed acid fermentation. Among them, *Klebsiella pneumonia*, *Klebsiella oxytoca*, and *Paenibacilus polymyxa* have been considered as unbeatable species in the efficient production of 2,3-Butanediol [81]. *Enterobacter aerogenes* and *Seratia marcescens* are also suggested as a promising microorganism for this application. Previous studies on 2,3-butanediol production in different bacteria are summarized in Table 2.4.

For 2,3-butanediol biosynthesis, two molecules of pyruvate are condensed to α-acetolactate by α-acetolactate synthase (ALS), and then α-acetolactate is further converted to acetoin through two different routes depending on the culture condition. Under unaerobic conditions, α-acetolactate is directly converted to acetoin catalyzed by α-acetolactate decarboxylase (ALDC). If oxygen is present, on the other hand, α-acetolactate is converted into diacetyl through spontaneous decarboxylation, followed by conversion of diacetly to acetoin by diacetyl reductase (DAR, also known as acetoin dehydrogenase). Finally 2,3-butanediol

Table 2.4 2,3-Butanediol production in bacteria

Strain	Substrates	2,3-Butanediol			Description	References
		Titer (g/L)	Productivity (g/(L·h))	Yield (g/g)		
Klebsiella pneumoniae	Glucose	150.0	3.95	0.40	Fed-batch, Optimizatioin of culture condition including medium composition	[82]
	Corncob malasses	78.9	1.29	0.39	Fed-batch	[83]
	Glycerol	70.0	0.47	0.39	Fed-batch	[84]
	Jerusalem artichoke tuber	84.0	2.10	0.29	Fed-batch, Simultaneous saccharification and fermentation (SSF)	[85]
Klebsiella oxytoca	Glucose	85.5	3.00	0.47	Fed-batch	[86]
	Glucose	130.0	1.62	0.47	Fed-batch, Construction of ethanol formation-deficient mutant by inactivating *aldA*	[87]
	Glucose	117.4	1.20	0.49	Fed-batch, Construction of engineered strain (Δ*adhE*Δ*ackA-pta*Δ*ldhA)*	[88]
	Corncob hydrolysate	35.7	0.59	0.50	Fed-batch, Investigation of the effects of acetate in hydrolysate and pH	[89]
	Molasses	118.0	2.35	0.41	Fed-batch	[90]
Enterobacter aerogenes	Glucose	110.0	5.40	0.49	Fed-batch, Cell recycle system	[91]
Enterobacter cloacae	1. Glucose + Xylose	152.0	3.50	0.49	Fed-batch, Construction of engineered strain Δ*bdh*Δ*ptsG*Δ*ldh*Δ*frdA overexpressing heterologous bdh and galP genes*	[92]
	2. Corn stover hydrolysate	119.4	2.30	0.48		

Table 2.4 2,3-Butanediol production in bacteria (*Continued*)

Strain	Substrates	2,3-Butanediol			Description	References
		Titer (g/L)	Productivity (g/(L·h))	Yield (g/g)		
Serratia marcescens	Sucrose	152.0	2.67	0.41	Fed-batch, Construction of a surfactant (serrawettin)-defficient mutant by inactivating *swrW*	[93]
	Sucrose	139.9	3.33	0.45	Fed-batch, Optimizatioin of culture condition including medium compsition and feeding strategy	[94]
Paenibacillus polymyxa	Sucrose	111.0	2.05	–	Fed-batch, Culture medium supplemented with 60 g /L yeast extracts	[95]
	Glucose	71.71	1.33	0.39	Fed-batch, Two-stage fermentation with vitimin C feeding	[96]
	Jerusalem artichoke tuber	36.9	0.88	0.50	Batch, Optimizatioin of culture condition including medium composition	[97]
Bacillus subtilis	Glucose	2.5	0.27	0.31	Batch, Investigation of the effect of dissolved oxygen level	[98]
	Glucose	6.1	0.40	–	Batch, Microaerophilic fermentation with acetate addition	[99]
Bacillus licheniformis	Glucose	8.7	0.47	0.12	Batch, Investigation of the effects of pH and temperature	[100]
Escherichia coli	Glucose	73.8	1.19	0.41	Fed-batch, Overexpression of heterogous gene cluster with optimization	[101]
Bacillus amyloliquefaciens	Glucose	33.0	–	0.33	Batch, Investigation of the effects of initial substrate concentration and aeration	[102]

dehydrogenase (BDH, also known as acetoin reductase (AR)) catalyzes the reduction of acetoin to 2,3-butanediol.

However, because of the potential pathogenicity of these native producers, 2,3-butanediol production using these bacteria has been considered unsuitable for industrial-scale fermentation [81, 103].

2.3.3. 2,3-Butanediol production in *S. cerevisiae*

Recently, several efforts have been made to produce 2,3-butanediol in *S. cerevisiae*, which is generally recognized as safe (GRAS) and widely used for the production of various chemicals and fuels because of its high tolerance to alcohols and harsh industrial conditions [11, 64-66]. *S. cerevisiae* does not have α-acetolactate decarboxylase responsible for direct production of acetoin form α-acetolactate. Therefore, α-acetolactate, produced by α-acetolactate synthase (Ilv2) in mitochondria, is converted to acetoin via diacetyl formation (Fig. 2.5). In addition, it has been reported that acetoin can be formed by the anomalous carboligase activity of pyruvate decarboxylase (PDC), which catalyzes condensation between pyruvate and acetaldehyde or two molecules of acetaldehyde [104-106]. Then, acetoin is converted to 2,3-butanediol by the action of 2,3-butanediol dehydrogenase, Bdh1.

Because *S. cerevisiae* has a strong tendency towards ethanol fermentation, is essential to reduce ethanol production and redirect this metabolic flux to 2,3-butanediol for high-yield production. Ethanol is produced from pyruvate via two

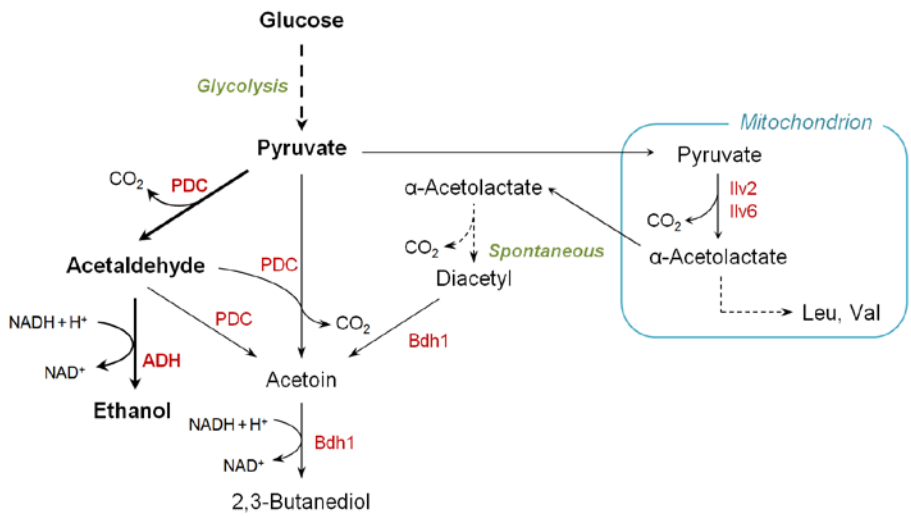

Figure 2.5 Metabolic pathway for 2,3-butanediol in *Saccharomyces cerevisiae*

Pyruvate produced from glucose by glycolysis, is mainly converted to ethanol via two steps, which consist of decarboxylation of pyruvate to acetaldehyde by pyruvate decarboxylase (PDC), and reduction of acetaldehyde to ethanol by alcohol dehydrogenase (ADH). Acetoin can be produced by anomalous carboligase activity of PDC, which catalyzes condensation between pyruvate and acetaldehyde or two molecules of acetaldehyde to acetoin. Also, pyruvate is converted to α-acetolactate by Ilv2 located in mitochondria, and then α-acetolactate is spontaneously decarboxylated to diacetyl. The reduction of diacetyl to acetoin is catalyzed by Bdh1. Finally acetoin is converted to 2,3-butanediol by Bdh1.

steps, which consist of decarboxylation of pyruvate to acetaldehyde by PDC and reduction of acetaldehyde to ethanol by alcohol dehydrogenase (ADH). Therefore, both PDC and ADH have been attractive disruption targets for 2,3-butanediol production in *S. cerevisiae*. In a previous study, deletion of *ADH1*, *ADH3*, and *ADH5* genes resulted in increased 2,3-butanediol production (2.29 g/L) with a yield of 0.113 g/g glucose under anaerobic condition [107]. Introduction of heterologous pathway consisting of α-acetolactate synthase (AlsS) and α-acetolactate decarboxylase (AlsD) from *B. subtilis* and endogenous Bdh1 to an evolved PDC-deficient strain led to successful production of 2,3-butanediol (96.2 g/L) with a high yield and productivity (0.28 g/g glucose and 0.39 g/(L·h), respectively) in fed-batch fermentation [108]. Although ethanol production can be completely eliminated by deleting *PDC1* and *PDC5* genes or all PDC genes (*PDC1*, *PDC*5, and *PDC6*), the resulting PDC-deficient strains have severe growth defects on glucose as a sole carbon source and require C_2 compounds such as acetate or ethanol for growth [15, 109]. Therefore, adaptively evolved PDC-deficient strains overcoming these defects have been used for metabolic engineering applications [108, 110-112]. Yeast strains producing 2,3-butanediol from xylose, galactose, or cellobiose apart from glucose, have also been developed [111, 113, 114]. Previous studies on 2,3-butanediol production in *S. cerevisiae* are summarized in Table 2.5.

Table 2.5 2,3-Butanediol production in *S. cerevisiae*

Reference Strain	Substrates	2,3-Butanediol			Description	References
		Titer (g/L)	Productivity (g/(L·h))	Yield (g/g)		
Saccharomoces cerevisiae						
V5	Glucose	7.4	0.06	0.03	Batch, *ald6Δ* and overexpression of *GPD1* and engineered *BDH1*	[115]
BY4742	Glucose	2.3	0.03	0.11	Batch, *adh1Δadh3Δadh5Δ*	[107]
D452-2	Glucose	96.2	0.39	0.28	Fed-batch, *pdc1Δpdc5Δ* (evolved) and overexpression of *alsS*, *alsD*, and *BDH1*	[108]
D452-2	1. Xylose	20.7	0.18	0.27	1. Batch, *pdc1Δpdc5Δ* (evolved) and overexpression of *XYL1*, *XYL2*, *XYL3*, *alsS*, a*lsD*, and *BDH1*	[113]
	2. Glucose + Xylose	43.6	0.20	–	2. Fed-batch, *pdc1Δpdc5Δ* (evolved) and overexpression of xylose assimilating enzymes (*XYL1*, *XYL2*, *XYL3*), *alsS*, a*lsD*, and *BDH1*	
D452-2	Cellobiose	5.3	0.22	0.29	Batch, *pdc1Δpdc5Δ* and overexpression of cellodextrin transporter (*cdt*), β-glucosidase (*gh1-1*), *alsS*, and *alsD*	[114]
CEN.PK2-1C	Glucose + Galactose	~100*	0.33*	–	Fed-batch, *pdc1Δpdc5Δpdc6Δ* (evolved) and overexpression of *ILV2* (cytosolic expression), *alsD*, and *BDH1*	[111]
D452-2	Glucose	~30*	0.40	0.37	Batch, *pdc1Δpdc5Δpdc6Δ* and overexpression of *alsS*, *alsD*, *BDH1*, and NADH oxidase (*noxE*)	[116]
CEN.PK2-1C	Glucose	72.9	1.43	0.41	Fed-batch, *adh1Δadh2Δadh3Δadh4Δadh5Δ gpd1Δgpd2Δ* and overexpression of *alsS*, *alsD*, *BDH1*, and NADH oxidase (*noxE*)	This study (Chapter 8)

*approximate value

Chapter 3.

Materials and methods

3.1. Strains and media

All strains used in this study are listed in Table 3.1. *E. coli* strain DH5α [F^- Φ80d*lacZ*ΔM15 Δ(*lacZYA-argF*)U169 *recA1 endA1 hsdR17* (r_K^-, m_K^+) *phoA supE44* λ^- *th*i-*1 gyrA96 relA1*] was used for genetic manipulations. *E. coli* was cultured in Luria-Bertani (LB) medium (10 g/L tryptone, 5 g/L yeast extract, and 10 g/L NaCl) supplemented with 50 μg/mL ampicillin.

S. cerevisiae strain EBY100 (*MATa GAL1-AGA1::URA3 ura3-52 trp1 leu2Δ1 his3Δ200 pep4::HIS2 prb1Δ1.6R can1 GAL*) was used for surface display of scaffoldin or cellulase secretion. EBY100 transformants were grown in synthetic dextrose casamino acids (SD-CAA) medium (20 g/L dextrose, 6.7 g/L yeast nitrogen base, 5 g/L casamino acids, 5.4 g/L Na_2HPO_4, and 8.6 g/L $NaH_2PO_4 \cdot H_2O$). For the induction of scaffoldin cloned in pCTCON vector, cells grown in SD-CAA medium were harvested and resuspended in SG-CAA medium containing galactose instead of glucose, and further incubated for 24 h.

S. cerevisiae strain BY4741 (*MATa his3Δ1 leu2Δ0 met15Δ0 ura3Δ0*), *bdh1Δ* (BY4741, *bdh1Δ::KanMX6*), and CEN.PK2-1C (*MATa ura3-52 trp1-289 leu2-3,112 his3Δ1 MAL2-8C SUC2*) were obtained from EUROSCARF. The gene disruption mutants were constructed by using the Cre/*loxP* recombination system [117]. The gene deletion cassette was obtained by PCR amplification from pUG27, pUG72 or pUG73 as template, using a gene-specific primer pair of d_ORF F and d_ORF R. After confirmation of the correct integration of the cassette at the target

Table 3.1 Strains used in this study

Strain	Genotype	Reference
E. coli		
DH5α	F$^-$ Φ80d*lacZ*ΔM15 Δ(*lacZYA-argF*)U169 *recA1 endA1 hsdR17* (r_K^-, m_K^+) *phoA supE44* λ^- *th*i-*1 gyrA96 relA1*	
S. cerevisiae		
EBY100	*MATa GAL1-AGA1::URA3 ura3-52 trp1 leu2Δ1 his3Δ200 pep4::HIS2 prb1Δ1.6R can1 GAL*	Invitrogen
BY4741	*MATa his3Δ1 leu2Δ0 met15Δ0 ura3Δ0*	EUROSCARF
CEN.PK2-1C	*MATa ura3-52 trp1-289 leu2-3,112 his3Δ1 MAL2-8C SUC2*	EUROSCARF
bdh1Δ	BY4741, *bdh1Δ::KanMX6*	EUROSCARF
adh1Δ	CEN.PK2-1C *adh1Δ::loxP*	This study
adh1-5Δ	CEN.PK2-1C *adh1Δ::loxP adh2Δ::loxP adh3Δ::loxP adh4Δ::loxP adh5Δ::loxP*	This study
gpd1Δgpd2Δ	CEN.PK2-1C *gpd1Δ::loxP gpd2Δ::loxP*	This study
adh1Δgpd1Δgpd2Δ	CEN.PK2-1C *adh1Δ::loxP gpd1Δ::loxP gpd2Δ::loxP*	This study
adh1-5Δgpd1Δgpd2Δ	CEN.PK2-1C *adh1Δ::loxP adh2Δ::loxP adh3Δ::loxP adh4Δ::loxP adh5Δ::loxP gpd1Δ::loxP gpd2Δ::loxP*	This study
PYK1-Myc	CEN.PK2-1C *PYK1*-Myc	This study
PYK1-Coh-Myc	CEN.PK2-1C *PYK1*-cohesin-Myc	This study

gene locus through PCR analysis using the confirmation primers (c_ORF F and c_ORF R), the marker gene was removed by transformation of Cre recombinase-expression vector, pSH63 or p414G-Cre. Additional gene deletion was sequentially conducted using the same procedure. PYK1-myc and PYK1-Coh-myc strain were also constructed by PCR-mediated homologous recombination based on Cre/*loxP* recombination system. The integration cassettes were obtained by PCR amplification from pUG27-Myc and pUG27-Coh-Myc as templates, using a primer pair of i_PYK1 F and i_PYK1 R. After confirmation of the correct integration of the cassette at the 3' end of *PYK1* target gene locus through PCR analysis using the confirmation primers (c_PYK1 F and c_PYK1 R), the marker gene was removed by transformation of Cre recombinase-expression vector, p414GPD-Cre. Primers used for gene manipulations, including deletion and integration, are listed in Table 3.2.

Yeast cells were cultured in YP medium (10 g/L yeast extract and 20 g/L bacto-peptone) supplemented with 20 (YPD), 50 (YPD5), or 100 g/L glucose (YPD10), in synthetic complete (SC) medium (6.7 g/L yeast nitrogen base without amino acids, 1.4 g/L amino acids dropout mixture lacking His, Trp, Leu, and Ura) supplemented with auxotrophic amino acids as required and 20 or 50 g/L glucose, or in synthetic defined (SD) medium (20 or 50 g/L glucose, 6.7 g/L yeast nitrogen base without amino acids) supplemented with auxotrophic requirements (120 μg/mL Leu and 50 μg/mL each of His, Met, and Ura).

Table 3.2 Primers used for strain construction (gene manipulation)

Primers	Sequence (5'-3')
d_ADH1 F	*TTCAAGCTATACCAAGCATACAATCAACTATCTCATATACA* CAGCTGAAGCTTCGTACGC
d_ADH1 R	*CTTATTTAATAATAAAAATCATAAATCATAAGAAATTCGC* GCATAGGCCACTAGTGGAT
d_ADH2 F	*TACAATCAACTATCAACTATTAACTATATCGTAATACACA* CAGCTGAAGCTTCGTACGC
d_ADH2 R	*ATAATGAAAACTATAAATCGTAAAGACATAAGAGATCCGC* GCATAGGCCACTAGTGGAT
d_ADH3 F	*GTTAAAACTAGGAATAGTATAGTCATAAGTTAACACCATC* CAGCTGAAGCTTCGTACGC
d_ADH3 R	*ACAAAGACTTTCATAAAAAGTTTGGGTGCGTAACACGCTA* GCATAGGCCACTAGTGGAT
d_ADH4 F	*CAAGTTTACATTTGCAACAACTAATAGTCAAATAAGAAAA* CAGCTGAAGCTTCGTACGC
d_ADH4 R	*GCACACGCATAATTGACGTTTATGAGTTCGTTCGATTTTT* GCATAGGCCACTAGTGGAT
d_ADH5 F	*AGAAAATTATTTAACTACATATCTACAAAATCAAAGCATC* CAGCTGAAGCTTCGTACGC
d_ADH5 R	*TAAAAAGTAAAAATATATTCATCAAATTCGTTACAAAAGA* GCATAGGCCACTAGTGGAT
d_GPD1 F	*CACCCCCCCCCTCCACAAACACAAATATTGATAATATAAAG* CAGCTGAAGCTTCGTACGC
d_GPD1 R	*AAGTGGGGGAAAGTATGATATGTTATCTTTCTCCAATAAAT* GCATAGGCCACTAGTGGAT
d_GPD2 F	*TCTCTTTCCCTTTCCTTTTCCTTCGCTCCCCTTCCTTATCA* CAGCTGAAGCTTCGTACGC
d_GPD2 R	*GGCAACAGGAAAGATCAGAGGGGGAGGGGGGGGGAGAGTGT* GCATAGGCCACTAGTGGAT
i_PYK1 F	*CGGTGCTGGTCACTCCAACACTTTGCAAGTCTCTACCGTT* GGTGGTTCTGGTGCTAGT
i_PYK1 R	*TTCAAAAAAATAATATCTTCATTCAATCATGATTCTTTTT* GCATAGGCCACTAGTGGATC
c_ADH1 F (-350)	CACCATATCCGCAATGAC
c_ADH1 R (+303)	GTGTTGTCCTCTGAGGAC

Table 3.2 Primers used for gene manipulation (*Continued*)

Primers	Sequence (5'-3')
c_ADH2 F (-300)	ACCGGGCATCTCCAACTT
c_ADH2 R (+200)	CCATGTCTACAGTTTAGAGG
c_ADH3 F (-300)	ATGAGCAGCAGCCATTTTG
c_ADH3 R (+200)	TGATGGTGATAATGTCTCTCA
c_ADH4 F (-300)	AAGAACTAGTTTTTAGTTCGCG
c_ADH4 R (+205)	AGAACTTCCGTTCTTCTTTT
c_ADH5 F (-300)	CTGCTATCTGCTTGTAGAAG
c_ADH5 R (+200)	GAAACGTTTGTATAGGTTGT
c_GPD1 F (-300)	CGCCTTGCTTCTCTCCCCTT
c_GPD1 R (+300)	CCGACAGCCTCTGAATGAGT
c_GPD2 F (-300)	TACGGACCTATTGCCATTGT
c_GPD2 R (+300)	TTAAGGGCTATAGATAACAG
c_PYK1 F (300)	TGTCCACTTCCGGTACCACC
c_PYK1 R (+209)	ATGCAACACCTCATCGTT

3.2. Plasmids

Plasmids used in this study are listed in Table 3.3. Plasmid pCT-mini CipA for surface display of scaffoldin was constructed as follows. The DNA fragments encoding amino acids 28-559 (1.6 kb, two cohesin domains and CBM) and 1533-1698 (0.5 kb, a cohesin domain) of the *C. thermocellum* CipA were prepared by PCR amplification, using genomic DNA (ATCC 27405) as template. These PCR products were sequentially cloned into the restriction sites SacI/SpeI and SpeI/XhoI of p426GPD vector [47], and then amplified by using PCR primers, each containing 35 nt or 37 nt region homologous to the pCTCON vector [118]. PCR product was transformed into *S. cerevisiae* EBY100 together with the NheI and BamHI digested pCTCON vector, leading to an insertion of the PCR product into a pCTCON vector by homologous recombination. The resulting plasmid, pCT-mini CipA was isolated from the transformant and confirmed by DNA sequencing.

Plasmid p424-s.s for the secretion of cellulase was constructed as follows. The DNA fragment encoding secretion signal sequence from the *S. cerevisiae* α- factor prepro-peptide was prepared by PCR amplification, using pPICZαA as template and primers containing additional restriction enzyme recognition sites (ApaI, BamHI, BglII and NheI). The 330 bp PCR product was cloned into the SpeI and SalI sites of pRS424GPD vector resulting in p424-s.s vector. *C. thermocellum* CelA gene lacking signal sequence was amplified from genomic DNA (ATCC 27405) and cloned into the ApaI/NheI sites of p424-s.s vector. The dockerin

Table 3.3 Plasmids used in this study

Plasmid	Description	Reference
p413GPD	CEN/ARS, *HIS3*, P_{TDH3}, T_{CYC1}	[47]
P414GPD	CEN/ARS, *TRP1*, P_{TDH3}, T_{CYC1}	[47]
p415GPD	CEN/ARS, *LEU2*, P_{TDH3}, T_{CYC1}	[47]
p416ADH	CEN/ARS, *URA3*, P_{ADH1}, T_{CYC1}	[47]
p416GPD	CEN/ARS, *URA3*, P_{TDH3}, T_{CYC1}	[47]
p423GPD	2 μ, *HIS3*, P_{TDH3}, T_{CYC1}	[47]
p424GPD	2 μ, *TRP1*, P_{TDH3}, T_{CYC1}	[47]
p425GPD	2 μ, *LEU2*, P_{TDH3}, T_{CYC1}	[47]
p426GPD	2 μ, *URA3*, P_{TDH3}, T_{CYC1}	[47]
pCTCON	CEN/ARS, *TRP1*, $P_{GAL1\text{-}10}$-[Aga2-HA-Myc]-$T_{MF\alpha1}$	[118]
pUG27	Plasmid containing *loxP-Sp.his5*$^{+}$*-loxP* deletion cassette	EUROSCARF
pUG72	Plasmid containing *loxP-Kl.URA3-loxP* deletion cassette	EUROSCARF
pUG73	Plasmid containing *loxP-Kl.LEU2-loxP* deletion cassette	EUROSCARF
pFA6a-VN-HIS3MX6	Plasmid containing VN-*HIS3MX6* integration cassette	[120]
pFA6a-VC-HIS3MX6	Plasmid containing VC-*HIS3MX6* integration cassette	[120]
pSH63	CEN/ARS, *TRP1*, P_{GAL1}-*cre*-T_{CYC1}	EUROSCARF
p414GPD-Cre	CEN/ARS, *TRP1*, P_{TDH3}-*cre*-T_{CYC1}	This study
pCT-mni CipA	CEN/ARS, *TRP1*, $P_{GAL1\text{-}10}$-[Aga2-HA-Coh_1-Coh_2-CBM-Coh_9-Myc]-T_{CYC1}	This study
p424-s.s	2 μ, *TRP1*, P_{TDH3}-[α-factor prepro-peptide (s.s)]-T_{CYC1}	This study
p424-s.s-CelA	2 μ, *TRP1*, P_{TDH3}-[s.s-CelA]-T_{CYC1}	This study
p424-s.s-CBHII	2 μ, *TRP1*, P_{TDH3}-[s.s-CBHII]-T_{CYC1}	This study

Table 3.3 Plasmids used in this study (*Continued*)

Plasmid	Description	Reference
p424-s.s-BGL1	2 μ, *TRP1*, P_{TDH3}-[s.s-BGLI]-T_{CYC1}	This study
pCT-BGL1	CEN/ARS, *TRP1*, $P_{GAL1\text{-}10}$-BGL1-$T_{MF\alpha1}$	This study
p413GPD-Doc	CEN/ARS, *HIS3*, P_{TDH3}-Doc-T_{CYC1}	This study
p414GPD-Doc	CEN/ARS, *TRP1*, P_{TDH3}-Doc-T_{CYC1}	This study
p415GPD-Doc	CEN/ARS, *LEU2*, P_{TDH3}-Doc-T_{CYC1}	This study
p414GPD-VN-Doc	CEN/ARS, *TRP1*, P_{TDH3}-[VN-Doc]-T_{CYC1}	This study
p415GPD-VC-Doc	CEN/ARS, *LEU2*, P_{TDH3}-[VC-Doc]-T_{CYC1}	This study
p416GPD-GST	CEN/ARS, *URA3*, P_{TDH3}-GST-T_{CYC1}	This study
p416GPD-GST2	CEN/ARS, *URA3*, P_{TDH3}-GST (no stop codon)-T_{CYC1}	This study
p416GPD-GST-$[Coh]_2$	CEN/ARS, *URA3*, P_{TDH3}-[GST-$(Cohesin)_{x2}$]-T_{CYC1}	This study
p416GPD-GST-$[Coh]_3$	CEN/ARS, *URA3*, P_{TDH3}-[GST-$(Cohesin)_{x3}$]-T_{CYC1}	This study
p416GPD-GST-$[Coh]_7$	CEN/ARS, *URA3*, P_{TDH3}-[GST-$(Cohesin)_{x7}$]-T_{CYC1}	This study
p415GPD-HA-BDH1	CEN/ARS, *LEU2*, P_{TDH3}-[HA-*BDH1*]-T_{CYC1}	This study
p415GPD-HA-BDH1-Doc	CEN/ARS, *LEU2*, P_{TDH3}-[HA-*BDH1*-Doc]-T_{CYC1}	This study
p413GPD-alsS-Doc	CEN/ARS, *HIS3*, P_{TDH3}-[*alsS*-Doc]-T_{CYC1}	This study
p414GPD-alsD-Doc	CEN/ARS, *TRP1*, P_{TDH3}-[*alsD*-Doc]-T_{CYC1}	This study
p415GPD-BDH1-Doc	CEN/ARS, *LEU2*, P_{TDH3}-[*BDH1*-Doc] T_{CYC1}	This study
pUG27-Myc	Plasmid containing Myc-[*loxP-his5*$^+$*-loxP*] integration cassette	This study
pUG27-Coh-Myc	Plasmid containing Cohesin-Myc-[*loxP-his5*$^+$*-loxP*] integration cassette	This study
p415GPD-ldhA	CEN/ARS, *LEU2*, P_{TDH3}-*ldhA*-T_{CYC1}	This study

Table 3.3 Plasmids used in this study (*Continued*)

Plasmid	Description	Reference
p415GPD-ldhA$_{Doc}$	CEN/ARS, *LEU2*, P$_{TDH3}$-[*ldhA*-Doc]-T$_{CYC1}$	This study
p413-SDB	CEN/ARS, *HIS3*, P$_{TDH3}$-*alsS*-T$_{PYK1}$, P$_{TEF1}$-*alsD*-T$_{PYK1}$, P$_{TPI1}$-*BDH1*-T$_{TPI11}$	This study
p413-S$_{Doc}$DB	CEN/ARS, *HIS3*, P$_{TDH3}$-[*alsS*-Doc]-T$_{PYK1}$, P$_{TEF1}$-*alsD*-T$_{PYK1}$, P$_{TPI1}$-*BDH1*-T$_{TPI1}$	This study
p416ADH-EGFP	CEN/ARS, *URA3*, P$_{ADH1}$-EGFP-T$_{CYC1}$	This study
p416GPD-EGFP	CEN/ARS, *URA3*, P$_{TDH3}$-EGFP-T$_{CYC1}$	This study
p416[U$_n$C$_{ARO80}$]-EGFP (n=2, 3, 4)	CEN/ARS, *URA3*, [(UAS$_{ARO80}$)$_n$-Core$_{ARO80}$] promoter-EGFP-T$_{CYC1}$	This study
p416[U$_n$C$_{ARO9}$]-EGFP (n=2, 3, 4)	CEN/ARS, *URA3*, [(UAS$_{ARO80}$)$_n$-Core$_{ARO9}$] promoter-EGFP-T$_{CYC1}$	This study
p416[P$_{ARO9}$]-EGFP	CEN/ARS, *URA3*, P$_{ARO9}$-EGFP-T$_{CYC1}$	This study
p413[U$_4$C$_{ARO9}$]	CEN/ARS, *HIS3*, [(UAS$_{ARO80}$)$_{x4}$-Core$_{ARO9}$] promoter, T$_{CYC1}$	This study
p423[U$_4$C$_{ARO9}$]	2 μ, *HIS3*, [(UAS$_{ARO80}$)$_{x4}$-Core$_{ARO9}$] promoter, T$_{CYC1}$	This study
p415[U$_4$C$_{ARO9}$]	CEN/ARS, *LEU2*, [(UAS$_{ARO80}$)$_{x4}$-Core$_{ARO9}$] promoter, T$_{CYC1}$	This study
p425[U$_4$C$_{ARO9}$]	2 μ, *LEU2*, [(UAS$_{ARO80}$)$_{x4}$-Core$_{ARO9}$] promoter, T$_{CYC1}$	This study
p413[U$_4$C$_{ARO9}$]-alsS	CEN/ARS, *HIS3*, [(UAS$_{ARO80}$)$_{x4}$-Core$_{ARO9}$] promoter-*alsS*-T$_{CYC1}$	This study
p413[U$_4$C$_{ARO9}$]-alsS	CEN/ARS, *HIS3*, [(UAS$_{ARO80}$)$_{x4}$-Core$_{ARO9}$] promoter-*alsS*-T$_{CYC1}$	This study
p423[U$_4$C$_{ARO9}$]-alsS	2 μ, *HIS3*, [(UAS$_{ARO80}$)$_{x4}$-Core$_{ARO9}$] promoter-*alsS*-T$_{CYC1}$	This study
p415[U$_4$C$_{ARO9}$]-alsD	CEN/ARS, *LEU2*, [(UAS$_{ARO80}$)$_{x4}$-Core$_{ARO9}$] promoter-*alsD*-T$_{CYC1}$	This study

Table 3.3 Plasmids used in this study (*Continued*)

Plasmid	Description	Reference
p425[U_4C_{ARO9}]-alsD	2 μ, *LEU2*, [$(UAS_{ARO80})_{x4}$-$Core_{ARO9}$] promoter-*alsD*-T_{CYC1}	This study
p413[P_{UGA4}]-alsS	CEN/ARS, *HIS3*, P_{UGA4}-alsS-T_{CYC1}	This study
p425[P_{UGA4}]-alsD	CEN/ARS, *LEU2*, P_{UGA4}-*alsD*-T_{CYC}	This study
p413-SDBN	CEN/ARS, *HIS3*, P_{TDH3}-*alsS*-T_{PYK1}, P_{TEF1}-*alsD*-T_{GPM1}, P_{TPI1}-*BDH1*-T_{TPI1}, P_{FBA1}-*noxE*-T_{FBA1}	This study

domain of *C. thermocellum* CelS (DocS) was amplified and cloned into the NheI and SalI sites of p424-s.s vector. *T. reesei* CBHII and *A. aculeatus* BGLI genes lacking signal sequence were amplified from cDNA containing vectors [119] and cloned into the ApaI/NheI sites of p424-s.s-DocS and BamHI/NheI sites of p424-s.s vector, respectively.

The DNA fragments encoding GST with or without stop codon were prepared by PCR amplification, using pGEX-4T-1 as template, and cloned into p416GPD resulting p416GPD-GST and p416GPD-GST2. To construct scaffold expression vectors, the DNA fragments encoding amino acids 523-888 (two cohesins), 523-1053 (three cohesins), and 523-1698 (seven cohesins) of the *C. thermocellum* CipA were amplified by PCR using genomic DNA (ATCC 27405) as template, and cloned into p416GPD-GST2 resulting p416GPD-GST-$[Coh]_2$, p416GPD-GST-$[Coh]_3$, and p416GPD-GST-$[Coh]_7$, respectively. To construct dockerin-tagging vectors, dockerin domain from *C. thermocellum* CelS (amino acids 676-744) was amplified and cloned into p413GPD, p414GPD, and p415GPD vectors, resulting p413GPD-Doc, p414GPD-Doc, and p415GPD-Doc, respectively. Plasmids for expression of dockerin-tagged proteins were constructed as follows. VN fragment and VC fragment for BiFC were obtained from pFA6a-VN-HIS3MX6 and pFA6a-VC-HIS3MX6 by PCR amplification [120]. The *alsS* and *alsD* genes from *B. subtilis* and *BDH1* from *S. cerevisiae* were amplified by PCR using genomic DNA. HA-tagged *BDH1* was amplified by using PCR primer containing HA tag sequence. These PCR products were cloned into dockerin tagging vectors containing

appropriate marker, generating p414GPD-VN-Doc, p415GPD-VC-Doc, p413GPD-alsS-Doc, p414GPD-alsD-Doc, p415GPD-BDH1-Doc, and p415GPD-HA-BDH1-Doc, respectively.

To construct plasmid for chromosomal integration cassette, pUG27 plasmid containing *loxP-his5*$^{+}$*-loxP* cassette was used as a starting plasmid. The DNA fragment sequentially consisting of linker sequence (GGSG), Myc epitope tag, and *CYC1* terminator (T_{CYC1}) was cloned into HindIII and SalI sites of pUG27, resulting in pUG27-Myc plasmid. The cohesin domain was obtained by PCR amplification using p416GPD-GST-$[Coh]_2$ as template. The PCR product was cloned into BamHI site located between linker sequence and Myc epitope tag in pUG27-Myc plasmid, resulting in pUG27-Coh-Myc. In order to omit the procedure of galactose induction for the expression of Cre recombinase, the DNA fragment encoding *CRE* recombinase was obtained by cutting the pSH63 plasmid with SpeI and XhoI and cloned into p414GPD plasmid, resulting in p414G-Cre.

For gene overexpression, strong constitutive promoters (P_{TPI1} and P_{FBA1}) and terminators (T_{PYK1}, T_{GPM1}, T_{TPI1}, and T_{FBA1}) were prepared by PCR amplification, using CEN.PK2-1C genomic DNA as template. The *TDH3* promoter of p414GPD was removed by cutting the plasmid with SacI and SpeI, and replaced with the DNA fragments P_{TPI1} and P_{FBA1}, resulting p414_P_{TPI1} and p414_P_{FBA1}. The *CYC1* terminators of p414GPD (containing P_{TDH3}), p414TEF (containing P_{TEF1}), p414_P_{TPI1}, and p414_P_{FBA1} were removed by cutting the plasmids with XhoI and KpnI, and replaced with the DNA fragments T_{PYK1}, T_{GPM1}, T_{TPI1}, and T_{FBA1},

respectively, generating p414_P_{TDH3}/T_{PYK1}, p414_P_{TEF1}/T_{GPM1}, p414_P_{TPI1}/T_{TPI1}, and p414_P_{FBA1}/T_{FBA1}.

HA-tagged BDH1 was amplified by using PCR primer containing HA tag sequence and cloned into p415GPD, resulting in p415GPD-HA-BDH1. A plasmid p415GPD-HA-BDH1-Doc, expressing N-terminal HA-tagged Bdh1 with C-terminal dockerin fusion, was previously reported [121]. *ldhA* (LEUM_1756, D-lactate dehydrogenase) gene from *Leuconostoc mesenteroides subsp. mesenteroides* ATCC 8293 was kindly provided by Dr. N. S. Han (Chungbuk National University, Korea) [122]. The PCR products encoding *ldhA* gene with or without stop codon were prepared by PCR amplification and cloned into p415GPD and p415GPD-Doc, respectively, resulting in p415GPD-ldhA and p415GPD-$ldhA_{DOC}$. The *alsS* and *alsD* genes from *B. subtilis*, and *BDH1* from *S. cerevisiae* were amplified by PCR using each genomic DNA. These PCR products were cloned into appropriate plasmids, resulting in p414_P_{TDH3}-*alsS*-T_{PYK1}, p414_P_{TEF1}-*alsD*-T_{GPM1}, and p414_P_{TPI1}-*BDH1*-T_{TPI1}. To construct multigene-expression vector for 2,3-butanediol pathway, the *alsD*-expression cassette (P_{TEF1}-*alsD*-T_{GPM1}) flanked by MluI sites was obtained by PCR amplification using a universal primer pair, Univ F and Univ R containing AscI and NotI sites for additional cloning, and cloned into the BssHII sites of pRS413 vector. *BDH1*- and *alsS*-expression cassettes flanked by MluI and NotI sites were also obtained using the same primers and sequentially cloned into AscI and NotI sites, resulting in p413-SDB.

The DNA fragment encoding EGFP was prepared by PCR amplification and

cloned into p416GPD and p416ADH, resulting p416GPD-EGFP and p416ADH-EGFP, respectively. To construct the synthetic promoters, PCR amplifications were performed using the primers containing additional Aro80 binding sites, F_U_nC_{ARO80}/R_C_{ARO80} for *ARO80* core element (-129 to -1) and F_U_nC_{ARO9}/R_C_{ARO9} for *ARO9* core element (-132 to -1), generating [U_nC_{ARO80}] and [U_nC_{ARO9}] (n=2, 3, 4). The *ARO9* promoter (P_{ARO9}) was amplified by PCR using the primers, F_P_{ARO9}/R_C_{ARO9}. The *TDH3* promoter of p416GPD-EGFP was removed by cutting the plasmids with SacI and BamHI, and replaced with the DNA fragments [U_nC_{ARO80}], [U_nC_{ARO9}], or P_{ARO9} resulting in p416[U_nC_{ARO80}]-EGFP, p416[U_nC_{ARO9}]-EGFP and p416P_{ARO9}-EGFP, respectively. The selected tryptophan-inducible promoter, [U_4C_{ARO9}], was replaced the *TDH3* promoter of p413GPD, p423GPD, p415GPD, and p425GPD, generating p413[U_4C_{ARO9}], p423[U_4C_{ARO9}], p415[U_4C_{ARO9}], and p425[U_4C_{ARO9}], respectively. The *alsS* gene from *B. subtilis* was amplified by PCR using genomic DNA and cloned into p413[U_4C_{ARO9}] and p423[U_4C_{ARO9}], generating p413[U_4C_{ARO9}]-*alsS* and p423[U_4C_{ARO9}]-*alsS*. The *alsD* gene from *B. subtilis* was amplified by PCR using genomic DNA and cloned into p415[U_4C_{ARO9}] and p425[U_4C_{ARO9}], generating p415[U_4C_{ARO9}]-*alsD* and p425[U_4C_{ARO9}]-*alsD*. To construct GABA-inducible acetoin producing pathway, *UGA4* promoter sequence (-460 to -1) was prepared by PCR amplification and replaced the [U_4C_{ARO9}] promoter of p413[U_4C_{ARO9}]-*alsS* and p425[U_4C_{ARO9}]-*alsD*, creating p413[P_{UGA4}]-*alsS* and p425[P_{UGA4}]-*alsD*.

The *noxE* gene from *L. lactis* IL1403 were amplified by PCR using genomic

DNA. The PCR product was cloned into p414_P_{FBA1}/T_{FBA1}, resulting in p414_P_{FBA1}-*noxE*-T_{FBA1}. To construct multigene-expression vector for 2,3-butanediol pathway, the *alsD*-expression cassette (P_{TEF1}-*alsD*-T_{GPM1}) flanked by MluI sites was obtained by PCR amplification using universal primer sets, Univ F and Univ R containing AscI and NotI sites for additional cloning, and cloned into the BssHII sites of pRS413 vector. *BDH1*- and *alsS*-expression cassettes flanked by MluI and NotI sites were also obtained using the same primers and sequentially cloned into AscI and NotI sites, resulting in p413-SDB. The *noxE*-expression cassette (P_{FBA1}-*noxE*-T_{FBA1}) was additionally cloned into AscI and NotI sites of p413-SDB, resulting in p413-SDBN. Primers used for gene cloning are listed in Table 3.4.

Table 3.4 Primers used for gene cloning

Primers	Sequence (5'-3')
CipA-1 F	ATAGAGCTCGCGGCCACAATGACAGTCG
CipA-1 R	CCGACTAGTCGGATCATCTGACGGCGG
CipA-2 F	CCGACTAGTACACCGACAACAACAGAT
CipA-2 R	GGACTCGAGCTATCCTTCTATTACAGGTTTA
mini-CipA F	TGGTGGTGGTGGTTCTGGTGGTGGTGGTTCTGCTAGCGCGGCCA CAATGACAGTCG
mini-CipA R	ACAAGTCCTCTTCAGAAATAAGCTTTTGTTCGGATCCGGATGGC GGCGTTAGTATC
s.s-Myc F	CTCACTAGTATGAGATTTCCTTCAATTTTT
s.s-Myc R	CTCGTCGACTCAGCTAGCACGCGTAGATCTGGGCCCCAGATCCT CTTCTGAGATGAGTTTTTGTTCAGCTTCAGCCTCTCTTTTCTC
DocS F	CGACGCTAGCTCTACTAAATTATACGGCGA
DocS R	CCGCTCGAGTCAGTTCTTGTACGGCAATGT
linker-DocS F	ACTGCTGCAGGGTGGTTCTGGTGCTAGCTCTACTAAATTATACG GCGA
CelA F	AATGGGCCCGCAGGTGTGCCTTTTAACAC
CelA R	AATGCTAGCATAAGGTAGGTGGGGTATGC
CBHII F	GCACGGGCCCCAAGCTTGCTCAAGCGTC
CBHII R	GCAGGCTAGCCAGGAACGATGGGTTTGC
BGLI F	CGACAGATCTGATGAACTGGCGTTCTCTCC
BGLI R	AATAGCTAGCTTGCACCTTCGGGAGCGCC
GST F	ACTGACTAGTATGTCCCCTATACTAGGTTA
GST R	CCCGGGAATTCCGGGGATCC
linker-Coh F	ACTGGGATCCGGTGGTTCTGGTGGCAGTGTAGTACCATCA
Coh R	ACTGGACTGCTCGAGCTAATCCAGATCATCTGTTGT
F_U_2C_{ARO80}	CGCGAGCTCTTGCCGATGATAACCGAGATAAATG

Restriction enzyme sites are underlined

Table 3.4 Plasmids used for gene cloning (*Continued*)

Primers	Sequence (5'-3')
F_U_2C_{ARO80}	CGCGAGCTCTTGCCGATGATAACCGAGATAAATG
F_U_3C_{ARO80}	CGCGAGCTCTTGCCGATACTATCCGATGATAACCGAGATAAATG
F_U_4C_{ARO80}	CGCGAGCTCTTGCCGATGCTTACCGATACTATCCGATGATAACC GAGATAAATG
R_C_{ARO80}	CGCGGATCCAGAGGATAAAGCAGTGCTTAATG
F_U_2C_{ARO9}	CGCGAGCTCTTGCCGATGATAACCGAACCATCATTGGGGTAGGA AAC
F_U_3C_{ARO9}	CGCGAGCTCTTGCCGATACTATCCGATGATAACCGAACCATCAT TGGGGTAGGAAAC
F_U_4C_{ARO9}	CGCGAGCTCTTGCCGATGCTTACCGATACTATCCGATGATAACC GAACCATCATTGGGGTAGGAAAC
F_P_{ARO9}	CGCGAGCTCCATTGCCGATGCTTACCGAGATTTGCCGCG
R_C_{ARO9}	CGCGGATCCTGAGTCGATGAGAGAGTGTAATTGTGG
F_EGFP	GAGGGATCCATGTCTAAAGGTGAAGAATTATTCAC
R_EGFP	GAGGAATTCTTATTTGTACAATTCATCCATACCATG
P_{PYK1} F	GTCAGAGCTCGAAAGTTTTTCCGGCAAGCT
P_{PYK1} R	GTCAACTAGTTGTGATGATGTTTTATTTGTTTTG
T_{PYK1} F	GTCACTCGAGAAAAAGAATCATGATTGAATGAAG
T_{PYK1} R	GTCAGGTACCGTACCCATGTATAACCTTCC
P_{PGK1} F	GTCAGAGCTCAGAAGTACCTTCAAAGAATGG
P_{PGK1} R	GTCAACTAGTTGTTTTATATTTGTTGTAAAAAG
T_{PGK1} F	GTCACTCGAGATTGAATTGAATTGAAATCGA
T_{PGK1} R	GTCAGGTACCAGGAAGAATACACTATACTGGA
P_{GPM1} F	GTCAGAGCTCTAGTCGTGCAATGTATGACT
P_{GPM1} R	GTCAACTAGTTATTGTAATATGTGTGTTTGT
T_{GPM1} F	GTCACTCGAGGTCTGAAGAATGAATGATTTG

Restriction enzyme sites are underlined

Table 3.4 Plasmids used for gene cloning (*Continued*)

Primers	Sequence (5'-3')
P_{GPM1} F	GTCAGAGCTCTAGTCGTGCAATGTATGACT
P_{GPM1} R	GTCAACTAGTTATTGTAATATGTGTGTTTGT
T_{GPM1} F	GTCACTCGAGGTCTGAAGAATGAATGATTTG
T_{GPM1} R	GTCAGGTACCTATTCGAACTGCCCATTCA
P_{FBA1} F	GTCAGAGCTCATCCAACTGGCACCGCTG
P_{FBA1} R	GTCAACTAGTTTTGAATATGTATTACTTGGTTATG
T_{FBA1} F	GTCACTCGAGTAAGTTAATTCAAATTAATTGATATAG
T_{FBA1} R	GTCAGGTACCCAAAAGATGAGCTAGGCTTT
alsS F	CTGAGGATCCATGACAAAAGCAACAAAAGAAC
alsS R	CTGACTCGAGCTAGAGAGCTTTCGTTTTCA
alsS R2	CTGACTCGAGGAGAGCTTTCGTTTTCATGA
alsD F	CTGAGGATCCATGAAACGAGAAAGCAACAT
alsD R	CTGACTCGAGTTATTCAGGGCTTCCTTCAG
alsD R2	CTGACTCGAGTTCAGGGCTTCCTTCAGTTG
HA-BDH1 F	ACTGACTAGTATGTATCCGTATGACGTCCCGGACTATGCAGGAT CCTCTGAAATTACTTTGGGTAA
BDH1 F	ACTGGGATCCATGAGAGCTTTGGCATATTTCA
BDH1 R	ACTGCTCGAGTTACTTCATTTCACCGTGATTGT
BDH1 R2	ACTGCTGCAGCTTCATTTCACCGTGATTGTT
Univ F	GACTACGCGTGGAACAAAAGCTGGAGCTC
Univ R	GACTACGCGTGCGGCCGCTAATGGCGCGCCATAGGGCGAATTGG GTACC

Restriction enzyme sites are underlined

3.3. Culture conditions

3.3.1. Cellulosic ethanol production using a yeast consortium

OD_{600} of 50 of cells were harvested and resuspended in YP-PASC medium (10 g/L yeast extract, 20 g/L peptone, and 1% PASC as the sole carbon source). Ethanol fermentation was carried out as previously described with minor modification [119]. Cell mixture was anaerobically incubated in a 30 mL-serum bottle with 10 mL reaction volume.

3.3.2. 2,3-Butanediol production using synthetic scaffold-based substrate channeling

OD_{600} of 0.3 of pre-cultured cells were harvested and resuspended in the 5 mL of appropriate SC medium in a 50 mL conical tube. For fed-batch cultivation, cells were cultured in 50 mL of SC-His-Trp-Leu-Ura medium containing 50 g/L glucose in 100 mL flask. The feeding solution (800 g/L glucose) was added to the culture medium, when glucose was depleted.

3.3.3. Redirection of pyruvate flux through enzyme coupling

For the production of lactic acid, yeast cells harboring p415GPD-ldhA or p415GPD-ldhA_{Doc} were pre-cultured in SC-Leu medium containing 20 g/L glucose and diluted to OD_{600} of 0.3 in 7.5 mL of SC-Leu medium containing 50 g/L glucose in a 50 mL conical tube with shaking at 170 rpm. For the production of 2,3-butanediol, yeast cells harboring p413-SDB or p413-S_{Doc}DB were cultured in

the same condition of lactate production in SC-His medium instead of SC-Leu medium.

3.3.4. Promoters inducible by aromatic amino acids and γ-aminobutyrate for metabolic engineering applications

For the experiments investigating the promoter inducibility on aromatic amino acids, overnight culture cells were diluted to OD_{600} of 0.45, incubated for 6 h in SD-Ura containing 20 g/L glucose, and then induced with 200 μg/mL tryptophan, phenylalanine or tyrosine. Tryptophan and phenylalanine were dissolved in distilled water at a concentration 10 mg/mL and used as stock solution. For tyrosine induction, instead of treatment of tyrosine using stock solution, the culture medium was exchanged with SD-Ura containing 200 μg/mL tyrosine because of the low solubility of tyrosine in water.

Yeast cells harboring *alsS* and *alsD* genes in various plasmids, were pre-cultured in SD-His-Ura containing 20 g/L glucose and then inoculated to OD_{600} of 0.2 in SD-His-Ura containing 50 g/L glucose with indicated concentrations of tryptophan or γ-aminobutyrate (GABA) for acetoin production.

3.3.5. Efficient production of 2,3-butanediol by eliminating ethanol and glycerol production and redox rebalancing

Yeast cells harboring appropriate plasmids were pre-cultured in SC-His medium containing 20 g/L glucose and diluted to OD_{600} of 0.3 in 8 mL of SC-His medium containing 50 g/L glucose in a 50 mL conical tube with shaking at 170 rpm. For

shake flask fed-batch fermentation, cells harboring p413-SDBN plasmid were pre-cultured in SC-His medium containing 20 g/L glucose, diluted to OD_{600} of 10, and cultured in 25 mL of YPD10 medium in a 250 mL flask with shaking at 170 rpm with an intermittent addition of glucose using 800 g/L stock solution.

3.4. β-glucosidase activity assay

The activity of β-glucosidase BGL1 was determined by measuring the amount of *p*-nitrophenol released from *p*-nitrophenyl-β-D-glucopyranoside (*p*NPG) used as substrate. OD_{600} of 10 cells were washed twice with distilled water and twice with reaction buffer (50 mM sodium acetate, pH 5.2). Cells were resuspended in a reaction buffer containing 1 mM *p*NPG and incubated at 30ºC. The amount of hydrolyzed *p*-nitrophenol was quantified by measuring the optical density at 400 nm using 96-well plate spectrophotometer (Multiskan GO, Thermo Scientific).

3.5. Endo/exoglucanase activity assays

Yeast cells, each harboring the surface-display plasmid for mini CipA or secretion plasmid for CelA or CBHII were grown in SD-CAA medium and then mixed in various combinations in SG-CAA medium for 24 h. OD_{600} of 10 of cells were harvested and washed with reaction buffer (50 mM sodium acetate, pH 5.2). Cells were resuspended in a reaction buffer containing 1% PASC and then incubated for 4 h at 30ºC. The amount of reducing sugars in the reaction supernatant was

determined by DNS method as described elsewhere [123].

3.6. *In vivo* GST-pull down assay

CEN.PK2-1C cells were co-transformed with p415GPD-HA-BDH1-Doc and one of the three GST-tagged scaffolds or GST expression vector. Cells harboring the appropriate constructs were grown in SC-Leu-Ura and harvested. Whole-cell extracts were prepared by glass bead lysis by using IP150 buffer [50 mM Tris-HCl (pH 7.4), 150 mM NaCl, 2 mM $MgCl_2$, and 0.1% NP-40)]. After cell lysates were incubated with glutathione-agarose beads for 3 h at 4ºC, the beads were washed three times with IP150 buffer and the bound proteins were eluted by boiling in sample buffer for 10 min. Samples were resolved by SDS-PAGE and proteins were detected by immunoblotting with antibodies against GST and HA epitope tag.

3.7. Bimolecular fluorescence complementation analysis

CEN.PK2-1C cells were co-transformed with p414GPD-VN-Doc, p415GPD-VC-Doc, and one of the p416GPD-GST-$[Coh]_x$ vectors or p416GPD-GST as a control. Cells harboring the appropriate constructs were grown in SC-Trp-Leu-Ura and harvested at exponential phase. After harvested cells were washed and suspended with PBS buffer, fluorescence microscopy was performed as previously described [120].

3.8. Co-immunoprecipitation

The PYK1-Coh-Myc strain harboring p415GPD-HA-BDH1 or p415GPD-HA-BDH1-Doc was grown in SC-Leu medium containing 20 g/L glucose and harvested in early log phase. Whole-cell lysates were prepared by glass bead lysis by using IP150 buffer [50 mM Tris-HCl (pH 7.4), 150 mM NaCl, 2 mM $MgCl_2$, and 0.1% NP-40)] supplemented with 0.1% protease inhibitor cocktail (Calbiochem) and 1 mM phenylmethylsulfonyl fluoride (PMSF). Whole-yeast lysates (700 μg of total protein) were incubated with 1 μg c-Myc antibody (Santa Cruz Biotechnology) for 3 h at 4˚C followed by addition of 15 μL protein G PLUS-Agarose beads (Santa Cruz Biotechnology). After further incubation for 90 min at 4˚C, samples were washed three times with IP150 buffer and the bound proteins were eluted by boiling in sample buffer for 10 min. Samples were resolved by SDS-PAGE and proteins were detected by immunoblotting with use of antibodies against Myc and HA epitope tag.

3.9. RNA preparation and quantitative reverse transcription PCR

The 1 mL of cells was harvested and frozen at -80ºC in 300 μL of lysis buffer [10 mM Tris-HCl (pH 7.4), 10 mM EDTA, 0.5% SDS]. 300 μL of acidic phenol was added to each sample and incubated at 65ºC for 20 min with occasional vortexing. Prior to chloroform extraction, the solution was chilled on ice for 10 min. After

centrifugation and ethanol precipitation, the resulting RNA pellets were dissolved in RNase-free water. The relative amount of mRNA was determined by quantitative reverse transcription PCR (qRT-PCR) as previously described [124]. Reverse transcription (RT) of 2 μg of total RNA was carried out with 0.1 μg of oligo-(dT) for 1 h at 42ºC using M-MLV reverse transcriptase (M-biotech, Inc., Korea), followed by heat inactivation for 10 min at 75ºC. PCR mixture containing 1 μL of 20 μL RT reaction solution, 1xSYBR master mix (Roche Diagnostics), and gene-specific primers, was subjected to qPCR reaction with 45 cycles of 95ºC for 10 s, 55ºC for 20 s, and 72ºC for 20 s using Roche LightCycler 480 real-time PCR system (Roche Diagnostics). Primer sequences used for qRT-PCR are as follows:

q_EGFP F, 5'-GTTCTGTTCAATTAGCTGAC-3';

q_EGFP R, 5'-TTATTTG TACAATTCATC-3';

q_ENO1 F, 5'-CTATCGAAAAGAAGGCTGCC-3';

q_ENO1 R, 5'-CGTGGTGGAAGTTTTCACCAGC-3'

3.10. Measurement of EGFP fluorescence intensity

To measure the EGFP fluorescence intensity, cells were harvested at appropriate point and resuspended with phosphate-buffered saline (PBS). The EGFP fluorescence intensity was measured by a TECAN GeNios Pro microplate reader (TECAN) at excitation wavelength of 485 nm and emission wavelength of 535 nm. Cell density was measured by using microplate reader Multiskan GO (Thermo Scientific) at 600 nm.

3.11. Analytic methods

Cell growth was monitored by optical density at 600 nm (OD_{600}) using a spectrophotometer (Cary 50 Conc, Varian). To quantify the concentration of metabolites, culture supernatants were collected and filtered through a 0.22 μm syringe filter. The concentrations of glucose, succinate, lactate, glycerol, acetate, acetoin, 2,3-butanediol and ethanol were determined by using high performance liquid chromatography (HPLC). The concentrations of acetoin and 2,3-butanediol were determined by using HPLC or gas chromatography (GC). HPLC analysis was performed in UltiMate 3000 HPLC system (Thermo Scientific, Dionex) equipped with an Aminex HPX-87H column (300 mm x 7.8 mm, 5μm, Bio-Rad) and a refractive index (RI) detector. The column was eluted with 5 mM H_2SO_4 as a flow rate of 0.6 mL/min at 60ºC and RI detector was kept at 35ºC. GC analysis was operated in a Varian GC-450 gas chromatograph equipped with a DB-WAX capillary column (30 m x 0.32 mm ID, 0.25 μm film thickness) and a flame ionization detector at 300ºC. The oven temperature program was initiated at 40ºC for 5 min and increased to 170ºC at 10°C/min, and then to 230ºC at 30ºC/min. Chemicals for standard solution were purchased from Sigma-Aldrich.

In the case of cellulosic ethanol production, HPLC analysis was performed in Finnigan Surveyor Plus (Thermo Scientific) with a flow rate of 0.8 mL/min. The other conditions were the same as previously described.

Chapter 4.

Cellulosic ethanol production using a yeast consortium displaying a minicellulosome and β-glucosidase

4.1. Introduction

Recently, there has been a growing interest in production of cellulosic bioethanol as a promising alternative to fossil fuels [125-127]. Cellulosic biomass is the most abundant materials in nature and insulated from the ethical concerns raised against the use of food-based materials such as corn and sugarcane [128, 129]. Despite these advantages, however, the recalcitrant nature and high cost of cellulase are the major obstacles to utilize cellulosic biomass [130, 131].

To completely degrade cellulose to fermentable glucose, the cooperative actions of at least three types of cellulases, endoglucanase, exoglucanase, and β-glucosidase, are required. Endoglucanase randomly breaks the β-1,4-glycosidic bonds within amorphous regions in crystalline cellulose. Exoglucanase further hydrolyzes the cellulose chains from their reducing or non-reducing ends, releasing cellodextrins, mainly cellobiose, which are finally converted to glucose by β-glucosidase [61, 62].

Several anaerobic cellulolytic bacteria such as *Clostridium* and *Ruminococcus* species produce intricate multi-enzyme machines, termed cellulosome, that allow highly efficient cellulose degradation [132, 133]. The assembly of cellulosome is mediated through structural scaffoldin that contains cohesin domains, which interact with dockerin domains in enzymes (Fig.4.1). It has been generally considered that cellulosome complex leads to synergistic degradation of cellulosic substrate afforded by spatial proximity of the tethered cellulases. In addition,

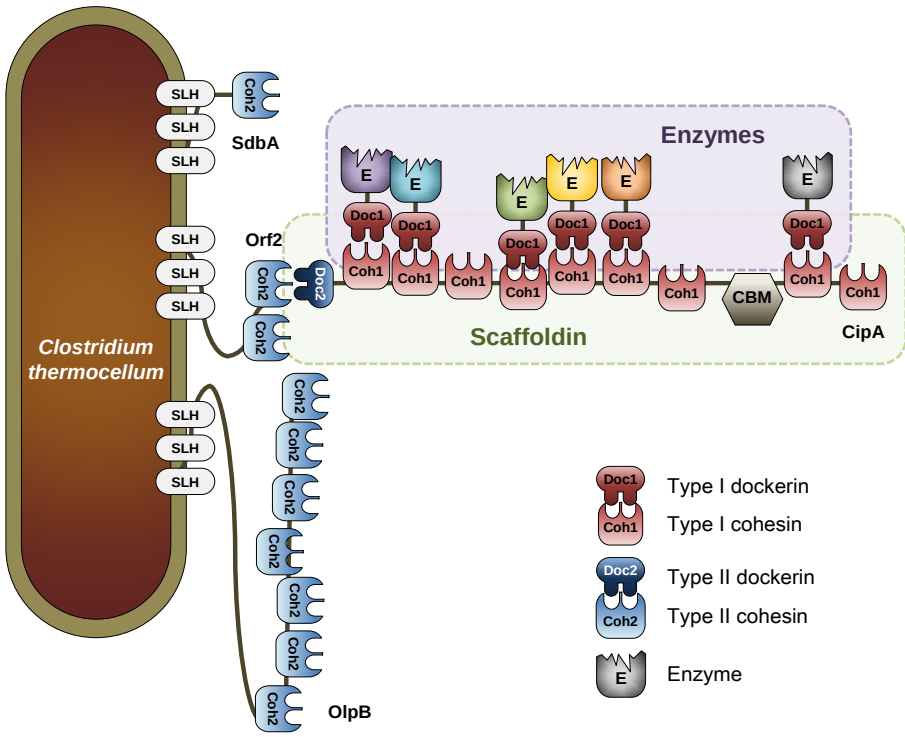

Figure 4.1 Schemetic diagram of cellulosome of *Clostridium thermocellum*

cellulose-binding module (CBM) in scaffoldin might also contribute to the cellulolytic efficiency via efficient substrate targeting [134]. Consolidated bioprocessing (CBP), combining cellulase production, saccharification, and fermentation into one step, has been proposed as the most efficient way to reduce the production cost of ethanol from cellulosic biomass [61, 63]. In recent years, some efforts have been made to develop cellulolytic yeast strains for CBP by imitating the cellulosome structure [71-74]. Zhao group reported the first successful assembly of tri-functional minicellulosomes on the surface of *S. cerevisiae* [71]. In their concept, three cellulases and a scaffoldin, containing a single type of cohesin and dockerin pair form *Clostridium thermocellum*, were co-expressed in a single strain, allowing a random assembly of the enzymes to the scaffoldin. However, expression of multiple genes in a single cell could cause metabolic burden and saturation of the cellular secretion system, which might restrict the efficiency of cellulosome assembly on the yeast surface.

On the other hand, Chen group constructed site-specific minicellulosomes using a scaffoldin carrying three divergent cohesin domains originated from three different strains, which allows site-specific binding of three enzymes, each tagged with the matching dockerin domain [73]. In addition, they introduced a consortium concept by expressing each cellulosome component, three cellulases and one scaffoldin, separately, and optimized the cellulolytic and ethanol production performance by adjusting the ratio of different populations in the consortium. Although site-specific interaction between cohesin and dockerin is capable of

providing highly controllable ordering of each enzyme, there is a limitation as the ratio among the enzymes is fixed depending ultimately on the ratio of the corresponding cohesin. Moreover, such a site-specific assembly system would be disadvantageous for expanding the list of enzymes to be incorporated into the cellulosome complex.

Therefore, in this chapter, the advantages of the consortium concept and the random assembly of cellulosome components are combined. A scaffoldin (mini CipA) composed of the same type of cohesins was constructed, which enables assembly of the dockerin-containing enzymes in a random manner. Since it was newly found that β-glucosidase can bind to the yeast surface without any modification, endoglucanase and exoglucanase, but not β-glucosidase, were incorporated as cellulosome components. The cellulosome activity for ethanol production was optimized by controlling the combination ratio among the four yeast strains, capable of either displaying the mini CipA or secreting one of the three enzymes.

4.2. Construction of a minicellulosome structure on the yeast surface

The basic design of this chapter is composed of four different yeast strains, one of which for displaying the mini CipA, and the others for secreting one of the three types of cellulases (Fig. 4.2). Mini CipA, a modified *C. thermocellum* scaffoldin containing a CBM and three cohesin domains, was expressed under the control of

GAL1 promoter as an Aga2-fusion protein on the surface of yeast EBY100 strain (Fig. 4.3A). In order to hydrolyze cellulose to glucose, endoglucanase CelA from *C. thermocellum*, exoglucanase CBHII from *T. reesei*, and β-glucosidase BGLI from *Aspergillus aculeatus* were secreted using α-factor prepro-peptide (Fig. 4.3B). CelA and CBHII were expressed with the native dockerin (DocA) and exogenous dockerin from *C. thermocellum* CelS (DocS), respectively.

BGLI, on the other hand, was expressed without a dockerin domain since it already has a cell adhesion characteristic without any additional anchor system. As shown in Figure 4.4, the harvested yeast cells harboring BGLI-secretion vector (p424-s.s-BGLI) showed β-glucosidase activity comparable to the cells containing pCT-BGLI, displaying BGLI on the surface as an Aga2-fusion protein. This observation might be in line with the cell wall-binding properties of the β-glucosidases reported in several fungi including *Aspergillus kawachii*, *Aspergillus oryzae*, *Neurospora crassa*, *Pichia etchellsii*, and *T. reesei* [135-139]. Therefore, in this study, dockerin fused-enzymes, CelA and CBHII, were randomly assembled to the scaffoldin structure via cohesin-dockerin interactions, whereas BGLI was assembled to the cell surface independently (Fig. 4.2). To confirm display of mini CipA on the yeast cell surface, immunofluorescence labeling of the cells was carried out using mouse anti-HA antibody as the primary antibody and goat anti-mouse IgG conjugated with FITC as the secondary antibody. As shown in Figure 4.5A, yeast cells expressing mini CipA were clearly distinguished by green fluorescence, whereas no fluorescence was observed on the cell surface of the

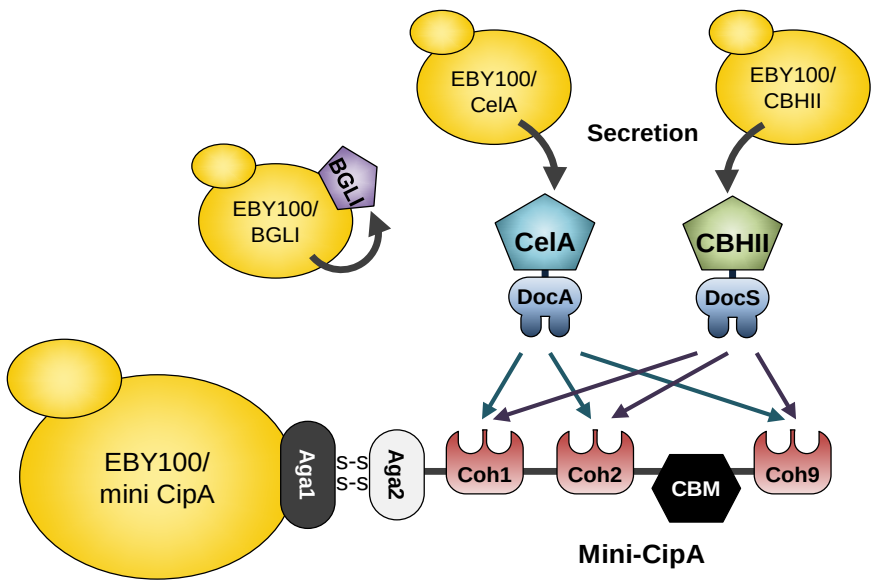

Figure 4.2 Schematic diagram of the overall concept of this research

The basic design of the research in this chapter is composed of four different yeast strains, one for displaying the mini CipA, and the others for secreting three types of cellulases. Mini CipA, a modified scaffoldin including a CBM and three cohesin domains, was expressed as an Aga2-fusion protein. The dockerin fused-enzymes, *C. thermocellum* CelA and *T. reesei* CBHII, were randomly assembled to mini CipA via cohesin-dockerin interactions, whereas the secreted *A. aculeatus* BGLI was independently bound to the cell surface through its own cell surface adhesion characteristic. Coh, cohesin; CBM, carbohydrate binding module; DocA and DocS, native dockerin in CelA and exogenous dockerin from *C. thermocellum* CelS, respectively.

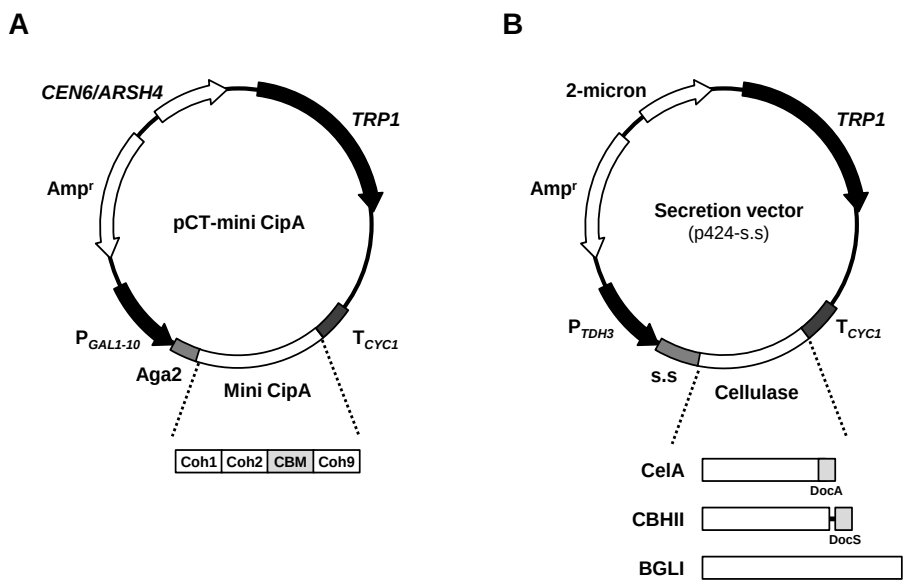

Figure 4.3 Design and construction of plasmids for cellulosome composition

A. Construction of a surface display vector, pCT-mini CipA. Mini CipA, a modified scaffoldin containing a CBM and three cohesin domains, was expressed under the control of *GAL1* promoter as an Aga2-fusion protein for displaying on the yeast surface.

B. Construction of cellulase secretion vectors. α-factor prepro-peptide (s.s) was used as a signal sequence.

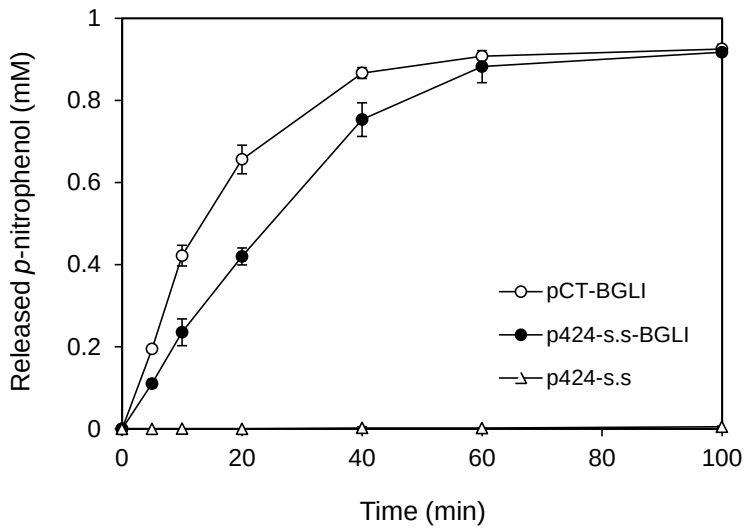

Figure 4.4 Yeast surface adhesion characteristic of *A. aculeatus* BGLI

The β-glucosidase activity was measured by pNPG assay using the harvested cells containing pCT-BGLI (BGL1 surface display vector, open circle), p424-s.s-BGLI (BGL1 secretion vector, closed circle), or p424-s.s (negative control, open triangle).

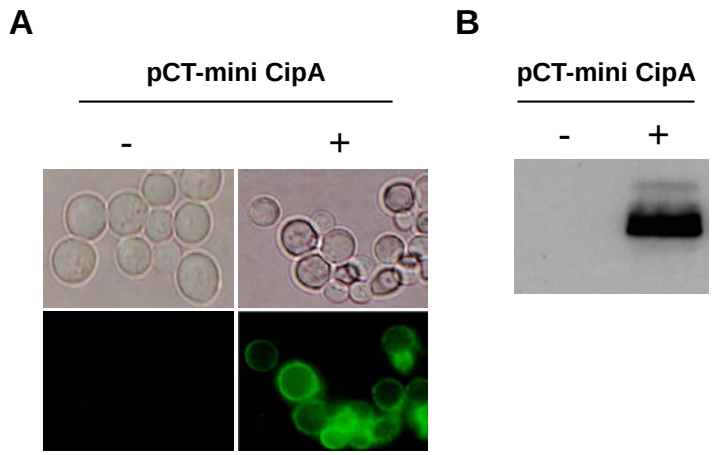

Figure 4.5 Surface-displayed mini CipA

A. Immunofluorescence labeling of EBY100 expressing mini CipA. EBY100 strain containing pCT-mini CipA was labeled with mouse anti-HA IgG and goat anti-mouse IgG conjugated with FITC. Yeast cells prior to galactose induction were used as a negative control (-).

B. Expression of mini CipA was confirmed by by immunoblotting (IB) with anti-HA antibody.

control cell. Also the expression of mini CipA was evaluated by immunoblotting with anti-HA antibody (Fig. 4.5B). These results confirmed that the mini CipA was successfully displayed on the cell surface.

With the successful display of mini CipA on cell surface, the assembly of secreted CelA onto surface-displayed mini CipA was examined. The culture medium for EBY100 containing p424-s.s-CelA (EBY100/CelA) was incubated with mini CipA displayed cells (EBY100/mini CipA) or control cells, followed by immunofluorescence microscopy using the anti-HA (for detection of mini CipA) or anti-myc antibody (for detection of CelA). As shown by fluorescence in Figure 4.6, secreted CelA was successfully assembled on the cell surface via mini CipA.

4.3. Cellulosic ethanol production using the optimized cellulosome

For complete degradation of pure cellulose to glucose, at least three different enzyme activities, including endoglucanase, exoglucanase, and β-glucosidase, are required [61]. However, each enzyme activity required for effective hydrolysis is depending on the types of enzymes and substrates, as well as the experimental conditions [140-143]. Therefore, cellulosome activity was optimized by controlling the combination ratio among the yeast strains capable of either displaying the mini CipA or secreting one of the three enzymes.

First, in order to simplify possible combinations, the mini CipA portion of

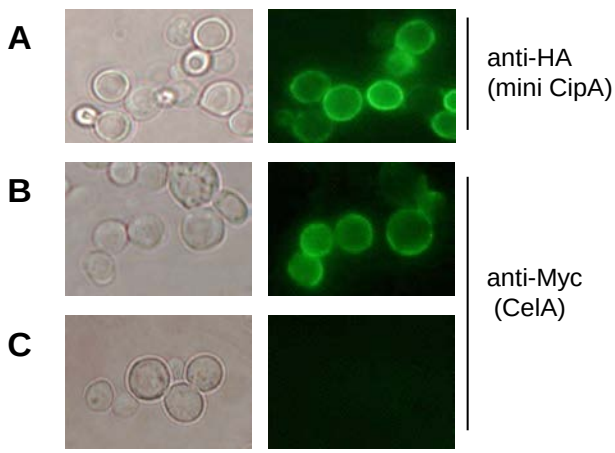

Figure 4.6 Assembly of secreted CelA to surface-displayed mini CipA

The culture medium for EBY100 containing p424-s.s-CelA (EBY100/CelA) was incubated with mini CipA displayed cells (EBY100/mini CipA) (A and B) or control cells (C), followed by immunofluorescence microscopy using the anti-HA (for detection of mini CipA) (A) or anti-myc antibody (for detection of CelA) (B and C) with goat anti-mouse IgG conjugated with FITC.

total population, which makes the amount of displayed enzymes on the cell-surface maximum, was investigated. EBY100 containing p424-s.s-CelA (EBY100/CelA) was regarded as a representative of cells secreting dockerin-fused enzymes. EBY100/CelA and EBY100 containing pCT-mini CipA (EBY100/mini CipA) were co-cultured for 24 h in SG-CAA medium in various ratios. The harvested cells were incubated with phosphoric acid swollen cellulose (PASC), and the released reducing sugars were measured by DNS method. Detection of the CelA endoglucanase activity in the harvested cells indicates successful binding of the secreted CelA to the mini CipA displayed on the surface (Fig. 4.7). In addition, mini CipA-dependent display of CelA on the yeast surface was previously confirmed by indirect immunofluorescence (Fig 4.6). The amount of released reducing sugars reached a peak at mini CipA:CelA ratio of 1:3.

Thereafter, the ratio between EBY100/CelA and EBY100/CBHII was investigated while fixing the amount of EBY100/mini CipA as 1/4 of total cells. As shown in Figure 4.8, the optimal ratio of EBY100/CelA:EBY100/CBHII, which produced the highest amounts of reducing sugars, was 1:1. Although CBHII alone did not show any significant PASC hydrolysis activity, the concentration of the released reducing sugars were higher in the presence of both CelA and CBHII (maximum 790 mg/L) than in the presence of CelA alone (maximum 460 mg/L), confirming the cooperative actions between the endoglucanase and exoglucanase.

Finally, EBY100/BGLI strain was included to the optimized minicellulosome system and ethanol production was determined after three-day fermentation in 5

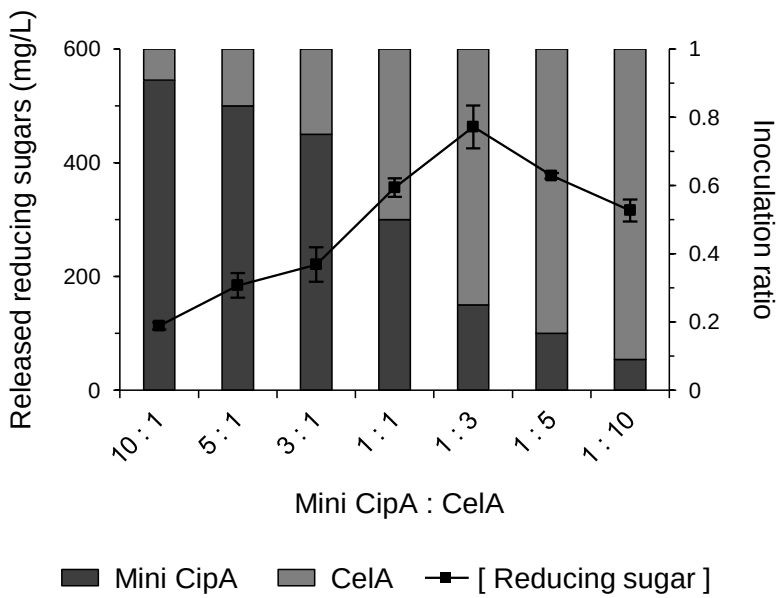

Figure 4.7 The optimal ratio of mini CipA (cohesin) to CelA (dockerin)

CelA was regarded as a representative of total cells harboring dockerin-fused enzymes. EBY100 cells displaying mini CipA and secreting CelA were combined as the indicated ratios, and the released reducing sugars from PASC were detected using the harvested cells.

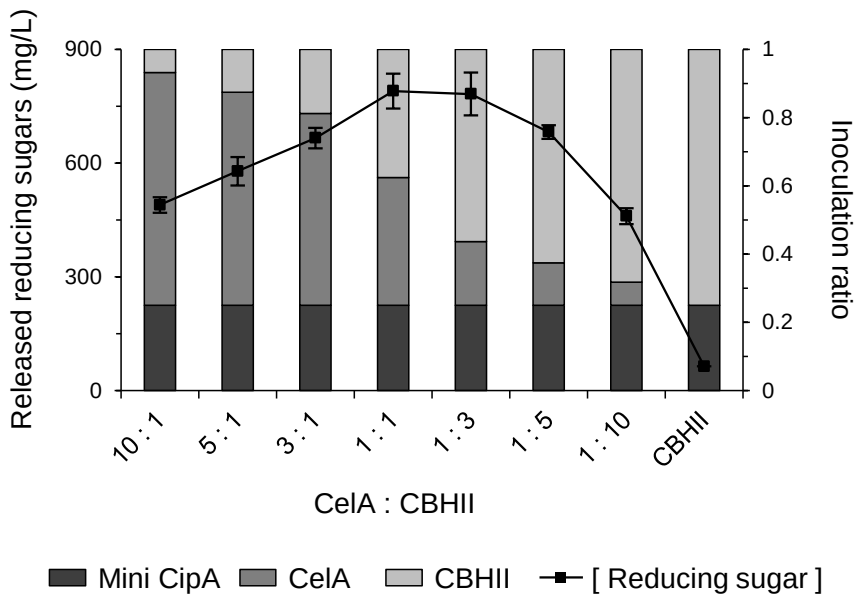

Figure 4.8 The optimal ratio of CelA to CBHII

The optimal CelA:CBHII ratio for PASC hydrolysis was determined while fixing the amount of cells displaying mini CipA as 1/4 of total cells.

mL YP-PASC. Fixing the mini CipA:CelA:CBHII ratio of 2:3:3, EBY100/BGLI strain was added with various ratios. As shown in Fig. 4.9, BGLI:the other cells (mini CipA, CelA, and CBHII) in a ratio of 1:15 produced the highest concentration of ethanol. This result indicates that very small amount of BGLI, compared with other enzymes, is sufficient to hydrolyze the cellodextrins generated by CelA and CBHII. Taken together, the cellulosome activity showed the maximum performance at mini CipA:CelA:CBHII:BGLI in a ratio of 4:6:6:1 (2:3:3:0.53).

The ability of direct ethanol fermentation from PASC was examined using a mixture of cells composed of the optimized ratio and an equal amount of each cell type. The maximum ethanol production was 1.80 g/L after 94 h in a consortium of the optimized ratio, which indicated about 1.2-fold increase compared with a consortium composed of an equal ratio (1.48 g/L) (Fig. 4.10).

4.4. Conclusions

In this chapter, cellulosic ethanol was produced by using a cellulolytic yeast consortium, which is composed of four different yeast strains capable of either displaying a scaffoldin (mini CipA) containing three cohesin domains derived from *C. thermocellum*, or secreting one of the three types of cellulases, *C. thermocellum* CelA containing its own dockerin, *T. reesei* CBHII fused with an exogenous dockerin from *C. thermocellum*, or *A. aculeatus* BGLI. The secreted dockerin-

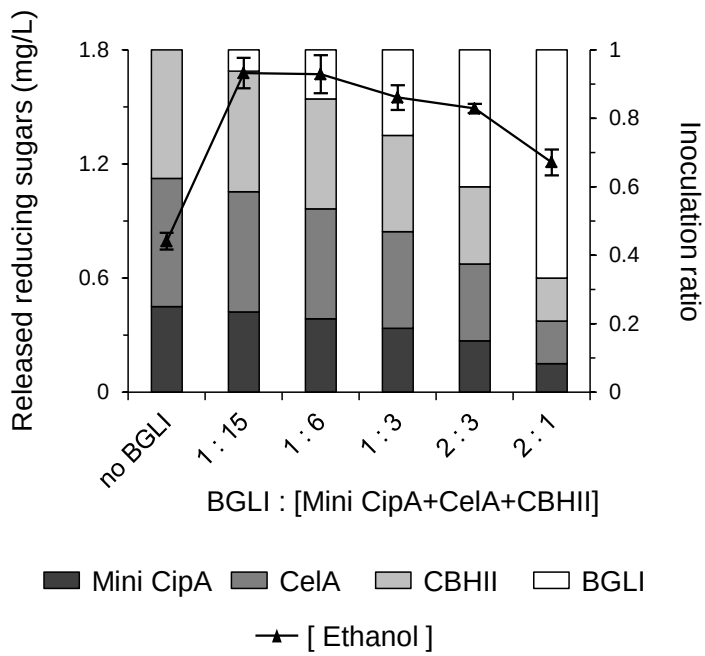

Figure 4.9 The optimal ratio of BGLI to cellulosome for ethanol production

The optimal amount of BGL1 for ethanol production was determined while fixing the mini CipA:CelA:CBHII ratio of 2:3:3. The bar graph represents inoculation portion of cells containing each plasmid. The square line graph represents released reducing sugars from PASC in each ratio. The triangle line graph represents ethanol concentration after three-day fermentation in each ratio.

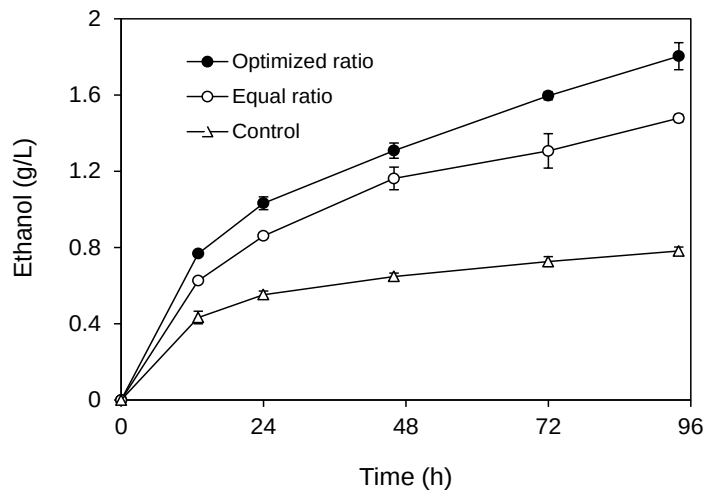

Figure 4.10 Direct fermentation of amorphous cellulose to ethanol

Time course of ethanol production from a yeast consortium composed of the mini CipA:CelA:CBHII:BGLI ratio of 4:6:6:1 (optimized ratio, closed circle) or 1:1:1:1 (equal ratio, open circle), or EBY100 cells containing pCT-mini CipA (control, open triangle).

containing enzymes, CelA and CBHI, were randomly assembled to the surface-displayed mini CipA via cohesin-dockerin interactions. On the other hand, BGLI was independently assembled to the cell surface since it already has a cell adhesion characteristic. The cellulosome activity and ethanol production were optimized by controlling the combination ratio among the four yeast strains. A mixture of cells with the optimized mini CipA:CelA:CBHII:BGLI ratio of 2:3:3:0.53 produced 1.80 g/l ethanol after 94 h, indicating about 20% increase compared with a consortium composed of an equal amount of each cell type (1.48 g/l).

Chapter 5.

Synthetic scaffold based on a cohesin-dockerin interaction for improved production of 2,3-butanediol in *Saccharomyces cerevisiae*

5.1. Introduction

Spatial organization of sequential enzymes in a metabolic pathway enables substrate channeling, which facilitates direct transfer of an intermediate from one enzyme to the next enzyme, while protecting the intermediate from competing reaction pathways or unstable environment. Therefore, substrate channeling has been applied to metabolic engineering to accelerate overall reaction rates [24, 144].

Cellulosome, found on the surface of anaerobic cellulolytic bacteria such as *Clostridium* and *Ruminococcus*, is a multi-enzyme complex composed of structural scaffolds containing cohesin domains and cellulases containing dockerin domains [125, 133]. The cohesin domain binds to the dockerin domain with a high affinity ($Kd < 10^{-11}M$), which is responsible for the assembly of cellulosome complex [145, 146]. The spatial proximity of the tethered cellulases in cellulosome structure provides the efficiency of degrading cellulosic substrate [147]. The high affinity cohesin-dockerin interaction has been widely used not only to express synthetic mini-cellulosomes in heterologous bacteria [72, 148] and yeasts [71, 73, 74, 149], but also for various applications such as protein purification [150, 151], biosensor [152], and construction of static enzyme complexes *in vitro* [153] and on the cell surface [154].

5.2. Construction of substrate channeling modules for substrate channeling in the cytosol of *S. cerevisiae*

In this chapter, inspired by the cellulosome structure, which is one of the natural substrate channeling complexes, cytosolic substrate channeling modules in *S. cerevisiae* was constructed by using the cohesin-dockerin interaction. Scaffold expression vectors, p416GPD-GST-$[Coh]_x$, containing two, three, or seven cohesin domains from *C. thermocellum* CipA, were constructed with N-terminal GST tag (Fig. 5.1A). Dockerin tagging vectors for the expression of metabolic enzymes were constructed by using the dockerin domain of *C. thermocellum* CelS (Fig. 5.1B).

5.3. The assembly of dockerin-tagged proteins to the scaffold

To determine whether these scaffold systems work *in vivo*, the recruitment of a dockerin-tagged enzyme to the cohesin-containing synthetic scaffolds was investigated by *in vivo* GST pull-down assay. Bdh1, a 2,3-butanediol dehydrogenase, was selected for the experiment. A plasmid p415GPD-HA- BDH1-Doc, expressing N-terminal HA-tagged Bdh1 with C-terminal dockerin fusion, was co-transformed into *S. cerevisiae* CEN.PK2-1C strain with a plasmid expressing one of the three GST-tagged scaffolds or GST as a control. Although the expression levels of the GST-tagged scaffold proteins decreased as increasing the number of cohesin domains, HA-Bdh1-Doc was successfully pulled down by GST-

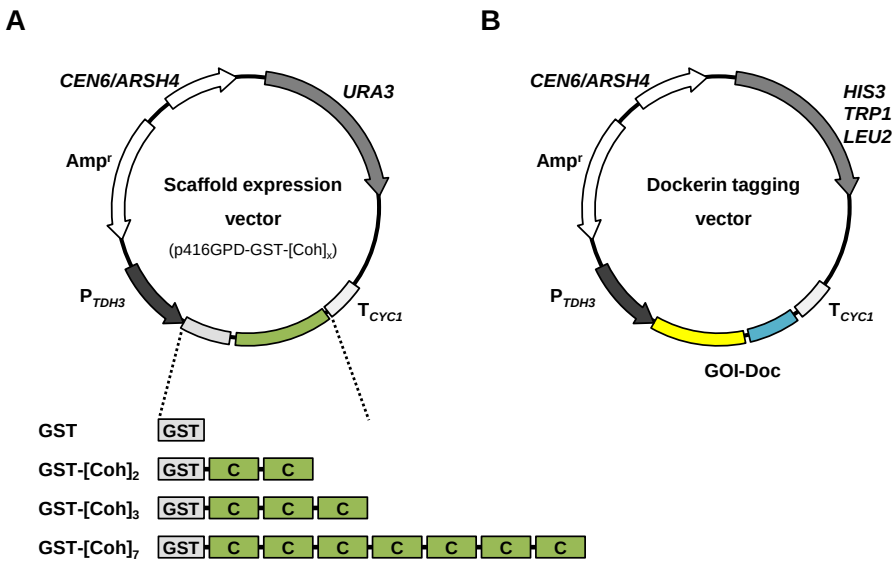

Figure 5.1 Plasmids to generate cohesin-dockerin interaction-based substrate channeling modules

A. Construction of scaffold expression vectors, p416GPD-GST-[Coh]x. A varying number of cohesin domains are from *C. thermocellum* CipA.

B. Construction of dockerin tagging vectors. Dockerin domain from *C. thermocellum* CelS was cloned into p413GPD (*HIS3* marker), p414GPD (*TRP1* marker), or p415GPD (*LEU2* marker) vector. The resulting plasmids were used to clone various gene of interest (GOI) for the expression of GOI-Doc proteins.

tagged scaffolds (Fig. 5.2). However, no interaction was observed with the control GST protein, suggesting that the dockerin domain of HA-Bdh1-Doc interacts specifically with the cohesin domains in the scaffolds *in vivo*. The assembly of multiple dockerin-tagged proteins to the scaffold was further investigated by bimolecular fluorescent complementation (BiFC) assay. Although BiFC assay has been commonly used to visualize a direct interaction between two partner proteins [120, 155], it was used to verify the spatial proximity of the dockerin-tagged proteins formed through their simultaneous binding to a scaffold protein (Fig. 5.3A). Both N-terminal and C-terminal fragment of an YFP variant known as Venus were each fused to a dockerin domain at their C-terminal ends. As shown in Figure 5.3B, the BiFC signals were detected only when the scaffolds were co-expressed. Strong punctate signals were observed with an increase in the number of cohesin domains, suggesting that aggregations might occur among the assembled Venus proteins due to an increase in local protein concentrations. These data demonstrate successful assembly of multiple dockerin-tagged proteins to the cohesin-containing scaffold in yeast cytoplasm. Therefore, this system might be suitable to construct a synthetic substrate channeling pathway in *S. cerevisiae.*

5.4. Substrate channeling effect in 2,3-butanediol synthesis

To demonstrate the feasibility of the synthetic scaffold for substrate channeling, this system was adopted to 2,3-butanediol production in *S. cerevisiae*. 2,3-

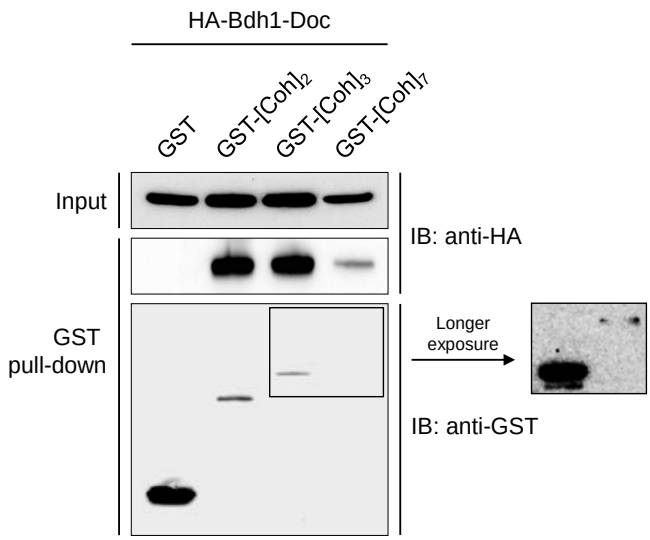

Figure 5.2 *In vivo* GST pull-down assay

CEN.PK2-1C cells were co-transformed with p415GPD-HA-BDH1-Doc and a plasmid expressing GST or one of the scaffold expression vectors. The cell lysates were incubated with glutathione-agarose beads for 3 h at 4ºC. After GST pull-down experiment, the samples were analyzed by immunoblotting (IB) with the indicated antibodies. The right panel represents a longer exposure of the two right lanes.

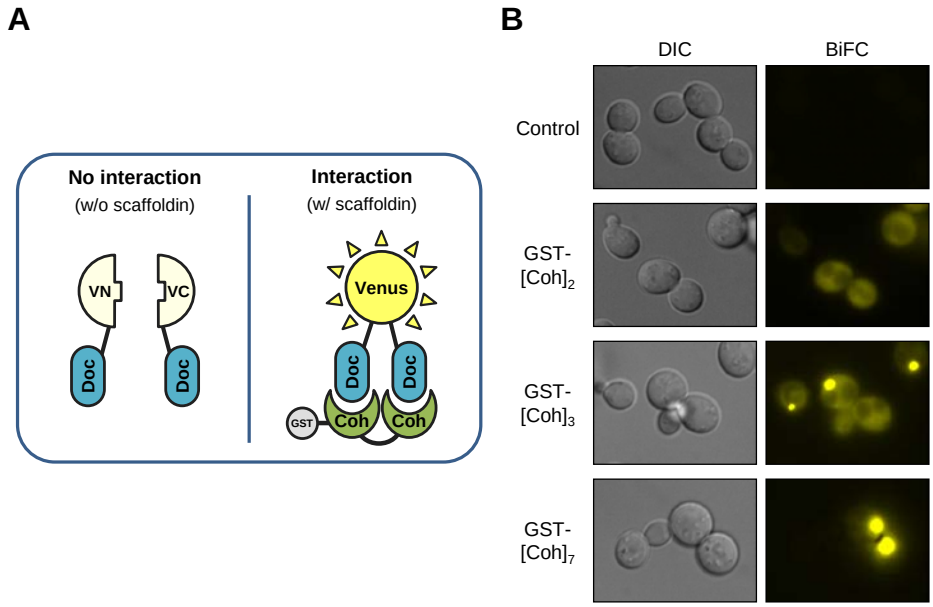

Figure 5.3 Development of a BiFC assay to detect interactions between a synthetic scaffold and dockerin-tagged proteins *in vivo*

A. Schematic diagram representing the BiFC assay. N-terminal Venus fragment (VN) and C-terminal Venus fragment (VC) are each C-terminally tagged with a dockerin domain.

B. BiFC assay monitoring the interaction between the scaffolds and dockerin-tagged proteins in vivo, as evidenced by intense YFP signals only in the presence of the scaffolds.

Butanediol is a promising high-value chemical that can be used in various areas, especially as a platform chemical and a liquid fuel [156]. In spite of the presence of innate pathways to produce 2,3-butanediol from pyruvate [105], the productivity and yield of 2,3-butanediol are extremely poor in wild type *S. cerevisiae* [81, 107]. Recently, a significant increase in 2,3-butanediol titer has been reported by introducing heterologous *alsS* and *alsD* genes from *Bacillus subtilis*, which encode α-acetolactate synthase and α-acetolactate decarboxylase, respectively, as well as overexpressing endogenous *BDH1* [108] (Fig. 5.4A). Therefore, *alsS*, *alsD*, and *BDH1* as C-terminal dockerin fusion proteins were overexpressed to investigate the substrate channeling effect in 2,3-butanediol synthesis. During the fermentation, pyruvate is mainly converted to ethanol via two steps involving pyruvate decarboxylase and alcohol dehydrogenase. Therefore, to increase pyruvate flux to 2,3-butanediol synthesis, *alsS*, *alsD*, and *BDH1* genes were expressed in *adh1Δ* strain, lacking the major alcohol dehydrogenase. The strain overexpressing dockerin-tagged *alsS* and *alsD* (*alsS*-Doc and *alsD*-Doc) produced increased amount of acetoin, confirming that the dockerin-tagged enzymes are functional (Fig. 5.4B, left). Additional overexpression of *BDH1*-Doc decreased acetoin titer, while increasing 2,3-butanediol production by 2-fold, suggesting that the dockerin-tagged Bdh1 is also functional (Fig. 5.4B). Cells overexpressing the dockerin-tagged *alsS*, *alsD*, and *BDH1* in the absence of a scaffold produced 8.0 g/L 2,3-butanediol (Fig. 5.4B, right). The 2,3-butanediol titers were gradually increased as increasing the number of cohesin domains in the co-expressed scaffolds,

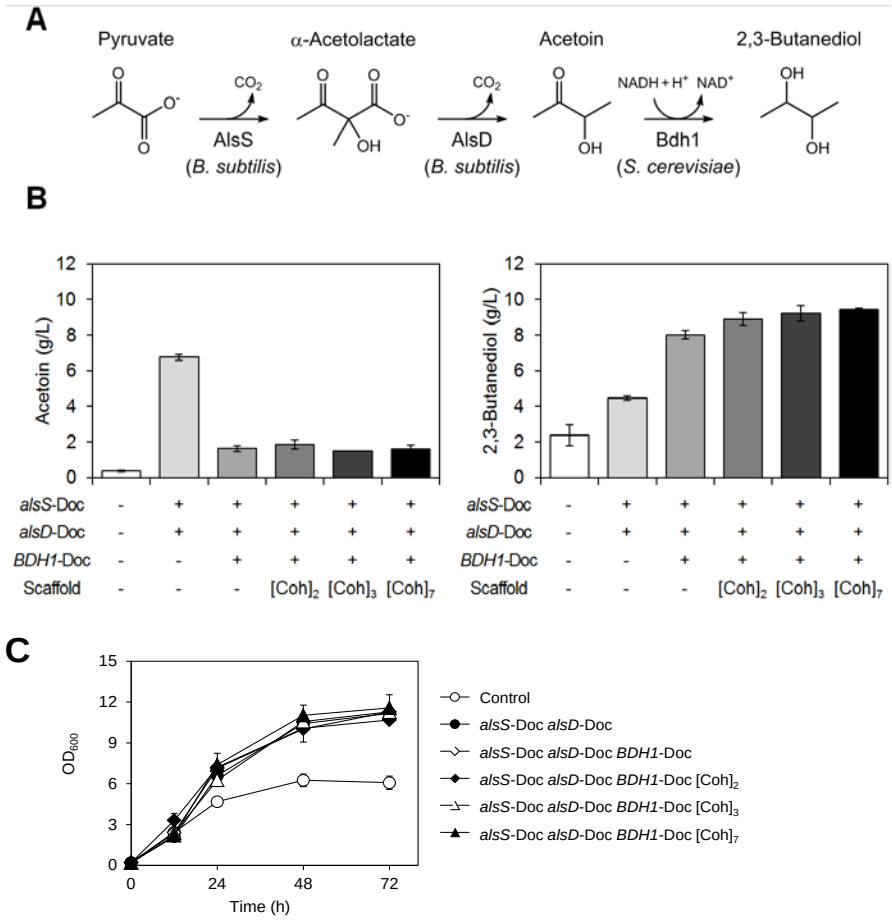

Figure 5.4 Improvement of 2,3-butanediol production by substrate channeling using synthetic scaffolds

A. Metabolic pathway for 2,3-butanediol production. Two molecules of pyruvate are converted to 2,3-butanediol via α-acetolactate and acetoin by the sequential actions of acetolactate synthase (AlsS), acetolactate decarboxylase (AlsD), and 2,3-butanediol dehydrogenase (Bdh1).

B. Acetoin and 2,3-butanediol production titers in scaffold systems after 48 h cultivation in synthetic complete (SC) medium.

C. Cell growth

demonstrating that the assembly of the dockerin-tagged enzymes to the cohesin domains in the synthetic scaffolds provide a substrate channeling effect in the biosynthetic pathway of 2,3-butanediol. The maximum 2,3-butanediol titer was 9.4 g/L after 48 h in the seven-cohesin scaffold system, which indicates about 20% increase compared with the scaffold-free system (Fig. 5.4B, right).

To further prove the effectiveness of our substrate channeling module, 2,3-butanediol production levels in the seven-cohesin scaffold system and the scaffold-free system were compared in fed-batch fermentation with an intermittent feeding of glucose. The seven-cohesin scaffold system produced 29.1 g/L 2,3-butanediol after 100 h, which is a 37% increase compared with that produced in the scaffold-free system (21.2 g/L) (Fig 5.5). These results further support our conclusion that the seven-cohesin scaffold system provide successful substrate channeling effect in 2,3-butanediol biosynthetic pathway. After the second feeding at 58 h, the glucose consumption rate reduced dramatically in the scaffold-free system, whereas it was maintained in the seven-cohesin scaffold system. The *adh1Δ* strain used in this study has a growth defect mainly because of the limited capability of NAD^+ regeneration through alcohol dehydrogenase. Introduction of the NAD^+-generating 2,3-butanediol pathway (Fig. 5.4A) can partly compensate for the NAD^+ limitation in *adh1Δ* strain, resulting in a growth recovery. Therefore, higher levels of 2,3-butanediol production in the presence of the substrate channeling system might provide advantages in cell growth, which can be more prominent in prolonged cultivation with repeated glucose addition.

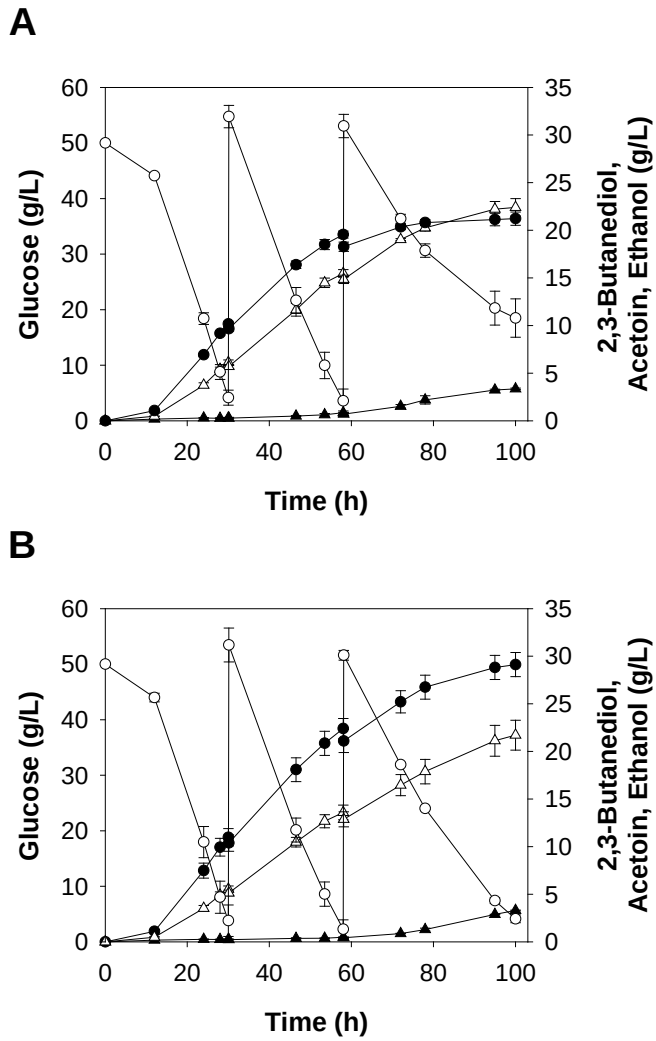

Figure 5.5 2,3-butanediol production in shake flask fed-batch cultivation

Production levels of 2,3-butanediol and other metabolites were measured in shake flask fed-batch culture with an intermittent addition of glucose in a scaffold-free system (A) and a seven-cohesin scaffold system (B). Symbols: glucose (open circle), 2,3-butanediol (closed circle), ethanol (open triangle), acetoin (closed triangle).

5.5. Conclusions

In summary, a cohesin-dockerin interaction-based synthetic scaffold system was newly developed for substrate channeling in *S. cerevisiae*. This system was successfully applied to the improved production of 2,3-butanediol. This is the first time that the interaction between cohesin and dockerin domains was confirmed in yeast cytosol and applied to metabolic engineering. In the case of 2,3-butanediol production using AlsS, AlsD, and Bdh1, this substrate channeling module increased the production titer up to 37%. Since it is reported that the degree of substrate channeling is drastically increased under the conditions of low substrate concentration and low-activity enzymes [157], it is expected that the substrate channeling system would be a more powerful tool for metabolic pathway containing low-activity enzymes. Also, the substrate channeling effect could be further optimized by fine-tuning the expression levels of scaffolds and metabolic enzymes, thus not only increasing the proportion of fully occupied scaffolds, but also adjusting the enzyme ratio participating in the enzyme complex. This system might serve as a platform for additional synthetic biology applications as well as a module for metabolic flux control in metabolic engineering.

Chapter 6.

Redirection of pyruvate flux through metabolite channeling in *Saccharomyces cerevisiae*

6.1. Introduction

In recent decades, metabolic engineering of microbial cells has received a great attention for the production of chemicals, fuels, and pharmaceuticals, as an attractive alternative to chemical synthesis [1, 2] . To achieve high titer and yield of production, both amplification of the metabolic pathway toward desired compound and inhibition of the competing pathways are usually required. To this end, various strategies, including modulation of gene copy number, promoter strength, or ribosome binding sites (RBS), have been used [3-5]. Recently, conditional knockout/down systems were also successfully applied to metabolic engineering [9, 10].

On the other hand, several efforts have been focused on the spatial organization of metabolic enzymes to accelerate intermediate processing. Expression of a fusion protein of 4-coumaroyl-CoA ligase and stilbene synthase in yeast resulted in up to 15-fold increased resveratrol production compared to co-expression of these enzymes [38]. Synthetic protein scaffold was applied to the heterologous mevalonate pathway in *E. coli*, resulting in a 77-fold increase in mevalonate titer with the optimized scaffold architecture [24]. In addition to protein scaffold, RNA- and DNA-based scaffold system have been constructed and used to produce various target products [39, 40]. The strategy of compartmentalization of metabolic pathways to organelle, especially mitochondria using N-terminal targeting sequence, has been also successfully applied to the

production of isobutanol, itaconic acid, and acetoin in *S. cerevisiae*, *Aspergillus niger*, and *Candida glabrata*, respectively [30, 41, 42].

These approaches, including fusion protein, scaffold-based enzyme complex, and localization to subcellular compartments or organelles, lead to substrate channeling effect, which has several potential advantages such as prevention of the loss of intermediates, reduction of the accumulation of toxic intermediates, and protection of unstable intermediates, as well as improved conversion rates.

In the previous chapter, channeling modules were designed based on cohesin-containing scaffolds and dockerin-containing enzymes and the improvement of 2,3-butanediol production was achieved by using this system in *S. cerevisiae*. The aim of this chapter is to test the effect of metabolite channeling on the flux partitioning at a metabolic branch point. Specifically, pyruvate and pyruvate kinase, which catalyzes the conversion of phosphoenolpyruvate (PEP) to pyruvate, the last step of glycolysis, were focused as a target metabolite and key enzyme for channeling. By tethering the pyruvate-converting enzyme to pyruvate kinase (Pyk1) using cohesin-dockerin interaction, pyruvate flux was successfully redirected to desired pathways.

6.2. Construction of PYK1-Coh strain as a platform strain for the channeling of pyruvate flux

Pyruvate is a key metabolite of the central metabolism and serves as an important precursor for biosynthesis of several products such as carboxylic acid, alcohols,

and amino acids. In *S. cerevisiae*, because pyruvate produced by glycolysis is mainly converted to ethanol via acetaldehyde (Fig. 6.1), it is very important to redirect the carbon flux to desired target products from ethanol.

The cohesin-dockerin interaction, found in cellulosome complex, has been demonstrated the feasibility in various applications based on its high affinity, such as protein purification and enzyme immobilization. In this study, this interaction was applied to recruit pyruvate-converting enzymes to a pyruvate-forming enzyme, Pyk1. Although *S. cerevisiae* has another gene encoding pyruvate kinase, *PYK2*, Pyk1 is known as a main pyruvate kinase [158]. To construct PYK1-Coh-Myc strain, expressing Pyk1 as a C-terminally tagged with cohesin domain and Myc epitope tag, chromosomal integration was performed by PCR-mediated homologous recombination and confirmed by PCR amplification. As a control strain, PYK1-Myc strain was also constructed.

6.3. Identification of the interaction between cohesin-fused Pyk1 and dockerin-fused enzyme by co-immunoprecipitation

To ensure the interaction between cohesin and dockerin domains, fused to Pyk1 and a pyruvate-converting enzymes, respectively, co-immunoprecipitation (co-IP) was performed. PYK1-Coh-Myc strain was transformed with p415-HA-Bdh1-Doc or p415-HA-Bdh1, which expressing N-terminal HA-tagged Bdh1 (HA-Bdh1) with or without C-terminal dockerin domain (Doc). As shown in Figure 6.2, HA-Bdh1

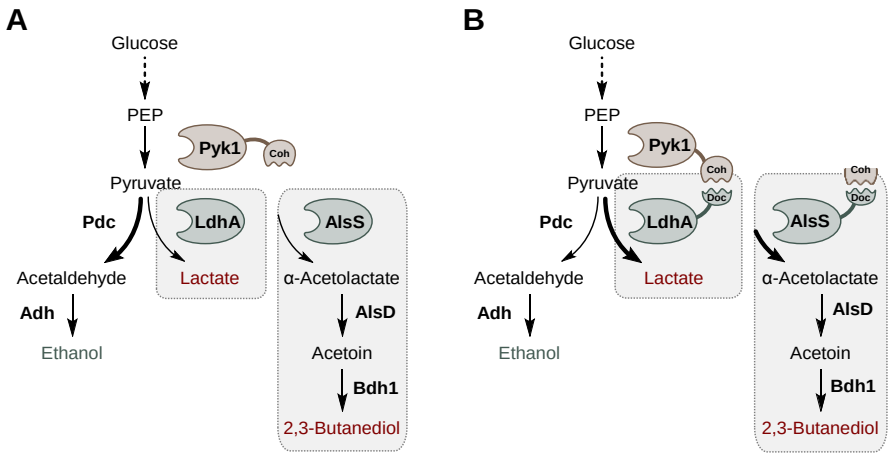

Figure 6.1 Schematic diagram of the overall concept of this chapter

Pyruvate kinase (Pyk1) catalyzes the conversion of phosphoenolpyruvate (PEP) to pyruvate, the last step of glycolysis. Pyruvate is mainly converted to ethanol by the sequential actions of pyruvate decarboxylase (Pdc) and alcohol dehydrogenase (Adh) in *S. cerevisiae*. The PYK1-Coh-Myc strain was constructed as a platform strain for the pyruvate channeling.

A. Overexpression of LdhA for lactate production or AlsS, AlsD, and Bdh1 for 2,3-butanediol production.

B. Overexpression of LdhA-Doc for lactate production or AlsS-Doc, AlsD, and Bdh1 for 2,3-butanediol production. In PYK1-Myc-Coh strain, cohesin-dockerin interaction provides spatial proximity between Pyk1 and the dockerin-tagged enzyme.

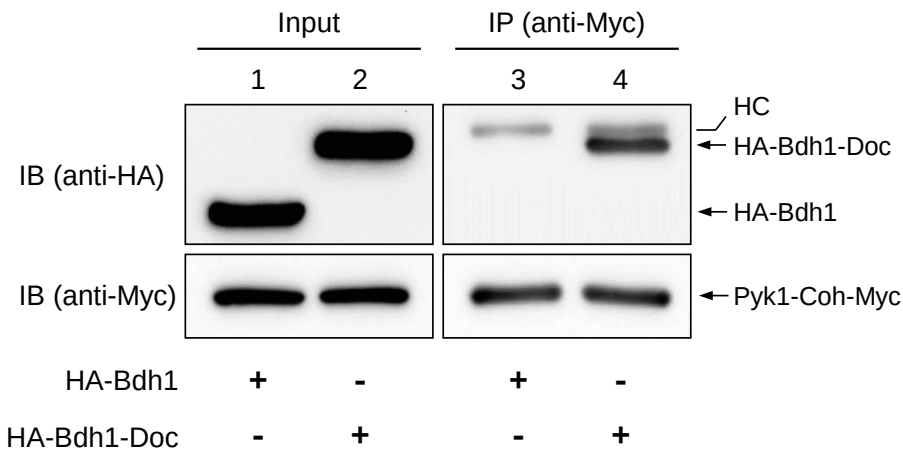

Figure 6.2 Co-immunoprecipitation between Pyk1-Coh-Myc and dockerin-tagged enzyme

Myc-tagged Pyk1 (Pyk1-Coh-Myc) was immunoprecipitated with anti-Myc antibody from PYK1-Coh-Myc strains expressing either HA-Bdh1 (lanes 1 and 3) or HA-Bdh1-Doc (lane 2 and 4). Cell lysates before immunoprecipitation (Input) and immunoprecipitates (IP) were analyzed by SDS-PAGE and immunoblotting (IB) indicated antibodies. HC indicates the position of the heavy chain of the immunoprecipitation antibody (anti-Myc antibody).

with a C-terminal dockerin domain (HA-Bdh1-Doc) was successfully co-precipitated with Pyk1-Coh-Myc, while no interaction was detected between HA-Bdh1 and Pyk1-Coh-Myc protein. These results demonstrate that the dockerin domain of HA-Bdh1-Doc interact specifically with the cohesin domain of Pyk1. Therefore, this approach connecting Pyk1 and to pyruvate-connecting enzymes based on cohesin-dockerin interactions might be able to applied for channeling of pyruvate produced by Pyk1 toward desired products.

6.4. Lactate production using the pyruvate channeling system

In order to test whether co-localization of Pyk1 and pyruvate-converting enzymes through cohesin-dockerin interaction could bring to metabolic channeling of pyruvate to desired metabolic pathways, this system was first adopted to lactate production in *S. cerevisiae*. Although *S. cerevisiae* cannot produce lactate naturally, due to their robust characteristics such as high tolerance to low pH, there are many attempts to engineer *S. cerevisiae* for lactate production by introducing heterologous lactate dehydrogenase.

To produce lactate from pyruvate, lactate dehydrogenase LdhA from *Leuconostoc mesenteroides subsp. mesenteroides* ATCC 8293 was introduced into *S. cerevisiae*. First, the effect of introducing native LdhA into PYK1-Myc or PYK1-Coh-Myc strain was verified. Although the rate of glucose consumption and lactate production in PYK1-Coh-Myc strain were slightly slow than that of PYK1-

Myc strain, the final yields of ethanol and lactate production were almost the same (Fig. 6.3A). Next, substrate channeling effect on pyruvate distribution between lactate and ethanol was investigated by expressing dockerin-tagged LdhA (LdhA-Doc) in PYK1-Myc or PYK1-Coh-Myc strain (Fig. 6.3B). The PYK1-Myc control strain harboring p415G-$LdhA_{Doc}$ produced 4.2 g/L lactate and 18.2 g/L ethanol after 36 h cultivation in SC-Leu medium containing 50 g/L glucose. On the other hand, PYK1-Coh-Myc strain harboring p415G-$LdhA_{Doc}$, exhibited 91% increase in lactate production (8.0 g/L) and 9% decrease in ethanol production (16.5 g/L) compared with the control strain (Fig. 6.3B), demonstrating a successful substrate channeling effect between Pyk1 and LdhA. However, unfortunately, the final titer and yield of lactate were reduced in both strains expressing dockerin-fused LdhA compared with those in the strains expressing native LdhA (Fig 6.3C). This result might be due to the reduced activity of lactate dehydrogenase by tagging with dockerin.

6.5. 2,3-Butanediol production using the pyruvate channeling system

To further confirm the effect of metabolite channeling for pyruvate redistribution, PYK1-Coh-Myc strain was applied to produce 2,3-butanediol (Fig. 6.1). 2,3-Butanediol production from pyruvate using heterologous acetoin production pathway in *S. cerevisiae* has been described previously. In previous chapter, to verify substrate channeling using a protein scaffold, three enzymes converting

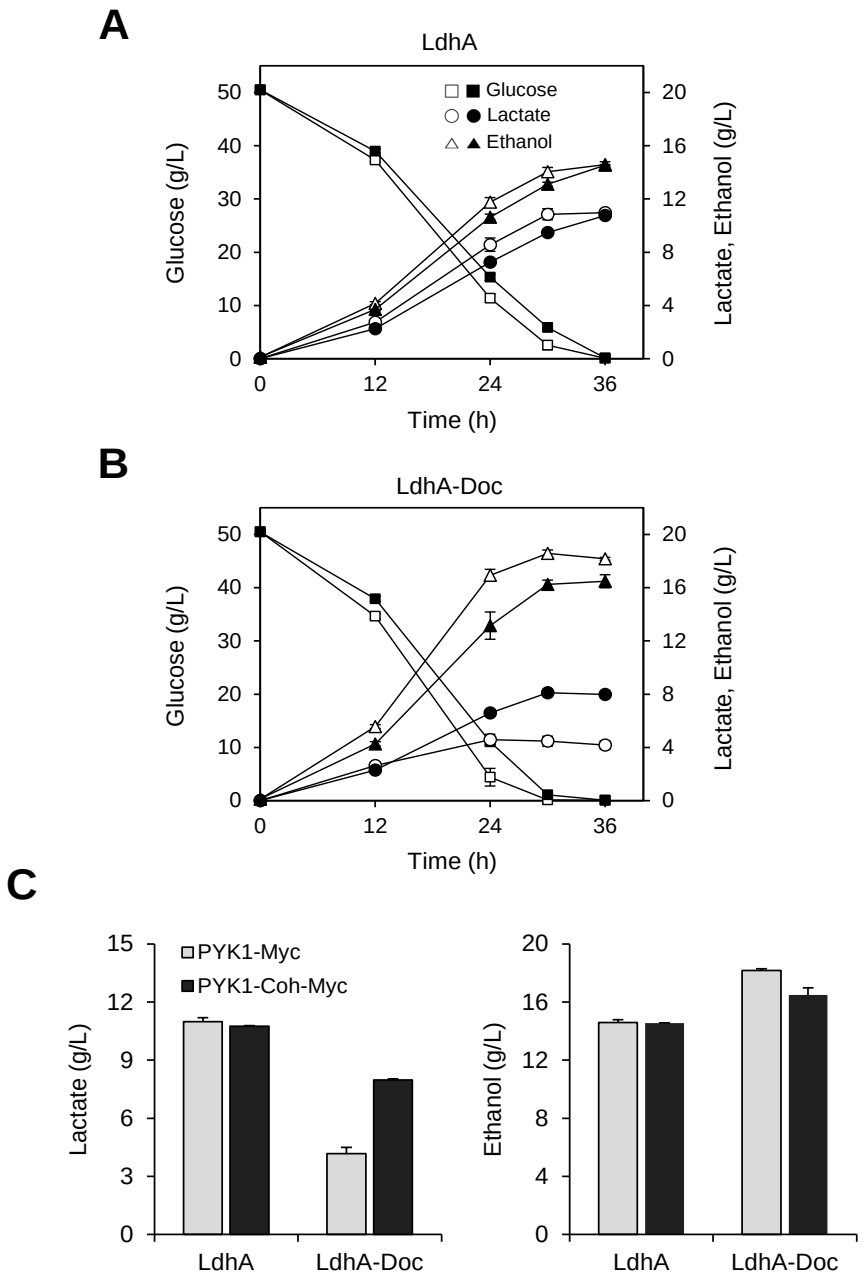
A
LdhA
Glucose
Lactate
Ethanol
Glucose (g/L)
Lactate, Ethanol (g/L)
Time (h)
B
LdhA-Doc
Glucose (g/L)
Lactate, Ethanol (g/L)
Time (h)
C
PYK1-Myc
PYK1-Coh-Myc
Lactate (g/L)
Ethanol (g/L)
LdhA
LdhA-Doc
LdhA
LdhA-Doc

Figure 6.3 The effect of substrate channeling on lactate production

Cells were grown in SC-Leu media containing 50 g/L glucose. Error bars indicate standard deviations of three independent experiments.

A. Fermentation profiles of PYK1-Myc (open symbol) and PYK1-Coh-Myc (closed symbol) strains, both harboring p415G-ldhA.

B. Fermentation profiles of PYK1-Myc (open symbol) and PYK1-Coh-Myc (closed symbol) strains, both harboring p415-ldhA_{Doc}.

C. The bar graphs show the production titers of lactate (left) and ethanol (right) after 36 h fermentation.

pyruvate to 2,3-butanediol including AlsS, AlsD, and BDH1, were expressed as dockerin-fused proteins. Because this study aimed to demonstrate the effect of metabolite channeling on the flux partitioning at a metabolic branch point, acetolactate synthase AlsS was focused as pyruvate converting enzyme. Therefore, AlsS was expressed as dockerin-fusion enzyme that enables its recruitment to Pyk1 via its cohesin domain (Fig. 6.1).

The effect of introducing native AlsS together with AlsD and Bdh1 into PYK1-Myc or PYK1-Coh-Myc strain was tested. As shown in Figure 4A, there were no significant differences between these two strains, including glucose consumption rate and metabolite production patterns. After 30 h fermentation, PYK1-Myc and PYK-Coh-Myc strains overexpressing native AlsS, AlsD, and Bdh1 from p413-SDB plasmid produced nearly the same amount of 2,3-butanediol (9.9 g/L and 10.1 g/L, respectively) and ethanol (8.3 g/L and 8.1 g/L, respectively) (Fig. 6.4A). These metabolites production profiles during fermentation were maintained in PYK1-Myc strain overexpressing dockerin tagged-AlsS, AlsD, and Bdh1 from p413-S_{Doc}DB, which produced 9.8 g/L 2,3-butanediol and 7.9 g/L ethanol after 30 h (Fig. 6.4B). In contrast, PYK1-Coh-Myc strain overexpressing AlsS-Doc, AlsD, and Bdh1 produced 13.6 g/L 2,3-butanediol, which indicates about 38% increase compared with that produced in PYK1-Myc strain. Consistent with this increase in 2,3-butanediol titer, ethanol production decreased by 46% (4.3 g/L after 30 h fermentation). These results demonstrate that the pyruvate flux was successfully redistributed toward 2,3-butanediol through the spatial organization of

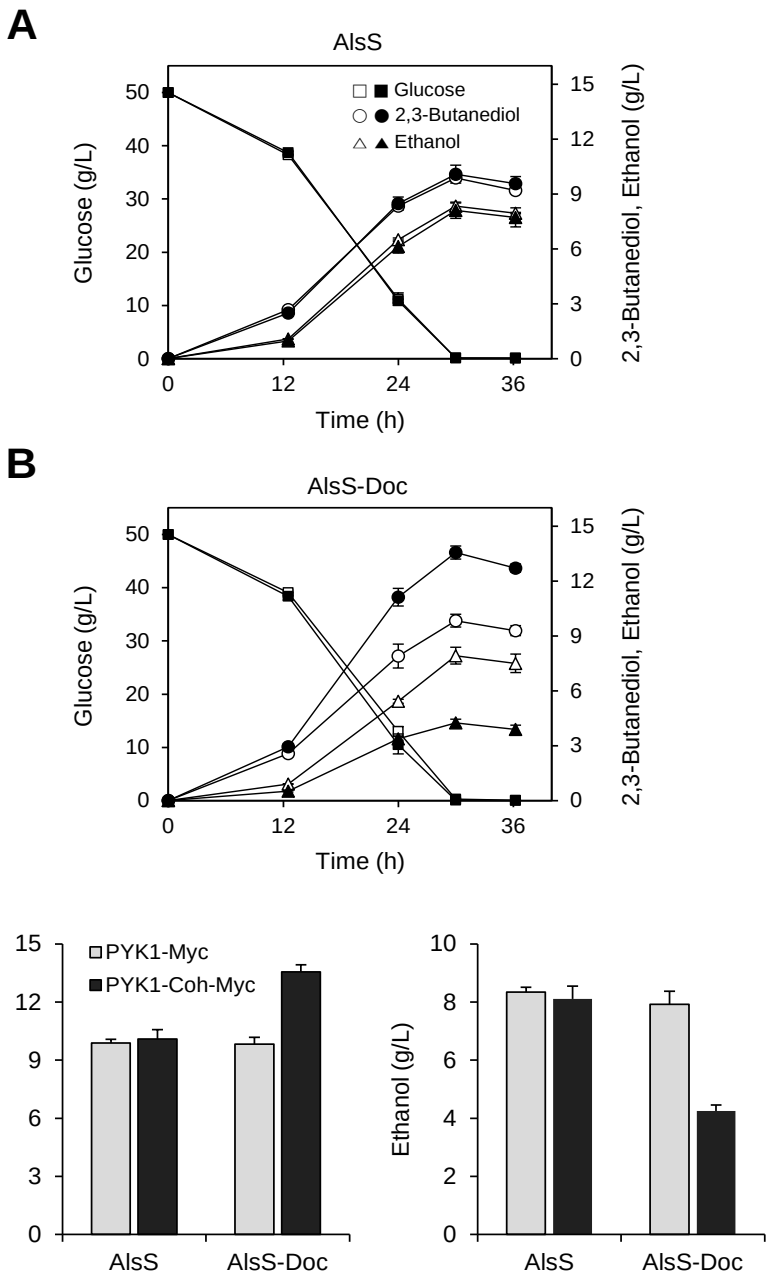
A
AlsS
Glucose
2,3-Butanediol
Ethanol
Glucose (g/L)
2,3-Butanediol, Ethanol (g/L)
Time (h)
B
AlsS-Doc
Glucose (g/L)
2,3-Butanediol, Ethanol (g/L)
Time (h)
C
PYK1-Myc
PYK1-Coh-Myc
2,3-Butanediol (g/L)
Ethanol (g/L)
AlsS
AlsS-Doc
AlsS
AlsS-Doc

Figure 6.4 The effect of substrate channeling on 2,3-butanediol production

Cells were grown in SC-His media containing 50 g/L glucose. Error bars indicate standard deviations of three independent experiments.

A. Fermentation profiles of PYK1-Myc (open symbol) and PYK1-Coh-Myc (closed symbol) strains, both harboring p413-SDB.

B. Fermentation profiles of PYK1-Myc (open symbol) and PYK1-Coh-Myc (closed symbol) strains, both harboring p413-S_{Doc}DB.

C. The bar graphs show the production titers of lactate (left) and ethanol (right) after 30 h fermentation.

Pyk1 and AlsS.

6.6. Conclusions

In this chapter, the effect of metabolite channeling on the flux partitioning at a metabolic branch point was investigated by focusing on pyruvate metabolism in *S. cerevisiae*. As a platform strain for pyruvate channeling, PYK1-Coh-Myc strain was constructed, and the assembly of dockerin-tagged enzymes to cohesin-tagged Pyk1 was confirmed by co-immunoprecipitation assay. In the case of both lactate production and 2,3-butanediol production, pyruvate flux toward the target products was significantly enhanced, coinciding with a decrease in ethanol production. As a result, it has been demonstrated that spatial organization of enzymes located at metabolic branch point could provide competitive advantages over the other pathways, within the frame of metabolite channeling effect.

Chapter 7.

Promoters inducible by aromatic amino acids and γ-aminobutyrate for metabolic engineering applications in *Saccharomyces cerevisiae*

7.1. Introduction

Controlling the expression of genes in metabolic pathways or in regulatory networks is an essential component in metabolic engineering and synthetic biology [2, 43]. Although gene expression can be regulated at multiple points, promoter-driven transcriptional initiation is a key regulatory step in determining gene expression levels and timing [44]. Successful pathway engineering requires diverse range of constitutive and inducible promoters, which allow sophisticated transcriptional regulation of each gene participating in the pathway [44, 45]. Therefore, numerous efforts have been made to isolate native promoters [46, 47] or to develop synthetic promoters suitable for genetic engineering [44, 48-50]

S. cerevisiae is a well-studied eukaryotic model system with great potential as microbial cell factories for the production of fuels and chemicals [20, 159]. Strong constitutive promoters in the glycolytic pathway, P_{TDH3} (also known as P_{GPD}), P_{PGK1}, P_{TPI1}, and P_{PDC1}, and the promoter of translation elongation factor (P_{TEF1}) have been widely used for gene expression in *S. cerevisiae*, along with other weaker constitutive promoters such as P_{CYC1} and P_{ADH1} [45-47, 160]. Although constitutive promoters are convenient to maintain gene expression without additional manipulation, they are not suitable for the metabolic pathway containing toxic intermediates or for the expression of target genes at a specific time point [45]. Inducible or regulated promoters can complement these problems. The galactose-inducible P_{GAL1} and P_{GAL10} promoters have been mostly used in metabolic

engineering applications although other inducible promoters such as P_{CUP1}, P_{PHO5}, and P_{MET25} are also available in *S. cerevisiae* [161-164]. The *GAL* promoters are tightly repressed in the presence of glucose, resulting in about 1000-fold induction by galactose [54, 165]. Recently, a series of synthetic galactose-inducible promoters with higher basal activity and dynamic range of galactose-induced expression levels have been generated by combining various upstream activation sequences (UASs) and core promoter elements [54]. However, the *GAL* promoters have several disadvantages. Because of the glucose repression effect, *GAL* promoters cannot be induced by direct addition of galactose if the culture medium contains glucose [166, 167]. Therefore, complete medium exchange is necessary for cells grown in glucose. In addition, galactose is used not only as an inducer, but also as a carbon source. Since galactose is a less preferred carbon source than glucose, shifting the glucose-grown cells into galactose medium reduces cell growth rate, and the galactose-induced expression levels decrease as galactose is consumed during growth [168].

The *GAL* promoters are activated by Gal4 transcription factor, which belongs to the Zn_2Cys_6 family of fungal-specific transcription factors [169, 170]. These transcription factors form homodimers and each Zn_2Cys_6 domain binds to CGG half sites aligned in various orientations (inverted repeat, $CGGN_xCCG$; everted repeat, $CCGN_xCGG$; direct repeat, $CGGN_xCGG$, and reverse direct repeat, $CCGN_xCCG$) and spacing [169, 170]. Although galactose-dependent activation of Gal4 is mediated by relieving the Gal80-dependent repression of Gal4, other

Zn_2Cys_6 transcription factors are activated by direct binding of specific inducers [169]. For example, proline directly binds and activates Put3 transcription factor, involved in proline utilization [171], and Leu3, involved in branched chain amino acids biosynthesis, is activated by binding of α-isopropylmalate, a pathway-specific intermediate [172, 173]. Therefore, the promoters of other Zn_2Cys_6 family proteins might have the potential to be developed as inducible promoters for genetic engineering applications. When selecting inducible promoters for biotechnological purposes, several factors have to be considered, which include the basal activity and induction fold of the promoter, and the cost and side effects of the inducer [174].

Aro80, a member of Zn_2Cys_6 family, is involved in the utilization of aromatic amino acids as nitrogen sources through transcriptional activation of *ARO9* and *ARO10* in the presence of aromatic amino acids [124, 175]. Aro9 and Aro10 act as transaminase and decarboxylase, respectively, in the degradation of aromatic amino acids through Ehrlich pathway [176]. *ARO9* and *ARO10* genes are also regulated by nitrogen catabolite repression (NCR), thus activated by GATA transcription activators (Gat1 and Gln3) in the absence of good nitrogen sources [124]. However, the availability of aromatic amino acids is the major determinant for the transcriptional activation of these genes [124]. Aro80 is believed to act as a dimer like other Zn_2Cyc_6 family of transcription factors [169]. Aro80 binding site consists of two CCG direct repeats separated by 7 base pairs ($CCGN_7CCG$), and the binding sites are repeated twice in the promoters of *ARO9* and *ARO10*,

allowing binding of up to two Aro80 dimers. *S. cerevisiae* genome contains two additional genes containing Aro80 binding sites; *ARO80* itself and *ESBP6* encoding a protein homologous to a monocarboxylate permease [177]. However, these genes, containing only one copy of the $CCGN_7CCG$ element in their promoters, are largely insensitive to the induction by aromatic amino acids [124].

In this chapter, Aro80 binding site was used to design promoters inducible by aromatic amino acids. A wide range of tryptophan-induced expression levels could be achieved by modulating the number of Aro80 binding sites, plasmid copy numbers, and the concentrations of inducer. The effectiveness of the tryptophan-inducible promoters was demonstrated by applying this promoter system to express heterologous genes for the production of acetoin in *S. cerevisiae*. In addition, the possibility of using γ-aminobutyrate (GABA)-inducible *UGA4* promoter for metabolic engineering was also demonstrated. The *UGA4* promoter is regulated by Uga3, another member of the Zn_2Cyc_6 family of transcription factors.

7.2. Construction of aromatic amino acids-inducible synthetic promoters

The possibility of using Aro80 binding site to design synthetic promoters inducible by aromatic amino acids was investigated. *ARO80* and *ARO9* promoters contain two and four CCG repeats, respectively, and the binding of Aro80 to these promoters has been confirmed by chromatin immunoprecipitation assays [124].

However, aromatic amino acids induce transcription of only *ARO9*, but not *ARO80* [124]. Therefore, it was hypothesized that the number of Aro80 binding site in the promoter might affect the inducibility by aromatic amino acids. To prove this, one or two CCG half sites were fused to the native *ARO80* promoter consisting of UAS_{ARO80} (U_2) and the core promoter (C_{ARO80}), generating U_3C_{ARO80} and U_4C_{ARO80} (Fig. 7.1). The synthetic promoters were fused to an EGFP reporter gene, and then cloned into p416, a CEN/ARS-based low copy number plasmid vector containing *CYC1* terminator, to test tryptophan-dependent transcriptional induction. However, the addition of more Aro80 binding sites to the *ARO80* promoter failed to induce transcriptional activation in the presence of tryptophan (Fig. 7.2). On the contrary, when the same Aro80 binding sites were fused to the *ARO9* core promoter (C_{ARO9}), the transcription of EGFP was induced by tryptophan depending on the increasing number of Aro80 binding sites, without affecting the basal expression levels (Fig. 7.2). The U_4C_{ARO9} promoter showed about 20-fold induction after the treatment of 200 μg/mL tryptophan for 1 h. These results suggest that tryptophan-inducible synthetic promoters with different induction folds can be constructed by controlling the number of CCG repeating units, but the core promoter region also plays an important role for the transcriptional activation by Aro80. It needs further studies to elucidate which features of the *ARO80* core promoter prevent the Aro80-dependent activation. Next, the effects of different aromatic amino acids on the induction of the U_4C_{ARO9} promoter were investigated by measuring EGFP fluorescence intensities. Although all three aromatic amino acids induced EGFP

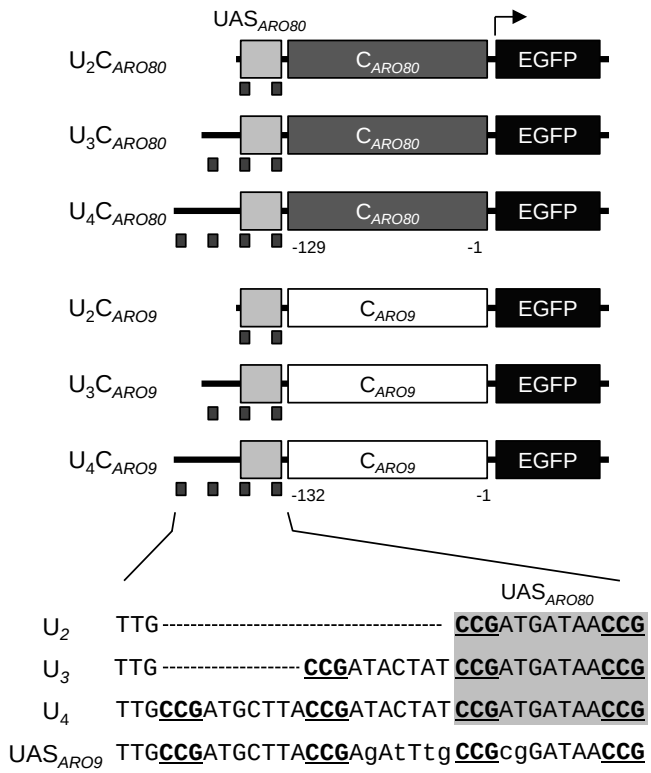

Figure 7.1 Construction of promoters inducible by aromatic amino acids

The promoter constructs contain core promoter region and additional upstream activating sequences (UAS). The EGFP gene was used as a reporter. The sequence details of UAS elements are shown below. CCG triplets, the binding sites of Aro80, are underlined. UAS$_{ARO9}$ is upstream activating sequence of native *ARO9* promoter and the sequences different from the synthetic UAS are represented in lowercase letters.

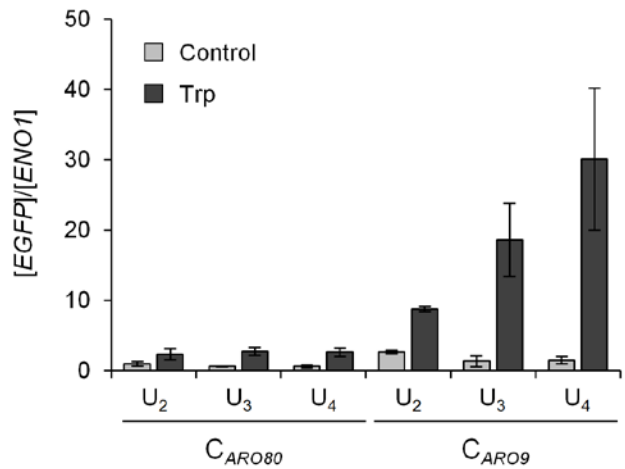

Figure 7.2 Tryptophan-dependent induction of synthetic promoters

Cells harboring p416-based plasmid expressing EGFP from the indicated promoter elements were treated with 200 μg/mL tryptophan for 1 h, and the EGFP mRNA levels were determined by qRT-PCR normalized to *ENO1*. Error bars represent standard deviation from triplicates.

expression, tyrosine was

less effective than tryptophan and phenylalanine (Fig. 7.3A). Moreover, because of its low solubility (< 0.5 g/L), tyrosine might not be suitable as a practical inducer of the U_4C_{ARO9} promoter. The EGFP expression levels decreased after 13 h of induction, which might reflect the degradation or utilization of the inducers. Although tryptophan exerted a little lower induction fold (8.1-fold) than did phenylalanine (9.1-fold) up to 4 h, tryptophan served as a better inducer than phenylalanine after 13 h. Note that since 200 μg/mL amino acids were used, the molar concentration of phenylalanine (1.21 mM) is slightly higher than that of tryptophan (0.98 mM). In the case of tryptophan, its degradation product tryptophol is also known as an activator of Aro80, which might be in part responsible for the longer induction period in the presence of tryptophan. Because the U_4C_{ARO9} promoter sequence is very similar to that of the native *ARO9* promoter (P_{ARO9}) (Fig. 7.1), the inducibility of P_{ARO9} by aromatic amino acids was also investigated. As expected, the aromatic amino acids-dependent induction pattern of the P_{ARO9} promoter was comparable to that of the U_4C_{ARO9} promoter (Fig. 7.3B).

It was also tested whether further addition of Aro80 binding sites to the native *ARO9* promoter can enhance the tryptophan-dependent induction levels. However, fusion of additional two or four half sites to the upstream of USA_{ARO9} rather reduced transcription levels in the presence of tryptophan (data not shown). Therefore, for Aro80-dependent activation, most efficient activation seems to be achieved by binding of two Aro80 dimers.

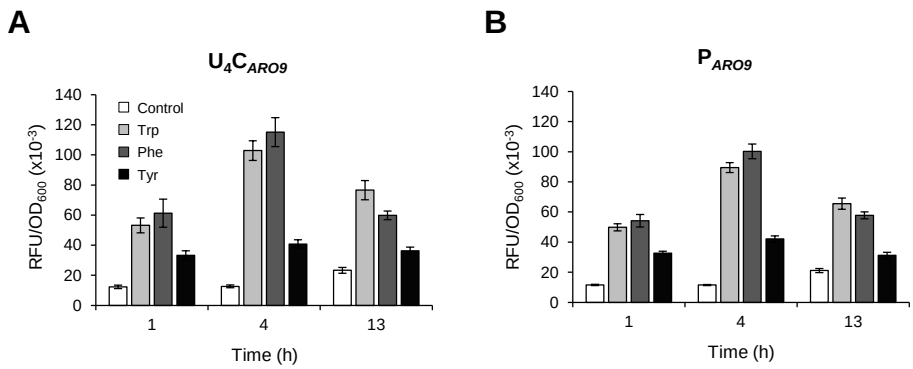

Figure 7.3 Effect of different aromatic amino acids on EGFP expression levels from the U_4C_{ARO9} promoter and the native *ARO9* promoter

Cells harboring p416[U_4C_{ARO9}]-EGFP (A) or p416[P_{ARO9}]-EGFP (B) were treated with 200 μg/mL tryptophan (Trp), phenylalanine (Phe), or tyrosine (Tyr) for the indicated time period, and the fluorescence intensities (RFU) were detected and normalized to the cell densities (OD_{600}).

7.3. Regulation of tryptophan-induced expression levels by plasmid copy numbers and tryptophan concentrations

Next, tryptophan-induced expression levels from the U_4C_{ARO9} promoter was examined depending on various tryptophan concentrations and plasmid copy numbers. Cells harboring low copy number plasmid, p416[U_4C_{ARO9}]-EGFP or high copy number plasmid, p426[U_4C_{ARO9}]-EGFP were treated with 50 to 800 μg/mL tryptophan, and transcription and protein expression levels were determined by qRT-PCR and fluorescence detection, respectively. The EGFP mRNA levels were gradually increased depending on tryptophan concentrations, resulting in up to 20- and 15-fold induction levels in low and high copy number plasmids, respectively, compared with each uninduced control (Fig. 7.4A). Because of the leaky basal expression from the U_4C_{ARO9} promoter, both uninduced and induced EGFP mRNA levels expressed from high copy number plasmid were about 10 to 15-fold higher than those expressed from low copy number plasmid. The activities of commonly used constitutive promoters, P_{ADH1} (in p416ADH-EGFP) and P_{TDH3} (in p416GPD-EGFP), were not affected by tryptophan. The U_4C_{ARO9}-controlled tryptophan-induced expression levels were comparable to the P_{ADH1}-driven expression levels when expressed from low copy number plasmid.

The EGFP protein expression levels detected by fluorescence intensities reflected the transcription induction patterns (Fig. 7.4B). Cells harboring p416[U_4C_{ARO9}]-EGFP plasmid showed a gradual increase in fluorescence

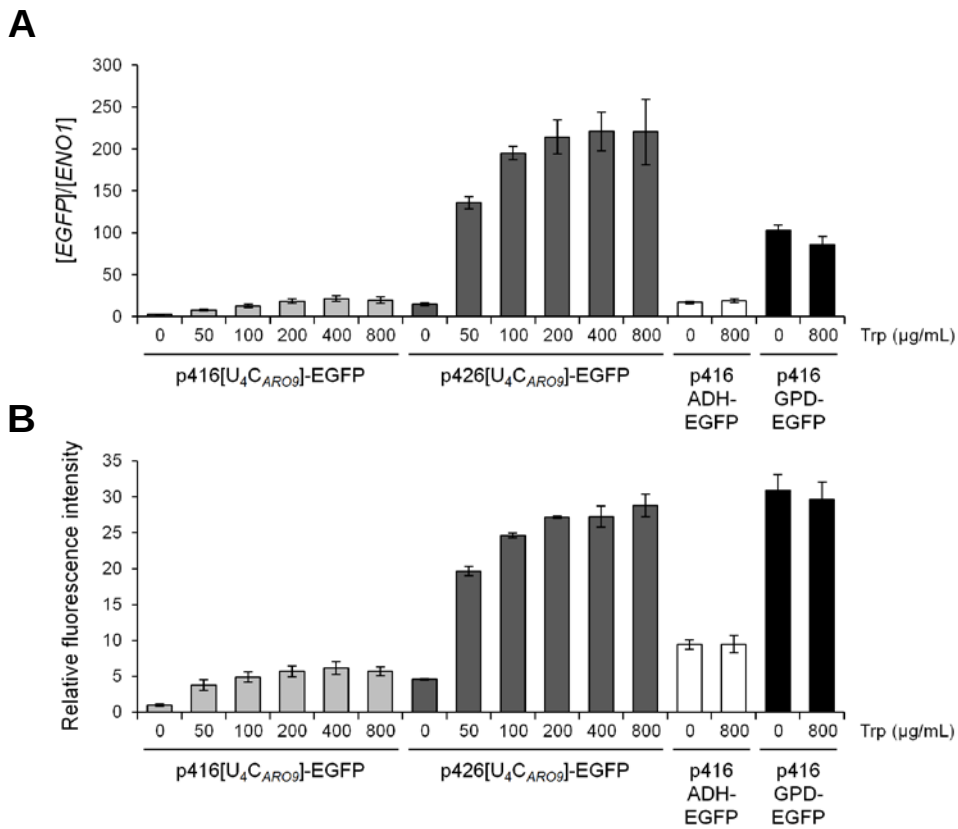

Figure 7.4 Effect of plasmid copy numbers and tryptophan concentrations on EGFP expression levels from the U_4C_{ARO9} promoter

Cells harboring the indicated plasmids were treated with the indicated concentrations of tryptophan for 1 h, and transcription and protein levels of EGFP were investigated. The constitutive promoters, P_{ADH1} and P_{TDH3}, were used as controls.

A. EGFP mRNA levels were determined by qRT-PCR normalized to *ENO1*. Error bars represent standard deviation from triplicates.

B. The RFU/OD_{600} value was normalized to that of untreated cells harboring p416[U_4C_{ARO9}]-EGFP, and represented as relative fluorescence intensity.

intensities as increasing tryptophan concentrations from 50 to 800 μg/mL with a maximum induction fold of 6 (Fig. 7.4B). Expression of [U_4C_{ARO9}]-EGFP from high copy number plasmid resulted in about 5-fold higher uninduced and induced expression levels, while keeping the tryptophan concentration-dependent induction profile (Fig. 7.4B). By using these two vectors and different tryptophan concentrations, a 29-fold range of expression levels could be achieved from the U_4C_{ARO9} promoter. Taken together, a wide range of tryptophan-inducible promoter strengths can be obtained by modulating the number of Aro80 binding sites, plasmid copy numbers, and tryptophan concentrations, thereby enabling the fine-tuning of transcription levels for metabolic engineering applications.

7.4. Acetoin production by using the U_4C_{ARO9} promoter

To verify the effectiveness of the tryptophan-inducible promoters in metabolic engineering, this system was applied to the biosynthetic pathway of acetoin, a potential high-value platform chemical for a broad range of applications such as food, flavor, and pharmaceutical industries [178]. For effective production of acetoin from pyruvate, a heterologous pathway consisting of acetolactate synthase (AlsS) and acetolactate decarboxylase (AlsD) from *Bacillus subtilis* were introduced into *S. cerevisiae*. Also, endogenous *BDH1* gene, encoding 2,3-butanediol dehydrogenase, was deleted to prevent the formation of 2,3-butanediol from acetoin (Fig. 7.5A).

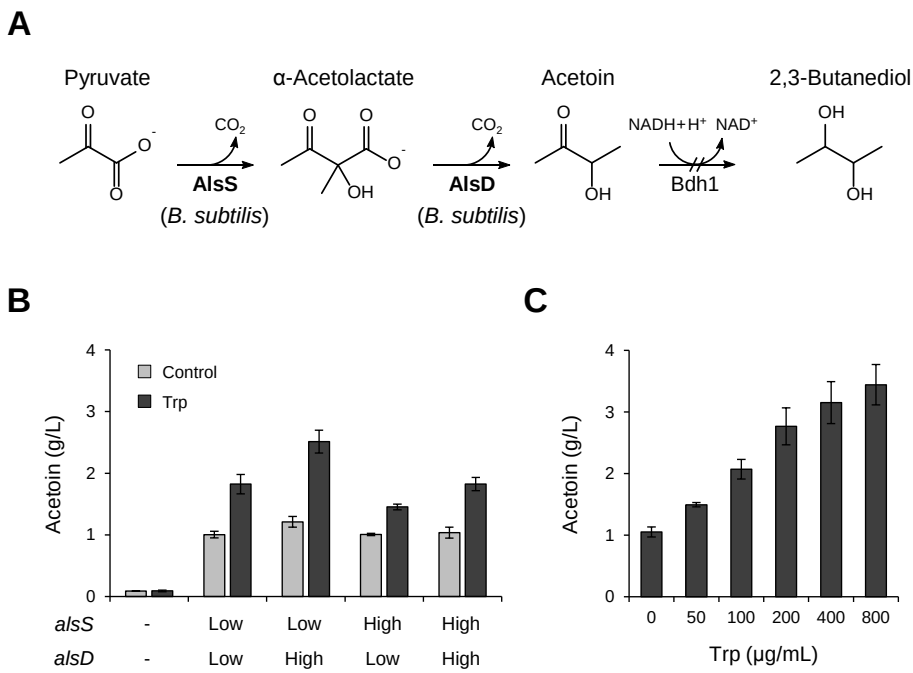

Figure 7.5 Application of the U_4C_{ARO9} promoter to metabolic engineering for acetoin production

A. Metabolic pathway for acetoin production. Two molecules of pyruvate are converted α-acetolactate by acetolactate synthase (AlsS), and then acetolactate decarboxylase (AlsD) converts α-acetolactate to acetoin. To block the 2,3-butanediol production from acetoin, *BDH1* gene encoding 2,3-butanediol dehydrogenase was deleted.

B. Cells carrying alsS expression vector, p413[U_4C_{ARO9}]-alsS (Low) or p423[U_4C_{ARO9}]-*alsS* (High), and *alsD* expression vector, p415[U_4C_{ARO9}]-*alsD* (Low) or p425[U_4C_{ARO9}]-*alsD* (High), in four different combinations were grown for 48 h in the absence or presence of 200 μg/mL tryptophan, and acetoin production levels were monitored.

C. Acetoin production depending on tryptophan concentrations in cells harboring p413[U_4C_{ARO9}]-*alsS* and p425[U_4C_{ARO9}]-*alsD*.

The *alsS* and *alsD* genes were expressed under the control of U_4C_{ARO9}, and the required balance between AlsS and AlsD was simply tested by cloning the genes into both low copy number (p413 or p415) and high copy number (p423 or p425) plasmids, and examining acetoin production levels in cells harboring four different combinations of plasmid types (Fig. 7.5B). In the presence of 200 μg/mL tryptophan, cells expressing *alsS* from low copy number plasmid (p413) and *alsD* from high copy number plasmid (p425), produced 2.5 g/L acetoin after 48 h, the highest concentration among the four combinations. Expressing both *alsS* and *alsD* from high copy number plasmids did not give the best result, exemplifying the importance of regulating and balancing gene expression levels in pathway engineering. Because of the basal activity of the U_4C_{ARO9} promoter, lower levels of acetoin production were also observed even in the absence of tryptophan (Fig. 7.5B). The acetoin titers increased gradually as increasing tryptophan concentrations, faithfully reflecting the tryptophan concentration-dependent increase in U_4C_{ARO9} promoter activity (Fig. 7.5C). As a result, up to 3.4 g/L acetoin was produced in the presence of 800 μg/mL tryptophan. Although promoters stronger than the U_4C_{ARO9} promoter could be more effective in maximizing acetoin production levels, these results demonstrate the usefulness of the tryptophan-inducible promoter in modulating metabolic flux simply by changing the concentrations of tryptophan.

7.5. Application of the GABA-inducible *UGA4* promoter to metabolic engineering

Since it was demonstrated that Aro80-dependent transcriptional regulation can be successfully used to design novel inducible promoters, other Zn_2Cys_6 family member of transcription factors, which are regulated by inducers suitable for genetic engineering, was investigated. Uga3 transcription factor is involved in the utilization of GABA as a nitrogen source by activating transcription of *UGA1*, *UGA2*, and *UGA4* genes in response to GABA [179-182]. In the *UGA4* promoter, the region from -404 to -386 was identified as UAS_{GABA} [180, 182], where CGG half sites are aligned in everted orientation ($CCGN_4CGG$) (Fig. 7.6A). It has been known that Uga3-dependent activation of UAS_{GABA} requires Uga35, another Zn_2Cys_6 protein with a pleiotropic function [183].

Therefore, it was investigated whether the GABA-inducible *UGA4* promoter can be applied to metabolic engineering for acetoin production. The *alsS* and *alsD* genes were expressed under the control of *UGA4* promoter (-460 to -1) from low copy number plasmid and high copy number plasmid, respectively. Cells harboring the two plasmids produced 0.1 g/L acetoin in the absence of GABA (Fig. 7.6B), which is about 10-fold lower than that produced in cells expressing *alsS* and *alsD* from the U_4C_{ARO9} promoter (Fig. 7.5C). Accordingly, the *UGA4* promoter might have a lower basal activity than that of U_4C_{ARO9} under our experimental conditions. However, acetoin production increased in correlation to GABA concentrations,

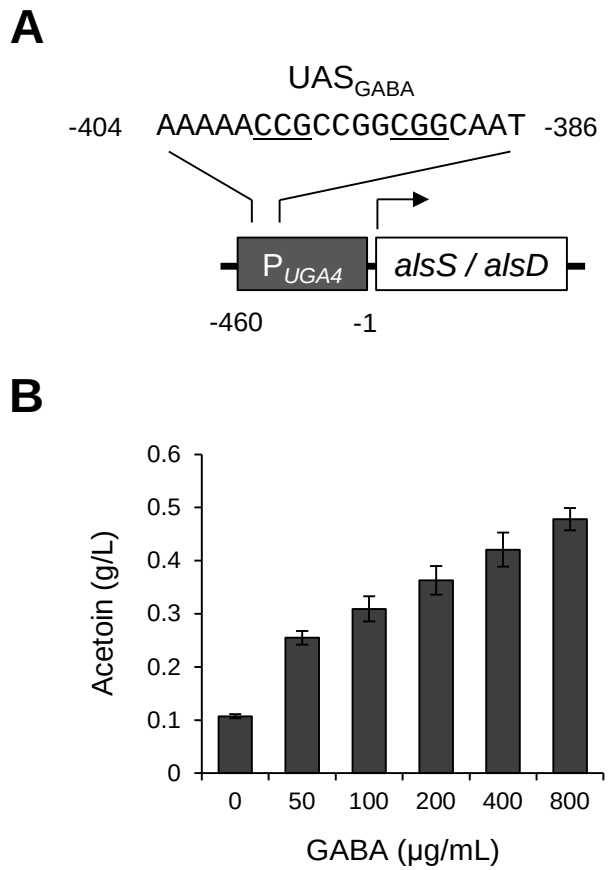

Figure 7.6 Application of GABA-inducible *UGA4* promoter for acetoin production

A. Construction of GABA-inducible system for acetoin production.

B. Cells harboring p413[P_{UGA4}]-*alsS* and p425[P_{UGA4}]-*alsD* were tested for acetoin production depending on GABA concentrations.

resulting up to 5-fold increase in acetoin titer in the presence of 800 μg/mL GABA. These results demonstrate that GABA can be used as a dose-dependent modulator of the *UGA4* promoter activity in metabolic engineering.

7.6. Conclusions

Promoters, the key determinants of transcriptional initiation, are essential components for controlling gene expression in metabolic engineering and synthetic biology [44, 174]. In this chapter, it was demonstrated that promoters regulated by Aro80 transcription factor can be used as tryptophan-inducible promoters for pathway engineering in *S. cerevisiae*. The tryptophan-induced expression levels can be modulated by changing the number of Aro80 binding sites, plasmid copy numbers, and the concentrations of inducer, providing a dynamic range of promoter strengths available for fine-tuning gene expression levels for pathway optimization. Furthermore, it was shown that GABA-inducible *UGA4* promoter, regulated by Uga3, can also be used in metabolic engineering.

Taken together, tryptophan- and GABA-inducible promoters were newly introduced as useful tools for metabolic engineering in *S. cerevisiae*. The wide range of controllable expression levels of these promoter systems might contribute to fine-tuning gene expression levels and timing for the pathway optimization.

Chapter 8.

Efficient production of 2,3-butanediol in *Saccharomyces cerevisiae* by eliminating ethanol and glycerol production and redox rebalancing

8.1. Introduction

Recently, microbial production of 2,3-butanediol has attracted great attention because of its extensive industrial applications as a platform chemical for the production of various derivatives such as 1,3-butadiene, methyl ethyl ketone (MEK), and diacetyl [103]. Many bacterial species, including *Klebsiella pneumonia*, *Klebsiella oxytoca*, and *Enterobacter aerogenes*, can produce 2,3-butanediol efficiently with high titer and productivity [81]. In these bacteria, two molecules of pyruvate are condensed to α-acetolactate by α-acetolactate synthase, and then α-acetolactate is further converted to acetoin through two different routes; direct conversion to acetoin by α-acetolactate decarboxylase or spontaneous decarboxylation to diacetyl, followed by conversion of diacetly to acetoin by diacetyl reductase. Finally 2,3-butanediol dehydrogenase catalyzes the reduction of acetoin to 2,3-butanediol. However, because of the potential pathogenicity of these native producers, 2,3-butanediol production using these bacteria has been considered unsuitable for industrial-scale fermentation [81, 103].

In this context, several efforts have been made to produce 2,3-butanediol in *S. cerevisiae* which is generally recognized as safe (GRAS) and widely used for the production of various chemicals and fuels because of its high tolerance to alcohols and harsh industrial conditions [11, 64-66].

Because *S. cerevisiae* has a strong tendency towards ethanol fermentation, it is essential to reduce ethanol production and redirect this metabolic flux to 2,3-

butanediol for high-yield production. Ethanol is produced from pyruvate via two steps, which consist of decarboxylation of pyruvate to acetaldehyde by PDC, and reduction of acetaldehyde to ethanol by alcohol dehydrogenase (ADH). Therefore, both PDC and ADH have been attractive disruption targets for 2,3-butanediol production in *S. cerevisiae*. In a previous study, deletion of *ADH1*, *ADH3*, and *ADH5* genes resulted in increased 2,3-butanediol production (2.29 g/L) with a yield of 0.113 g/g glucose under anaerobic condition [107]. Introduction of heterologus pathway consisting of α-acetolactate synthase (AlsS) and α-acetolactate decarboxylase (AlsD) from *B. subtilis* and endogenous Bdh1 to an evolved PDC-deficient strain led to successful production of 2,3-butanediol (96.2 g/L) with a high yield and productivity (0.28 g/g glucose and 0.39 g/(L·h), respectively) in fed-batch fermentation [108]. Although ethanol production can be completely eliminated by deleting *PDC1* and *PDC5* genes or all PDC genes (*PDC1*, *PDC*5, and *PDC6*), the resulting PDC-deficient strains have severe growth defects on glucose as a sole carbon source and require C_2 compounds such as acetate or ethanol for growth [15, 109]. Therefore, adaptively evolved PDC-deficient strains overcoming these defects have been used for metabolic engineering applications [108, 110-112]. Yeast strains producing 2,3-butanediol from xylose, galactose, or cellobiose apart from glucose, have also been developed [111, 113, 114].

It is also important to reduce or eliminate glycerol accumulation in terms of the efficient utilization of carbon source, because glycerol is one of the major products in *S. cerevisiae*. Especially, it has been reported that glycerol is further

accumulated by disrupting ADH activity due to the increased demand for NAD^+ regeneration [184]. Glycerol is produced from dihydroxyacetone phosphate (DHAP) by glycerol-3-phosphate dehydrogenase and glycerol-3-phosphatase (Fig. 8.1). *S. cerevisiae* has two isoforms of NAD^+-dependent glycerol-3-phosphate dehydrogenase, Gpd1 and Gpd2, which catalyze the reduction of DHAP to glycerol-3-phosphate (G3P) [185, 186] (Fig. 8.1). In spite of the same catalytic function with similar kinetics, Gpd1 and Gpd2 are known to serve distinct physiological roles attributed by different transcriptional regulation [65]. Gpd1 is responsible for osmotic stress-induced glycerol production, whereas Gpd2 is involved in redox regulation. A number of studies have attempted to reduce glycerol formation for the production of ethanol, succinic acid, and lactic acid by deleting *GPD1* or/and *GPD2*, replacing the promoter sequences of *GPD1* and *GPD2* to the lower strength promoters, or deleting *FPS1*, which encodes a plasma membrane transporter of glycerol [187-190].

Redox cofactors, especially NAD^+/NADH pair, play an essential role in cellular metabolism by participating in a large number of biochemical reactions [191, 192]. Consequently, changes in cellular redox status, such as the ratio between NAD^+ and NADH, lead to widespread effects on metabolic network. Therefore, maintaining redox balance is not only a fundamental requirement for sustained cellular metabolism and cell growth, but also an important strategy for metabolic engineering [193]. Metabolic cofactor imbalance caused by pathway engineering can be restored through removal of excess cofactor by enzymatic

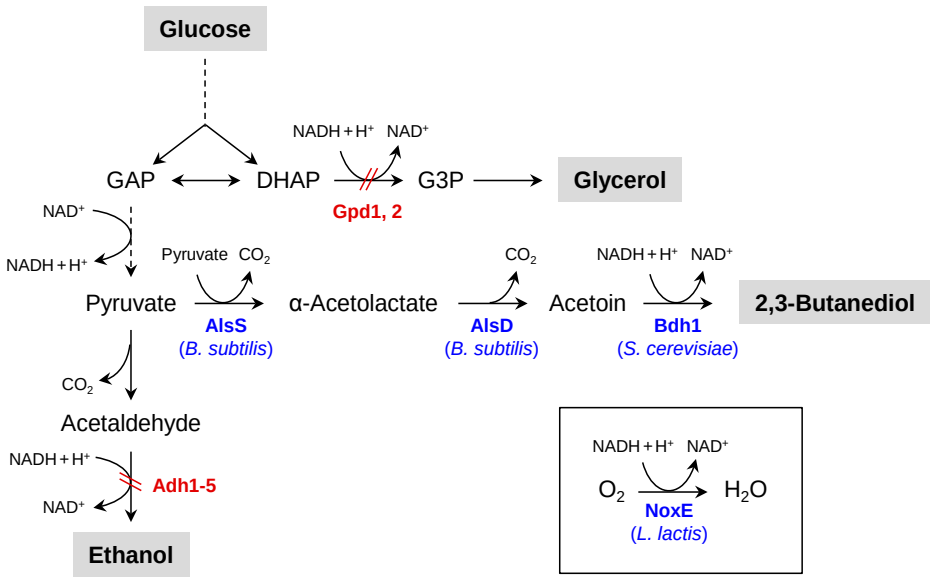

Figure 8.1 Metabolic pathway for 2,3-butanediol production used in this chapter

Two molecules of pyruvate are converted to one molecule of 2,3-butanediol via α-acetolactate and acetoin by sequential actions of α-acetolactate synthase (AlsS), α-acetolactate decarboxylase (AlsD), and 2,3-butanediol dehydrogenase (Bdh1). The water-forming NADH oxidase (NoxE) catalyzes the oxidation of NADH to NAD+ with the concomitant reduction of oxygen to water. Dashed arrows indicate multiple enzymatic steps. DHAP, dihydroxyacetone phosphate; G3P, glycerol-3-phosphate; GAP, glyceraldehyde-3-phosphate.

conversion using NADH oxidase or NADH kinase, or by modulating the cofactor specificity of pathway enzymes [194-196].

In this chapter, as an effort to develop *S. cerevisiae* strain for 2,3-butanediol production, 2,3-butanediol biosynthetic pathway was introduced into *S. cerevisiae* using a multigene-expression plasmid. To minimize byproduct formation, including ethanol and glycerol, genes encoding five alcohol dehydrogenases (*ADH1* to *ADH5*) and two glycerol-3-phosphate dehydrogenases (*GPD1* and *GPD2*) were deleted. Moreover, to relieve cofactor imbalance, water-forming NADH oxidase (NoxE) from *Lactococcus lactis* was expressed with 2,3-butanediol biosynthetic enzymes in the final strain *adh1-5Δgpd1Δgpd2Δ*, resulting in 2,3-butanediol production with dramatically improved productivity and high yield.

8.2. Construction of 2,3-butanediol biosynthetic pathway in *S. cerevisiae*

S. cerevisiae has an innate 2,3-butanediol production pathway, but the efficiency is very low. To enhance 2,3-butanediol production, heterologous acetoin biosynthetic pathway in *B. subtilis*, consisting of α-acetolactate synthase (AlsS) and α-acetolactate decarboxylase (AlsD), was introduced into *S. cerevisiae* which lacks α-acetolactate decarboxylase. Pyruvate is sequentially converted to α-acetolactate and acetoin by AlsS and AlsD, respectively, and then acetoin can be converted to 2,3-butanediol by endogenous 2,3-butanediol dehydrogenase (Bdh1) (Fig. 8.1).

This pathway has been successfully adopted to produce 2,3-butanediol in *S. cerevisiae* in previous studies [108, 121].

To construct multigene-expression plasmid for the expression of genes required for 2,3-butanediol biosynthesis, multiple cloning system was developed based on isocaudomer restriction enzyme pairs (BssHII-MluI and AscI-MluI) by using a CEN/ARS-based low copy number plasmid (pRS413) as a vector backbone (Fig. 8.2). The resulting plasmid p413-SDB is composed of *alsS*, *alsD*, and *BDH1* genes under the control of strong constitutive promoters, P_{TDH3}, P_{TEF1}, and P_{TPI1}, respectively, and different terminators.

The effect of introducing 2,3-butanediol pathway into *S. cerevisiae* was verified by transforming p413-SDB or empty p413GPD plasmid into CEN.PK2-1C strain. The control strain harboring p413GPD (WT [C]) produced only a trace amount of 2,3-butanediol (< 0.1 g/L), mainly producing ethanol with a titer of 22.0 g/L after 24 h fermentation in SC-His medium containing 50 g/L glucose (Fig. 8.3A). Whereas, CEN.PK2-1C strain harboring p413-SDB plasmid (WT [SDB]) produced 11.3 g/L 2,3-butanediol as a major product, 6.0 g/L ethanol, and 6.6 g/L glycerol after 31 h fermentation (Fig. 8.3B). However, 2,3-butanediol production pathway was reversed after glucose depletion, exhibiting a gradual conversion of 2,3-butanediol to acetoin (Fig. 8.3B). Taken together, the pyruvate flux was dramatically reconstructed to produce 2,3-butanediol just by overexpressing *alsS* and *alsD* genes from *B. subtilis* and native *BDH1*gene using multigene-expression plasmid.

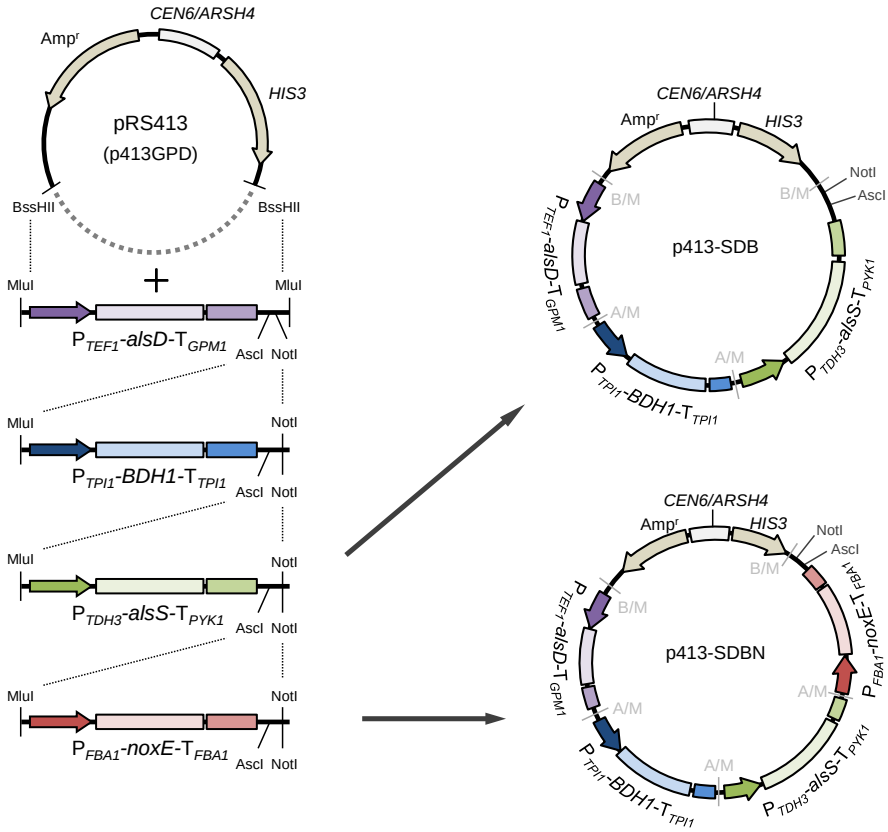

Figure 8.2 Construction of multigene-expression vector

Gene-expression cassettes flanked by MluI and AscI-NotI-MluI sites were obtained by PCR using primers carrying the restriction enzyme sites. First, MluI digested cassette was cloned into the BssHII sites of pRS413 vector, resulting in uncleavable BssHII-MluI ligation site (B/M) and AscI/NotI site for additional cloning. Additional cloning were sequentially carried out by ligating AscI/NotI digested vector and MluI/NotI digested gene expression cassette, resulting in uncleavable AscI-MluI ligation site (A/M), and new cloning sites (AscI and NotI sites). The experimental details are described in Materials and Methods.

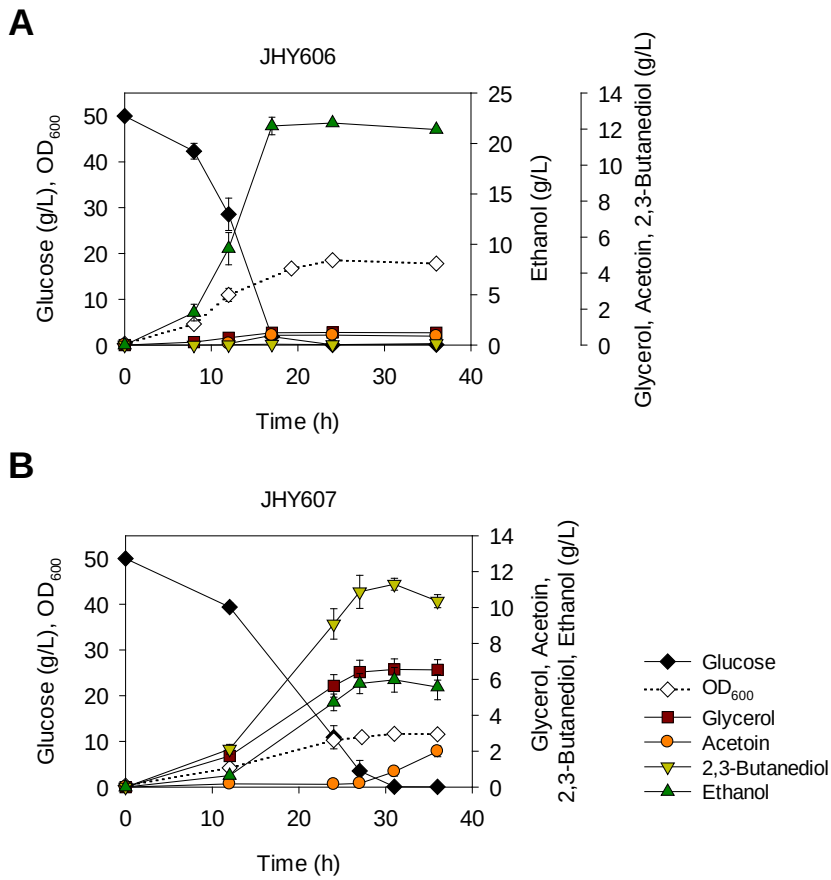

Figure 8.3 Improvement of 2,3-butanediol production by introducing 2,3-butanediol biosynthetic pathway in *S. cerevisiae*

The yeast strains WT [C] (A) and WT [SDB] (B) were grown in SC-His media containing 50 g/L glucose. Error bars indicate standard deviations of four independent experiments.

8.3. Disruption of competing pathways to improve 2,3-butanediol production

In WT [SDB] strain, ethanol and glycerol are the major byproducts. Therefore, to further improve 2,3-butanediol production, it is critical to minimize the metabolic pathways producing these byproducts. Although deletion of PDC could be the most efficient way of eliminating the competing pyruvate flux to ethanol, utilization of PDC-deficient strains is limited because of their severe growth defects in glucose medium. The growth defects of PDC-deficient strains are in part due to the limitation of producing cytosolic acetyl-CoA from acetaldehyde via acetate [109]. The problem of cytosolic acetyl-CoA can be solved by eliminating ADH instead of PDC, but the accumulation of toxic aldehyde could be a potential problem in ADH-deficient strains. However, the efficient redirection of pyruvate flux to 2,3-butanediol in WT [SDB] strain (Fig. 8.3B) suggests that AlsS activity might be high enough to compete with PDC, thus minimizing the accumulation of acetaldehyde even in the absence of ADH. Therefore, we chose to delete ADH genes instead of PDC genes to reduce ethanol production. In *S. cerevisiae*, there are at least five isozymes of NAD^+-dependent alcohol dehydrogenase, Adh1 to Adh5, among which Adh1 is known as the major enzyme [197, 198]. To reduce ethanol production, *ADH1* deletion strain (*adh1Δ*) was constructed and investigated the

effect on metabolites profile. The *adh1Δ* strain showed slow growth rate (Fig. 8.4A) because of the accumulation of NADH and acetaldehyde as previously reported [64, 107, 199]. When 2,3-butanediol pathway was introduced into *adh1Δ* strain (*adh1Δ* [SDB]), the growth defect was considerably recovered (Fig. 8.5A), which may be due to NAD^+-regeneration by Bdh1 and pyruvate flux to α-acetolactate instead of acetaldehyde formation. The *adh1Δ* [SDB] strain produced 3.4 g/L ethanol after 27 h (Fig 8.5A), indicating a 43% decrease compared with WT [SDB] strain (Fig. 8.5B). On the other hand, both 2,3-butanediol and glycerol production increased by 18% and 30%, reaching 13.3 g/L and 8.6 g/L, respectively, compared with WT [SDB] strain. Increase in glycerol production in response to reduced ethanol production is known as a compensation mechanism of regenerating NAD^+ to maintain redox balance [200] (Fig. 8.1). When all five *ADH* genes were deleted (*adh1-5Δ*), ethanol production was almost completely blocked (< 0.4 g/L) (Fig. 8.5B). However, *adh1-5Δ* [SDB] strain showed similar level of 2,3-butanediol production compared with *adh1Δ* [SDB] strain, while exhibiting further increase in glycerol production by 22% (10.5 g/L after 36 h).

In addition, the effect of deleting glycerol pathway on 2,3-butanediol production was investigated. Since glycerol-3-phosphate dehydrogenase is the rate-controlling enzyme in the glycerol production [201], both *GPD1* and *GPD2* were deleted to block the carbon flux to glycerol. In agreement with previous reports [65, 202], glycerol accumulation was completely eliminated in *gpd1Δgpd2Δ* strain containing p413-SDB plasmid (*gpd1Δgpd2Δ* [SDB]) (Fig 8.5C). In comparison

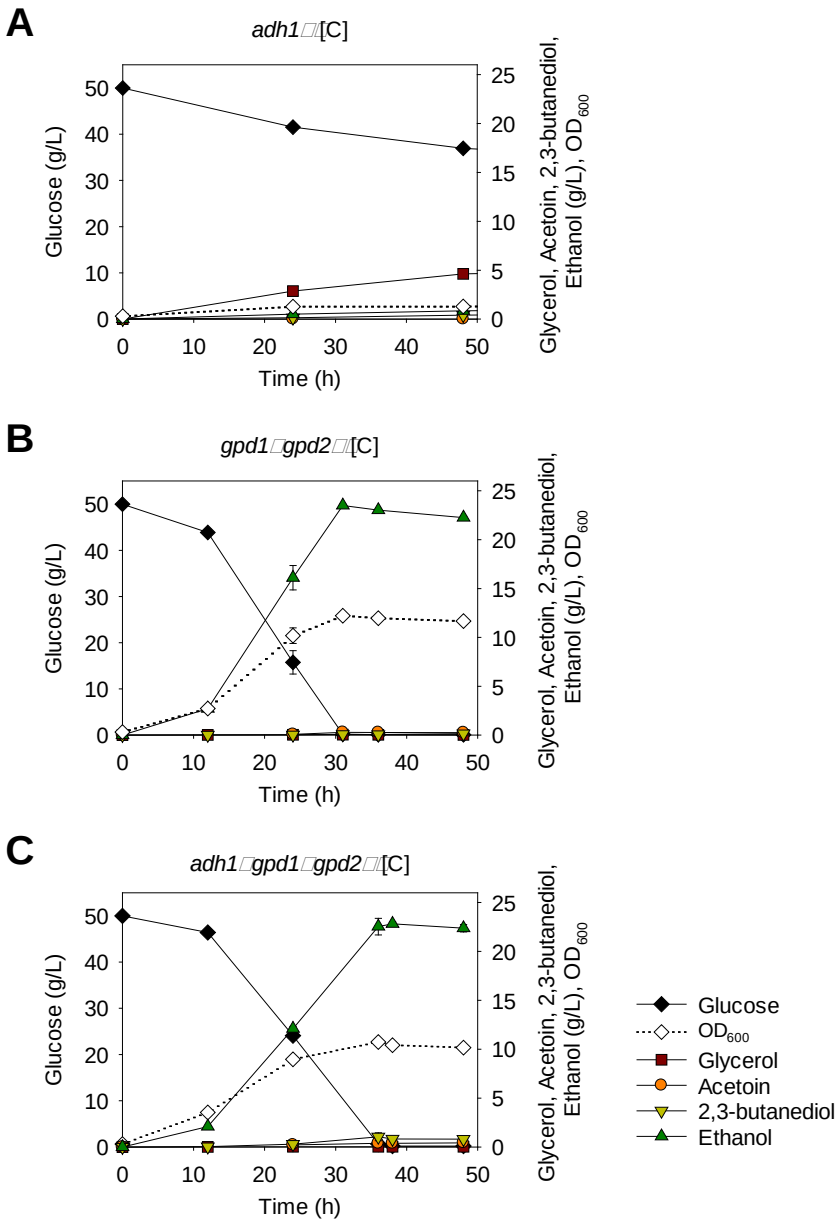
A
adh1□/□[C]
Glucose (g/L)
Glycerol, Acetoin, 2,3-butanediol, Ethanol (g/L), OD600
Time (h)
B
gpd1□gpd2□/□[C]
Glucose (g/L)
Glycerol, Acetoin, 2,3-butanediol, Ethanol (g/L), OD600
Time (h)
C
adh1□gpd1□gpd2□/□[C]
Glucose (g/L)
Glycerol, Acetoin, 2,3-butanediol, Ethanol (g/L), OD600
Time (h)
Glucose
OD600
Glycerol
Acetoin
2,3-butanediol
Ethanol

Figure 8.4 Metabolic profiles of engineered strains

Cells were pre-cultured in SC-His medium containing 20 g/L glucose and diluted to OD_{600} of 0.3 in 8 mL of SC-His medium containing 50 g/L glucose in a 50 mL conical tube with shaking at 170 rpm. Error bars indicate standard deviations of at least three independent experiments.

A. *adh1Δ* strain harboring empty p413GPD plasmid (*adh1Δ* [C])

B. *gpd1Δgpd2Δ* strain harboring empty p413GPD plasmid (*gpd1Δgpd2Δ* [C])

C. *adh1Δgpd1Δgpd2Δ* strain harboring empty p413GPD plasmid (*adh1Δgpd1Δgpd2Δ* [C])

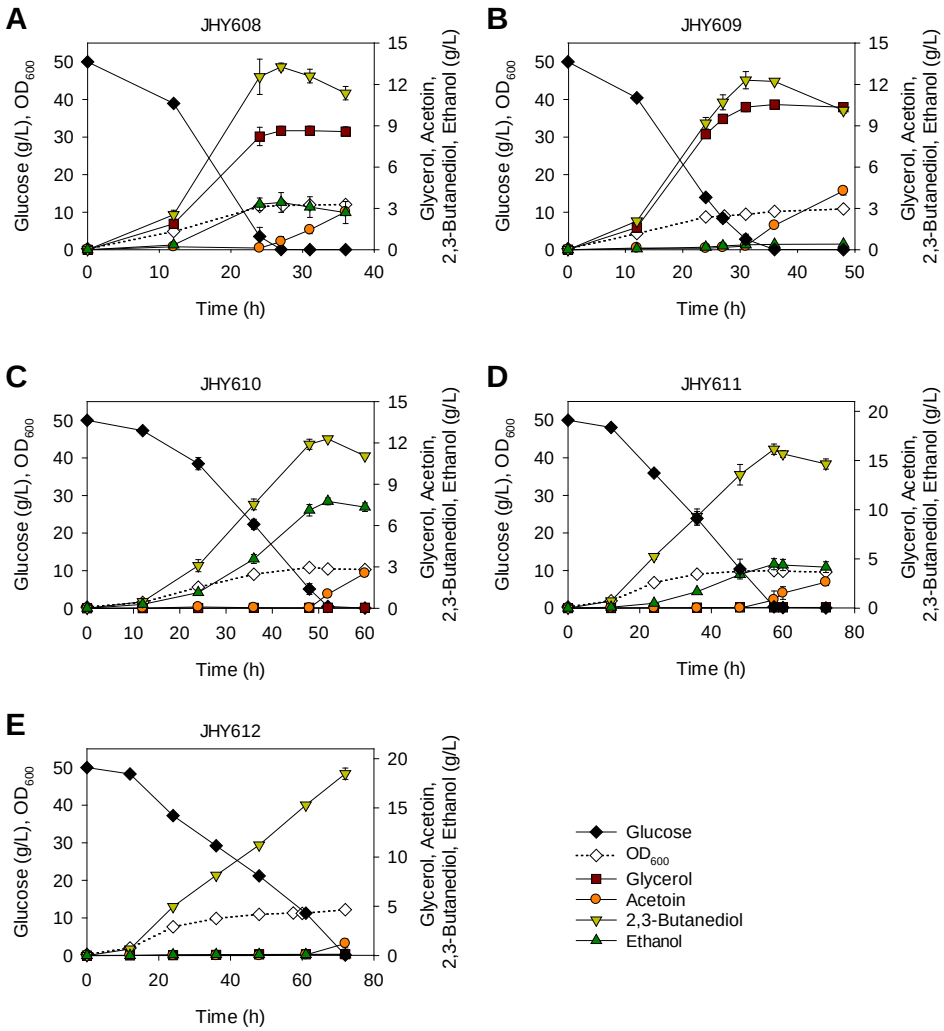

Figure 8.5 The effect of deleting competing pathways on 2,3-butanediol production

The yeast strains *adh1Δ* [SDB] (A), *adh1-5Δ* [SDB] (B), *gpd1Δgpd2Δ* [SDB] (C), *adh1Δgpd1Δgpd2Δ* [SDB] (D), and *adh1-5Δgpd1Δgpd2Δ* [SDB] (E) were grown in SC-His containing 50 g/L glucose. Error bars indicate standard deviations of four independent experiments.

with WT [SDB] (Fig 8.5B), 2,3-butanediol titer increased from 11.3 to 12.3 g/L, but ethanol titer also increased from 6.0 g/L to 7.8 g/L.

Next, 2,3-butanediol production upon deletion of both ethanol and glycerol pathways was investigated. In *adh1Δ* and *adh1-5Δ* strains, both *GDP1* and *GPD2* genes were additionally deleted to generate *adh1Δgpd1Δgpd2Δ* and *adh1-5Δgpd1Δgpd2* strains. Additional deletion of ADH genes in *gpd1Δgpd2Δ* strain led to a decrease in ethanol production, and the reduced ethanol levels in *adh1Δgpd1Δgpd2Δ* [SDB] and *adh1-5Δgpd1Δgpd2* [SDB] strains contributed to the increase in 2,3-butanediol production levels accordingly (Fig. 8.5D and E). The final *adh1-5Δgpd1Δgpd2* [SDB] strain produced up to 18.5 g/L 2,3-butanediol with a yield of 0.37 g/g glucose after 72 h, reaching 74% of maximum theoretical yield (Fig 5E and Table 8.1). In addition to high 2,3-butanediol yield, byproduct formation was dramatically reduced in this strain (0.07 g/L ethanol and 0.13 g/L glycerol).

8.4. Recovering redox imbalance by expressing water-forming NADH oxidase NoxE

In 2,3-butanediol production pathway, two molecules of NAD^+ are consumed in glycolysis to generate two molecules of pyruvate, but only one molecule of NAD^+ is regenerated from two molecules of pyruvate by reduction of acetoin to 2,3-butanediol (Fig 8.1). Therefore, introduction of metabolic pathway to produce 2,3-

butanediol from glucose leads to redox cofactor imbalance, resulting in glycerol accumulation as a compensation mechanism to regenerate NAD^+ (Fig 8.3). In this context, when glycerol production pathway was eliminated in order to improve 2,3-butanediol titer and yield, glucose consumption rate and 2,3-butanediol productivity were considerably reduced. (Fig. 8.5 and Table 8.1).

To alleviate the redox imbalance and improve the fermentation performance, the *noxE* gene from *L. lactis* encoding the water-forming NADH oxidase, which provides extra rout for NAD^+ regeneration, was coupled to 2,3-butanediol biosynthetic pathway (Fig. 8.2). The water-forming NADH oxidase regenerates NAD^+ from NADH by using molecular oxygen. Previous studies have demonstrated that NoxE mainly localizes in the cytosol in *S. cerevisiae* and has high affinity for NADH, which provides competitive advantage against endogenous NADH-dependent enzymes [193, 203]. Introducing *noxE* gene into xylose-utilizing *S. cerevisiae* led to increased ethanol production and decreased glycerol and xylitol accumulation [66, 204]. In addition, cofactor engineering using NADH oxidase has been successfully applied to acetoin production in *B. subtilis*, *K. pneumonia*, and *Serratia marcescens* [196, 205, 206].

The *noxE* gene under the control of strong constitutive promoter, P_{FBA1}, was cloned into p413-SDB plasmid, generating p413-SDBN plasmid (Fig 8.2). The *adh1-5Δgpd1Δgpd2* strain harboring p413-SDBN plasmid (*adh1-5Δgpd1Δgpd2* [SDBN]) showed significant improvement in 2,3-butanediol productivity (0.44 g/(L·h)) compared with *adh1-5Δgpd1Δgpd2* [SDB] strain (0.26 g/(L·h)), while

Table 8.1 Fermentation characteristics of recombinant strains

Strain	Description	Fermentation time (h)	Products (g/L)					Productivity of 2,3-BDO (g/(L·h))	Yield of 2,3-BDO (g/g glucose)
			Ethanol	Glycerol	Acetoin	2,3-BDO	Acetoin + 2,3-BDO		
Batch flask fermentation									
JHY606	WT [C]	24	22.03±0.11	0.70±0.01	0.56±0.05	0.03±0.00	0.59±0.05	0.001±0.000	0.001±0.000
JHY607	WT [SDB]	31	5.97±0.69	6.55±0.58	0.86±0.24	11.30±0.33	12.16±0.43	0.365±0.011	0.226±0.007
JHY608	*adh1Δ* [SDB]	27	3.44±0.72	8.64±0.32	0.60±0.37	13.27±0.28	13.87±0.59	0.492±0.010	0.266±0.006
JHY609	*adh1-5Δ* [SDB]	36	0.39±0.05	10.54±0.25	1.77±0.15	12.22±0.13	14.00±0.25	0.340±0.004	0.245±0.003
JHY610	*gpd1Δgpd2Δ* [SDB]	52	7.78±0.29	0.04±0.00	1.11±0.01	12.31±0.14	13.42±0.14	0.237±0.003	0.247±0.003
JHY611	*adh1Δgpd1Δgpd2Δ* [SDB]	60	4.38±0.57	0.07±0.01	1.54±0.65	15.67±0.34	17.20±0.34	0.261±0.006	0.314±0.007
JHY612	*adh1-5Δgpd1Δgpd2Δ* [SDB]	72	0.07±0.02	0.13±0.00	1.22±0.45	18.47±0.58	19.69±0.14	0.257±0.008	0.370±0.011
JHY613	*adh1-5Δgpd1Δgpd2Δ*[SDBN]	43	0.12±0.09	0.04±0.01	1.78±0.22	18.89±1.22	20.67±1.00	0.442±0.029	0.380±0.023
Fed-batch flask fermentation									
JHY613	*adh1-5Δgpd1Δgpd2Δ*[SDBN]	51	0.31±0.16	0.34±0.05	1.38±0.56	72.91±4.70	74.29±4.31	1.430±0.092	0.407±0.010

exhibiting similar levels of both 2,3-butanediol titer and yield (Fig. 8.6 and Table 8.1). This result indicates that redox imbalance caused by 2,3-butanediol production can be successfully restored by expressing NADH oxidase.

8.5. Fed-batch fermentation for 2,3-butanediol production

In order to order to further improve the fermentation performance to produce 2,3-butanediol in *adh1-5Δgpd1Δgpd2* [SDBN] strain (JHY613), various culture conditions were investigated. 2,3-Butanediol productivity was improved by increasing the initial cell density from OD_{600} of 0.3 to 10 (Fig. 8.6 and Fig. 8.7A). Similar to a previous report [111], fermentation in YPD medium exhibited slightly higher 2,3-butanediol productivity than that of in SC medium (Fig. 8.7). When aeration was increased by growing cells with 25 ml culture volume in a 250 ml flask, 2,3-butanediol productivity was remarkably improved compared with that obtained from the routine cultivation condition of 8 ml culture in a 50 ml conical tube (Fig. 8.8), suggesting that increased aeration might contribute to NAD^+ regeneration through respiration or increasing NoxE activity. Although NoxE has very low K_m constant for oxygen [207], oxygen concentration might affect the NoxE activity in the fermentation. Taken together, flask fed-batch fermentation was carried out in YPD10 medium containing 100 g/L glucose with initial high cell density of OD_{600} of 10. After 51 h fermentation, 72.9 g/L 2,3-butanediol was produced with a yield of 0.41 g/g glucose, reaching 81.4% of maximum theoretical

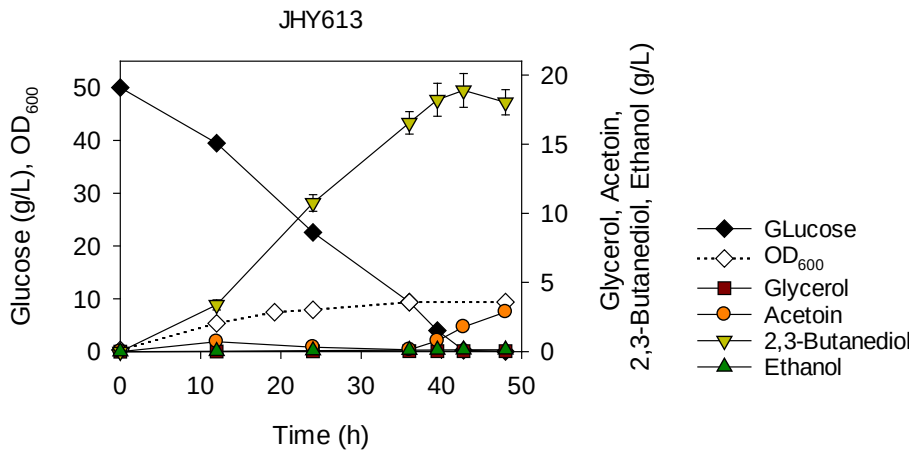

Figure 8.6 The effect of noxE expression on 2,3-butanediol production

The *adh1-5Δgpd1Δgpd2Δ* [SDBN] was grown in SC-His containing 50 g/L glucose. Error bars indicate standard deviations of four independent experiments.

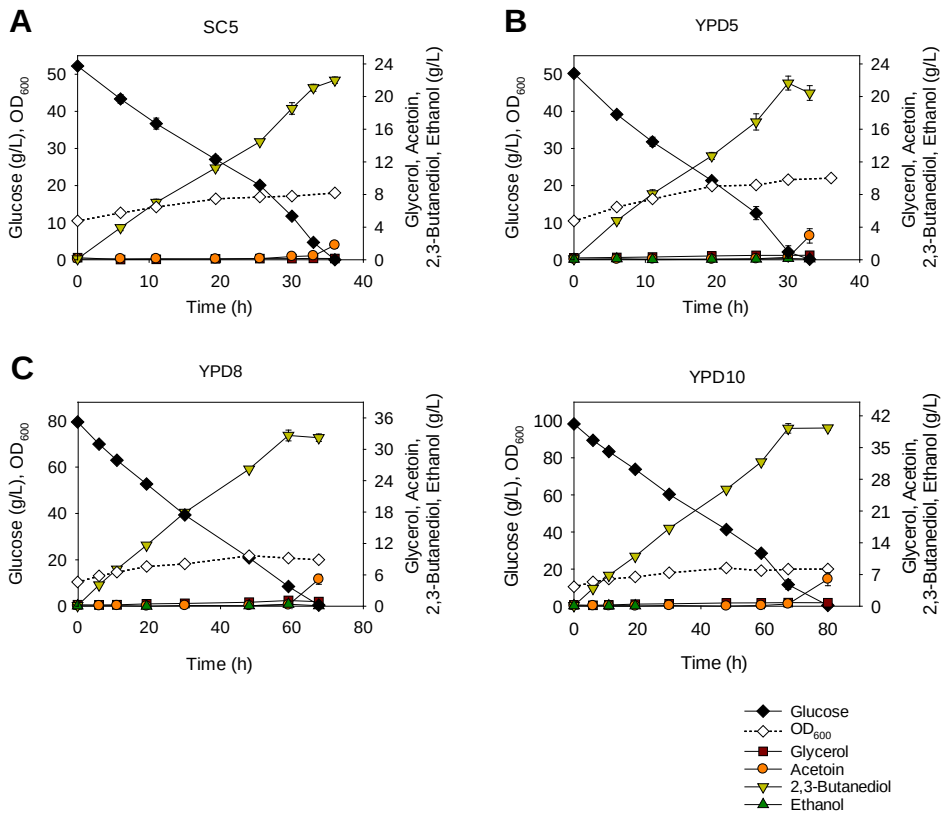

Figure 8.7 High cell density fermentation of *adh1-5Δgpd1Δgpd2Δ* [SDBN] strain (JHY613) in a 50 mL conical tube

Cells (OD_{600} of 10), pre-cultured in SC-His medium containing 20 g/L glucose, were harvested and cultured in SC-His medium containing 50 g/L glucose (SC5) (A) or YPD media with various concentrations of glucose; 50 g/L (YPD5) (B), 80 g/L (YPD8) (C), and 100 g/L (YPD10) (D). Error bars indicate standard deviations of at least three independent experiments.

yield (Fig. 8.9). Furthermore, 2,3-butanediol productivity was dramatically improved to 1.43 g/(L·h). Although 2,3-butanediol titer (72.9 g/L) was lower than that of previous reports (above 100 g/L) [108, 111], JHY613 strain achieved the highest yield and productivity ever reported in *S. cerevisiae*.

8.6. Conclusions

In this chapter, an engineered *S. cerevisiae* strain was developed for efficient 2,3-butanediol production by deleting competitive pathways producing ethanol and glycerol and introducing biosynthetic pathway consisting of AlsS and AlsD from *B. subtilis* and endogenous Bdh1, and expressing NADH oxidase (NoxE) from *L. lactis* for redox cofactor balance. In previous reports to produce 2,3-butanediol in *S. cerevisiae* strains with reduced ethanol production, significant amount of glycerol was accumulated as a regulatory mechanism to maintain redox balance, leading to a decrease in 2,3-butanediol yield [107, 113]. Although some attempts have been made to minimize glycerol accumulation by optimizing aeration conditions, glycerol production was considered as an inevitable phenomenon during 2,3-butanediol production in *S. cerevisiae* [107, 108, 113]. However, in this chapter, glycerol accumulation was completely eliminated by deleting both *GPD1* and *GPD2* genes, and the redox imbalance was successfully relieved by coupling the NAD^+-regenerating NADH oxidase to 2,3-butanediol production pathway. By using these strategies, both high yield and productivity in 2,3-butanediol

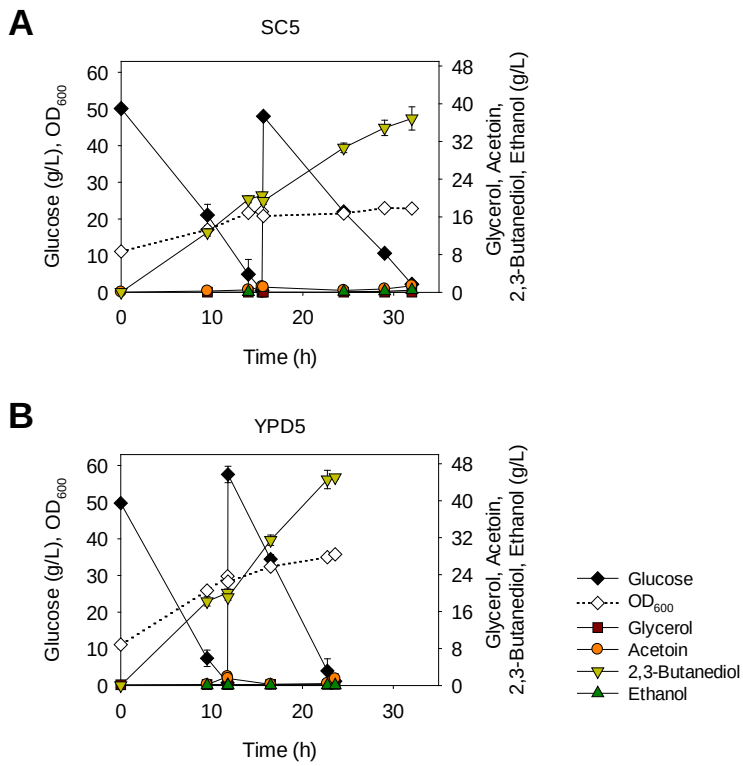

Figure 8.8 High cell density fermentation of *adh1-5Δgpd1Δgpd2Δ* [SDBN] strain (JHY613) in a 250 mL flask

Cells (OD_{600} of 10), pre-cultured in SC-His medium containing 20 g/L glucose, were harvested and cultured in 25 mL SC-His medium containing 50 g/L glucose (SC5) (A) or YPD medium with 50 g/L glucose (YPD5) (B). The feeding solution (800 g/L glucose) was added to the culture medium when glucose was depleted. Error bars indicate standard deviations of at least three independent experiments.

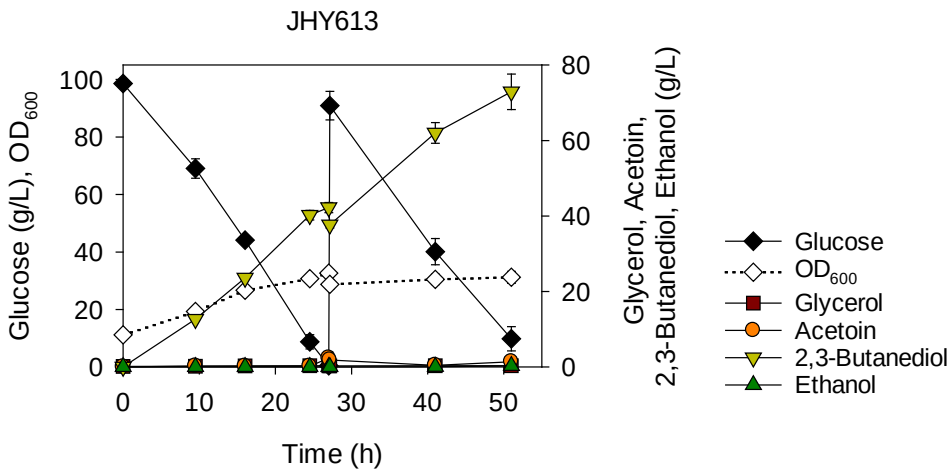

Figure 8.9 2,3-Butanediol fermentation profile in shake flask with glucose feeding

adh1-5Δ gpd1Δgpd2Δ [SDBN] was grown in YPD10 containing 100 g/L glucose. The feeding solution (800 g/L glucose) was added to the culture medium when glucose was depleted (after 27 h fermentation). Error bars indicate standard deviations of four independent experiments.

production could be achieved. In the final strain JHY613, 2,3-butanediol was produced up to 72.9 g/L after 51 h cultivation, with 84% of the maximum theoretical yield. To further improve 2,3-butanediol production, future works should be focused on further optimization of fermentation conditions and improvement of tolerance to 2,3-butanediol.

Chapter 9.

Overall discussion and recommendations

In this dissertation, several strategies, including substrate channeling, promoter engineering, and rational metabolic engineering, were developed and applied to produce cellulosic ethanol and 2,3-butanediol in *S. cerevisiae*. It is expected that this study will provide an expanded tool for metabolic engineering in *S. cerevisiae.*

In the first part, a novel cellulolytic yeast consortium was developed for cellulosic ethanol production. This consortium was composed of cells displaying mini cellulosomes generated via random assembly of CelA and CBHII to a mini CipA, and cells displaying BGLI independently. It is highly likely that the amount of each cellulase required for the maximum cellulolytic activity changes depending on the characteristics of target substrate and each cellulase. Therefore, one of the advantages of this system is the convenient optimization of ethanol production by simply changing the combination ratio of the different populations. In addition, not only cellulases used in this study, but also any other enzymes, including cellulases and hemicellulases, could be applied just by fusing dockerins to the enzymes. It means that there is no limitation on the number of cellulases to be incorporated to the cellulosome structure. In this study, it was also found that *A. aculeatus* BGLI can bind to yeast cell surface without any modification, which should be considered in interpreting or designing cellulolytic yeast system involving secreted BGLs originated from fungi. Furthermore, as well as bioethanol, various chemicals could be produced from cellulosic materials.

In the second part, a cohesin-dockerin interaction-based synthetic scaffold system was newly developed for substrate channeling in *S. cerevisiae*. This system

was successfully applied to the improved production of 2,3-butanediol. This is the first time that the interaction between cohesin and dockerin domains was confirmed in yeast cytosol and applied to metabolic engineering. Next, the effect of substrate channeling was further investigated at a metabolic branch point. Although there was not any gene modification such as deletion of competing pathways, except only cohesin tagging to target gene (*PYK1*), metabolic flux toward the target products was significantly enhanced with a decrease in byproduct formation. As a result, it has been demonstrated that spatial organization of enzymes located at metabolic branch point could provide competitive advantages over the other pathways, within the frame of metabolite channeling effect.

Since it is reported that the degree of substrate channeling is drastically increased under the conditions of low substrate concentration and low-activity enzymes [157], it is expected that the substrate channeling system would be a more powerful tool for metabolic pathway containing low-activity enzymes. Also, in synthetic scaffoldin system, the substrate channeling effect could be further optimized by fine-tuning the expression levels of scaffolds and metabolic enzymes, thus not only increasing the proportion of fully occupied scaffolds, but also adjusting the enzyme ratio participating in the enzyme complex.

In the third part, tryptophan- and GABA-inducible promoters were newly introduced as useful tools for metabolic engineering in *S. cerevisiae*. The tryptophan- or GABA-inducible promoters have advantages in that their promoter strengths can be easily modulated by adding different concentrations of inducers

directly into the culture medium. Therefore, these promoters might be useful in regulating gene expression levels at specific time points during the growth. Among the inducible promoters available in *S. cerevisiae*, the *CUP1* promoter can also be regulated by Cu^{2+} concentration-dependent manner, but the toxicity of Cu^{2+} can be a problem when using high concentrations of Cu^{2+} [164]. In the case of *GAL* promoters, complete medium exchange is necessary to prevent glucose repression effect [166, 167]. In addition, because galactose is used as a carbon source, it is not convenient to modulate galactose concentrations as a way to regulate expression levels. Other regulated promoters such as P_{ADH2}, P_{PHO5}, and P_{MET25} are repressed in the presence of glucose [208], inorganic phosphate [163], and methionine [161], respectively. Therefore, these promoters are useful for inducing gene expression when such nutrients or metabolite are depleted during the cultivation, but not appropriate for dose-dependent regulation by the regulating chemicals. The tryptophan-induced expression levels form the U_4C_{ARO9} promoter was within a similar range of the P_{ADH1}-deriven expression levels. Since P_{ADH1} promoter is weaker than other widely used strong promoters such as P_{TDH3} and P_{TEF1} [46, 47], the tryptophan-inducible promoters might be suitable for genes requiring low to intermediate-level expression in the metabolic pathway. The activity of tryptophan- or GABA-inducible promoters could be further enhanced by various promoter engineering strategies, which include combining the UAS with different core promoters and terminators [54, 209], or introducing poly(dA:dT) tracks that disfavor nucleosome assembly [210].

In the fourth part, an engineered *S. cerevisiae* strain for efficient 2,3-butanediol production was developed by combining metabolic pathway engineering and cofactor engineering. To minimize byproduct formation and improve 2,3-butanediol yield, competing pathways producing ethanol and glycerol, which are the major fermentation products in *S. cerevisiae*, were completely eliminated. In addition, the redox cofactor imbalance, caused by replacing ethanol and glycerol production with 2,3-butanediol production, was successfully restored by overexpressing water-forming NADH oxidase. As a result, the yield and productivity of 2,3-butanediol production in *S. cerevisiae* were significantly improved compared with previous studies. These results demonstrate that cofactor engineering with metabolic pathway engineering is a promising strategy to produce 2,3-butanediol with both yield and productivity. Although the encouraging results were obtained in this study, future works should be focused on further optimization of fermentation conditions and improvement of tolerance to 2,3-butanediol in order to further improve 2,3-butanediol production.

Various types of substrate channeling systems based on cohesin-dockerin interaction were successfully applied to metabolic engineering in *S. cerevisiae*, but the combinatorial effect with rational pathway engineering strategy was not yet confirmed. I expect that both of cytosolic substrate channeling systems, scaffold-based channeling system and PYK1-based channeling system, can be combined to JHY613 strain in order to further improve the performance of 2,3-butanediol production. Especially, the final strain JHY613 has native PDC genes, therefore,

PYK1-based channeling system is expected to further reduce the residual pyruvate flux toward acetaldehyde, which inhibits cellular functions and cell growth as a toxic intermediate.

Bibliography

[1] Woolston, B. M., Edgar, S., Stephanopoulos, G., Metabolic Engineering: Past and Future. *Annu. Rev. Chem. Biomol. Eng.* 2013, *4*, 259-288.

[2] Keasling, J. D., Manufacturing molecules through metabolic engineering. *Science* 2010, *330*, 1355-1358.

[3] Stephanopoulos, G., Metabolic fluxes and metabolic engineering. *Metab. Eng.* 1999, *1*, 1-11.

[4] Pitera, D. J., Paddon, C. J., Newman, J. D., Keasling, J. D., Balancing a heterologous mevalonate pathway for improved isoprenoid production in *Escherichia coli*. *Metab. Eng.* 2007, *9*, 193-207.

[5] Pfleger, B. F., Pitera, D. J., D Smolke, C., Keasling, J. D., Combinatorial engineering of intergenic regions in operons tunes expression of multiple genes. *Nat. Biotechnol.* 2006, *24*, 1027-1032.

[6] Liu, L. Q., Redden, H., Alper, H. S., Frontiers of yeast metabolic engineering: diversifying beyond ethanol and *Saccharomyces*. *Curr. Opin. Biotechnol.* 2013, *24*, 1023-1030.

[7] Bailey, J. E., Toward a Science of Metabolic Engineering. *Science* 1991, *252*, 1668-1675.

[8] Nielsen, J., Metabolic engineering. *Appl. Microbiol. Biotechnol.* 2001, *55*, 263-283.

[9] Brockman, I. M., Prather, K. L., Dynamic knockdown of *E. coli* central metabolism for redirecting fluxes of primary metabolites. *Metab. Eng.* 2015, *28*, 104-113.

[10] Soma, Y., Tsuruno, K., Wada, M., Yokota, A., Hanai, T., Metabolic flux redirection from a central metabolic pathway toward a synthetic pathway using a metabolic toggle switch. *Metab. Eng.* 2014, *23*, 175-184.

[11] Hong, K. K., Nielsen, J., Metabolic engineering of *Saccharomyces cerevisiae*: a key cell factory platform for future biorefineries. *Cell. Mol. Life Sci.* 2012, *69*, 2671-2690.

[12] Sellis, D., Callahan, B. J., Petrov, D. A., Messer, P. W., Heterozygote advantage as a natural consequence of adaptation in diploids. *Proc. Natl. Acad. Sci. USA* 2011, *108*, 20666-20671.

[13] Rodrigues, F., Ludovico, P., Leão, C., Sugar Metabolism in Yeasts: an Overview of Aerobic and Anaerobic Glucose Catabolism, in: Péter, G., Rosa, C. (Eds.), *Biodiversity and Ecophysiology of Yeasts*, Springer Berlin Heidelberg 2006, pp. 101-121.

[14]Blank, L. M., Sauer, U., TCA cycle activity in *Saccharomyces cerevisiae* is a function of the environmentally determined specific growth and glucose uptake rates. *Microbiology-Sgm* 2004, *150*, 1085-1093.

[15] Pronk, J. T., Yde Steensma, H., Van Dijken, J. P., Pyruvate metabolism in *Saccharomyces cerevisiae*. *Yeast* 1996, *12*, 1607-1633.

[16] Pfeiffer, T., Morley, A., An evolutionary perspective on the Crabtree effect. *Front Mol Biosci* 2014, *1*, 17.

[17] Lian, J., Zhao, H., Recent advances in biosynthesis of fatty acids derived products in *Saccharomyces cerevisiae* via enhanced supply of precursor metabolites. *J. Ind. Microbiol. Biotechnol.* 2015, *42*, 437-451.

[18] Strijbis, K., Distel, B., Intracellular Acetyl Unit Transport in Fungal Carbon Metabolism. *Eukaryot. Cell* 2010, *9*, 1809-1815.

[19] Nielsen, J., Jewett, M. C., Impact of systems biology on metabolic engineering of *Saccharomyces cerevisiae*. *FEMS Yeast Res.* 2008, *8*, 122-131.

[20] Nevoigt, E., Progress in metabolic engineering of *Saccharomyces cerevisiae*. *Microbiol. Mol. Biol. Rev.* 2008, *72*, 379-412.

[21] Spivey, H. O., Ovadi, J., Substrate channeling. *Methods-a Companion to Methods in Enzymology* 1999, *19*, 306-321.

[22] Jorgensen, K., Rasmussen, A. V., Morant, M., Nielsen, A. H., *et al.*, Metabolon formation and metabolic channeling in the biosynthesis of plant natural products. *Curr. Opin. Plant Biol.* 2005, *8*, 280-291.

[23] Elcock, A. H., Atomistic simulations of competition between substrates binding to an enzyme. *Biophys. J.* 2002, *82*, 2326-2332.

[24] Dueber, J. E., Wu, G. C., Malmirchegini, G. R., Moon, T. S., *et al.*, Synthetic protein scaffolds provide modular control over metabolic flux. *Nat. Biotechnol.* 2009, *27*, 753-759.

[25] Geck, M. K., Kirsch, J. F., A novel, definitive test for substrate channeling illustrated with the aspartate aminotransferase/malate dehydrogenase system. *Biochemistry* 1999, *38*, 8032-8037.

[26] Rudolph, J., Stubbe, J., Investigation of the mechanism of phosphoribosylamine transfer from glutamine phosphoribosylpyrophosphate amidotransferase to glycinamide ribonucleotide synthetase. *Biochemistry* 1995, *34*, 2241-2250.

[27] Srivastava, D. K., Smolen, P., Betts, G. F., Fukushima, T., *et al.*, Direct transfer of nadh between alpha-glycerol phosphate dehydrogenase and lactate dehydrogenase: fact or misinterpretation? *Proc. Natl. Acad. Sci. USA* 1989, *86*, 6464-6468.

[28] Conrado, R. J., Varner, J. D., DeLisa, M. P., Engineering the spatial organization of metabolic enzymes: mimicking nature's synergy. *Curr. Opin. Biotechnol.* 2008, *19*, 492-499.

[29] Steen, E. J., Chan, R., Prasad, N., Myers, S., *et al.*, Metabolic engineering of *Saccharomyces cerevisiae* for the production of n-butanol. *Microb. Cell Fact.* 2008, *7*.

[30] Avalos, J. L., Fink, G. R., Stephanopoulos, G., Compartmentalization of metabolic pathways in yeast mitochondria improves the production of branched-chain alcohols. *Nat. Biotechnol.* 2013, *31*, 335-341.

[31] Park, S. H., Kim, S., Hahn, J. S., Metabolic engineering of *Saccharomyces cerevisiae* for the production of isobutanol and 3-methyl-1-butanol. *Appl. Microbiol. Biotechnol.* 2014, *98*, 9139-9147.

[32] Lee, J. Y., Kang, C. D., Lee, S. H., Park, Y. K., Cho, K. M., Engineering cellular redox balance in *Saccharomyces cerevisiae* for improved production of L-lactic acid. *Biotechnol. Bioeng.* 2015, *112*, 751-758.

[33] Yan, D. J., Wang, C. X., Zhou, J. M., Liu, Y. L., *et al.*, Construction of reductive pathway in *Saccharomyces cerevisiae* for effective succinic acid fermentation at low pH value. *Bioresour. Technol.* 2014, *156*, 232-239.

[34] Chen, Y., Bao, J., Kim, I. K., Siewers, V., Nielsen, J., Coupled incremental precursor and co-factor supply improves 3-hydroxypropionic acid production in *Saccharomyces cerevisiae*. *Metab. Eng.* 2014, *22*, 104-109.

[35] Curran, K. A., Leavitt, J. M., Karim, A. S., Alper, H. S., Metabolic engineering of muconic acid production in *Saccharomyces cerevisiae*. *Metab. Eng.* 2013, *15*, 55-66.

[36] Xie, W., Lv, X., Ye, L., Zhou, P., Yu, H., Construction of lycopene-overproducing *Saccharomyces cerevisiae* by combining directed evolution and metabolic engineering. *Metab. Eng.* 2015, *30*, 69-78.

[37] Lee, H., DeLoache, W. C., Dueber, J. E., Spatial organization of enzymes for metabolic engineering. *Metab. Eng.* 2012, *14*, 242-251.

[38] Zhang, Y. S., Li, S. Z., Li, J., Pan, X. Q., *et al.*, Using unnatural protein fusions to engineer resveratrol biosynthesis in yeast and mammalian cells. *J. Am. Chem. Soc.* 2006, *128*, 13030-13031.

[39] Delebecque, C. J., Lindner, A. B., Silver, P. A., Aldaye, F. A., Organization of intracellular reactions with rationally designed RNA assemblies. *Science* 2011, *333*, 470-474.

[40] Collins, C. H., Yokobayashi, Y., Umeno, D., Arnold, F. H., Engineering proteins that bind, move, make and break DNA. *Curr. Opin. Biotechnol.* 2003, *14*, 371-378.

[41] Blumhoff, M. L., Steiger, M. G., Mattanovich, D., Sauer, M., Targeting enzymes to the right compartment: Metabolic engineering for itaconic acid production by *Aspergillus niger*. *Metab. Eng.* 2013, *19*, 26-32.

[42] Li, S. B., Liu, L. M., Chen, J., Compartmentalizing metabolic pathway in *Candida glabrata* for acetoin production. *Metab. Eng.* 2015, *28*, 1-7.

[43] Andrianantoandro, E., Basu, S., Karig, D. K., Weiss, R., Synthetic biology: new engineering rules for an emerging discipline. *Mol. Syst. Biol.* 2006, *2*, 2006 0028.

[44] Blazeck, J., Alper, H. S., Promoter engineering: recent advances in controlling transcription at the most fundamental level. *Biotechnology journal* 2013, *8*, 46-58.

[45] Da Silva, N. A., Srikrishnan, S., Introduction and expression of genes for metabolic engineering applications in *Saccharomyces cerevisiae*. *FEMS Yeast Res.* 2012, *12*, 197-214.

[46] Sun, J., Shao, Z., Zhao, H., Nair, N., *et al.*, Cloning and characterization of a panel of constitutive promoters for applications in pathway engineering in *Saccharomyces cerevisiae*. *Biotechnol. Bioeng.* 2012, *109*, 2082-2092.

[47] Mumberg, D., Muller, R., Funk, M., Yeast vectors for the controlled expression of heterologous proteins in different genetic backgrounds. *Gene* 1995, *156*, 119-122.

[48] Alper, H., Fischer, C., Nevoigt, E., Stephanopoulos, G., Tuning genetic control through promoter engineering. *Proc. Natl. Acad. Sci. USA* 2005, *102*, 12678-12683.

[49] Blount, B. A., Weenink, T., Vasylechko, S., Ellis, T., Rational diversification of a promoter providing fine-tuned expression and orthogonal regulation for synthetic biology. *PLoS One* 2012, *7*, e33279.

[50] Hartner, F. S., Ruth, C., Langenegger, D., Johnson, S. N., *et al.*, Promoter library designed for fine-tuned gene expression in *Pichia pastoris*. *Nucleic Acids Res.* 2008, *36*, e76.

[51] Nair, T. M., Kulkarni, B. D., On the consensus structure within the *Escherichia coli* promoters. *Biophys. Chem.* 1994, *48*, 383-393.

[52] Basehoar, A. D., Zanton, S. J., Pugh, B. F., Identification and distinct regulation of yeast TATA box-containing genes. *Cell* 2004, *116*, 699-709.

[53] Blount, B. A., Weenink, T., Vasylechko, S., Ellis, T., Rational diversification of a promoter providing fine-tuned expression and orthogonal regulation for synthetic biology. *PloS one* 2012, *7*.

[54] Blazeck, J., Garg, R., Reed, B., Alper, H. S., Controlling promoter strength and regulation in *Saccharomyces cerevisiae* using synthetic hybrid promoters. *Biotechnol. Bioeng.* 2012, *109*, 2884-2895.

[55] Reshamwala, S., Shawky, B. T., Dale, B. E., Ethanol-production from enzymatic hydrolysates of AFAX-treated coastal bermudagrass and switchgrass. *Appl. Biochem. Biotechnol.* 1995, *51-2*, 43-55.

[56] Cheung, S. W., Anderson, B. C., Laboratory investigation of ethanol production from municipal primary wastewater solids. *Bioresour. Technol.* 1997, *59*, 81-96.

[57] Boopathy, R., Biological treatment of swine waste using anaerobic baffled reactors. *Bioresour. Technol.* 1998, *64*, 1-6.

[58] Dewes, T., Hunsche, E., Composition and microbial degradability in the soil of farmyard manure from ecologically-managed farms. *Biol. Agric. Hortic.* 1998, *16*, 251-268.

[59] Sun, Y., Cheng, J. Y., Hydrolysis of lignocellulosic materials for ethanol production: a review. *Bioresour. Technol.* 2002, *83*, 1-11.

[60] van Zyl, W. H., Lynd, L. R., den Haan, R., McBride, J. E., Consolidated bioprocessing for bioethanol production using *Saccharomyces cerevisiae*. *Advances in biochemical engineering/biotechnology* 2007, *108*, 205-235.

[61] Lynd, L. R., Weimer, P. J., van Zyl, W. H., Pretorius, I. S., Microbial cellulose utilization: Fundamentals and biotechnology. *Microbiol. Mol. Biol. Rev.* 2002, *66*, 506-577.

[62] Kumar, R., Singh, S., Singh, O. V., Bioconversion of lignocellulosic biomass: biochemical and molecular perspectives. *J. Ind. Microbiol. Biotechnol.* 2008, *35*, 377-391.

[63] Lynd, L. R., van Zyl, W. H., McBride, J. E., Laser, M., Consolidated bioprocessing of cellulosic biomass: an update. *Curr. Opin.Biotech.*2005, *16*, 577-583.

[64] de Smidt, O., du Preez, J. C., Albertyn, J., Molecular and physiological aspects of alcohol dehydrogenases in the ethanol metabolism of *Saccharomyces cerevisiae*. *FEMS Yeast Res.* 2012, *12*, 33-47.

[65] Ansell, R., Granath, K., Hohmann, S., Thevelein, J. M., Adler, L., The two isoenzymes for yeast NAD^+-dependent glycerol 3-phosphate dehydrogenase encoded by *GPD1* and *GPD2* have distinct roles in osmoadaptation and redox regulation. *EMBO J.* 1997, *16*, 2179-2187.

[66] Hou, J., Suo, F., Wang, C., Li, X., *et al.*, Fine-tuning of NADH oxidase decreases byproduct accumulation in respiration deficient xylose metabolic *Saccharomyces cerevisiae*. *BMC Biotechnol.* 2014, *14*, 13.

[67] Den Haan, R., Mcbride, J. E., La Grange, D. C., Lynd, L. R., Van Zyl, W. H., Functional expression of cellobiohydrolases in *Saccharomyces cerevisiae* towards one-step conversion of cellulose to ethanol. *Enzyme Microb. Technol.* 2007, *40*, 1291-1299.

[68] Den Haan, R., Rose, S. H., Lynd, L. R., van Zyl, W. H., Hydrolysis and fermentation of amorphous cellulose by recombinant *Saccharomyces cerevisiae*. *Metab. Eng.* 2007, *9*, 87-94.

[69] Fujita, Y., Ito, J., Ueda, M., Fukuda, H., Kondo, A., Synergistic saccharification, and direct fermentation to ethanol, of amorphous cellulose by use of an engineered yeast strain codisplaying three types of cellulolytic enzyme. *Appl. Environ. Microbiol.* 2004, *70*, 1207-1212.

[70] Yanase, S., Yamada, R., Kaneko, S., Noda, H., *et al.*, Ethanol production from cellulosic materials using cellulase-expressing yeast. *Biotechnology Journal* 2010, *5*, 449-455.

[71] Wen, F., Sun, J., Zhao, H., Yeast surface display of trifunctional minicellulosomes for simultaneous saccharification and fermentation of cellulose to ethanol. *Appl. Environ. Microbiol.* 2010, *76*, 1251-1260.

[72] Hyeon, J. E., Jeon, W. J., Whang, S. Y., Han, S. O., Production of minicellulosomes for the enhanced hydrolysis of cellulosic substrates by recombinant *Corynebacterium glutamicum*. *Enzyme Microb. Technol.* 2011, *48*, 371-377.

[73] Tsai, S. L., Goyal, G., Chen, W., Surface display of a functional minicellulosome by intracellular complementation using a synthetic yeast consortium and its application to cellulose hydrolysis and ethanol production. *Appl. Environ. Microbiol.* 2010, *76*, 7514-7520.

[74] Fan, L. H., Zhang, Z. J., Yu, X. Y., Xue, Y. X., Tan, T. W., Self-surface assembly of cellulosomes with two miniscaffoldins on *Saccharomyces cerevisiae* for cellulosic ethanol production. *Proc. Natl. Acad. Sci. USA* 2012, *109*, 13260-13265.

[75] Lee, W. H., Nan, H., Kim, H. J., Jin, Y. S., Simultaneous saccharification and fermentation by engineered *Saccharomyces cerevisiae* without supplementing extracellular beta-glucosidase. *J. Biotechnol.* 2013, *167*, 316-322.

[76] Yamada, R., Yamakawa, S., Tanaka, T., Ogino, C., *et al.*, Direct and efficient ethanol production from high-yielding rice using a *Saccharomyces cerevisiae* strain that express amylases. *Enzyme Microb. Technol.* 2011, *48*, 393-396.

[77] Nakatani, Y., Yamada, R., Ogino, C., Kondo, A., Synergetic effect of yeast cell-surface expression of cellulase and expansin-like protein on direct ethanol production from cellulose. *Microb. Cell Fact.* 2013, *12*.

[78] van Rooyen, R., Hahn-Hagerdal, B., La Grange, D. C., van Zyl, W. H., Construction of cellobiose-growing and fermenting *Saccharomyces cerevisiae* strains. *J. Biotechnol.* 2005, *120*, 284-295.

[79] Yamada, R., Nakatani, Y., Ogino, C., Kondo, A., Efficient direct ethanol production from cellulose by cellulase- and cellodextrin transporter-co-expressing *Saccharomyces cerevisiae*. *AMB Express* 2013, *3*, 34.

[80] Goyal, G., Tsai, S. L., Madan, B., DaSilva, N. A., Chen, W., Simultaneous cell growth and ethanol production from cellulose by an engineered yeast consortium displaying a functional mini-cellulosome. *Microb. Cell Fact.* 2011, *10*.

[81] Celinska, E., Grajek, W., Biotechnological production of 2,3-butanediol - Current state and prospects. *Biotechnol. Adv.* 2009, *27*, 715-725.

[82] Ma, C. Q., Wang, A. L., Qin, J. Y., Li, L. X., *et al.*, Enhanced 2,3-butanediol production by *Klebsiella pneumoniae* SDM. *Appl. Microbiol. Biotechnol.* 2009, *82*, 49-57.

[83] Wang, A. L., Wang, Y., Jiang, T. Y., Li, L. X., *et al.*, Production of 2,3-butanediol from corncob molasses, a waste by-product in xylitol production. *Appl. Microbiol. Biotechnol.* 2010, *87*, 965-970.

[84] Petrov, K., Petrova, P., High production of 2,3-butanediol from glycerol by *Klebsiella pneumoniae* G31. *Appl. Microbiol. Biotechnol.* 2009, *84*, 659-665.

[85] Sun, L. H., Wang, X. D., Dai, J. Y., Xiu, Z. L., Microbial production of 2,3-butanediol from *Jerusalem artichoke* tubers by *Klebsiella pneumoniae*. *Appl. Microbiol. Biotechnol.* 2009, *82*, 847-852.

[86] Qureshi, N., Cheryan, M., Production of 2,3-butanediol by *Klebsiella oxytoca*. *Appl. Microbiol. Biotechnol.* 1989, *30*, 440-443.

[87] Ji, X. J., Huang, H., Zhu, J. G., Ren, L. J., *et al.*, Engineering *Klebsiella oxytoca* for efficient 2, 3-butanediol production through insertional inactivation of acetaldehyde dehydrogenase gene. *Appl. Microbiol. Biotechnol.* 2010, *85*, 1751-1758.

[88] Jantama, K., Polyiam, P., Khunnonkwao, P., Chan, S., *et al.*, Efficient reduction of the formation of by-products and improvement of production yield of 2,3-butanediol by a combined deletion of alcohol dehydrogenase, acetate kinase-phosphotransacetylase, and lactate dehydrogenase genes in metabolically engineered *Klebsiella oxytoca* in mineral salts medium. *Metab. Eng.* 2015, *30*, 16-26.

[89] Cheng, K. K., Liu, Q., Zhang, J. A., Li, J. P., *et al.*, Improved 2,3-butanediol production from corncob acid hydrolysate by fed-batch fermentation using *Klebsiella oxytoca*. *Process Biochem.* 2010, *45*, 613-616.

[90] Afschar, A. S., Bellgardt, K. H., Rossell, C. E. V., Czok, A., Schaller, K., The production of 2,3-butanediol by fermentation of high test molasses. *Appl. Microbiol. Biotechnol.* 1991, *34*, 582-585.

[91] Zeng, A. P., Biebl, H., Deckwer, W. D., Production of 2,3-butanediol in a membrane bioreactor with cell recycle. *Appl. Microbiol. Biotechnol.* 1991, *34*, 463-468.

[92] Li, L. X., Li, K., Wang, Y., Chen, C., *et al.*, Metabolic engineering of *Enterobacter cloacae* for high-yield production of enantiopure (2R,3R)-2,3-butanediol from lignocellulose-derived sugars. *Metab. Eng.* 2015, *28*, 19-27.

[93] Zhang, L. Y., Sun, J. A., Hao, Y. L., Zhu, J. W., *et al.*, Microbial production of 2,3-butanediol by a surfactant (serrawettin)-deficient mutant of *Serratia marcescens* H30. *J. Ind. Microbiol. Biotechnol.* 2010, *37*, 857-862.

[94] Zhang, L. Y., Yang, Y. L., Sun, J. A., Shen, Y. L., *et al.*, Microbial production of 2,3-butanediol by a mutagenized strain of *Serratia marcescens* H30. *Bioresour. Technol.* 2010, *101*, 1961-1967.

[95] Hassler, T., Schieder, D., Pfaller, R., Faulstich, M., Sieber, V., Enhanced fed-batch fermentation of 2,3-butanediol by *Paenibacillus polymyxa* DSM 365. *Bioresour. Technol.* 2012, *124*, 237-244.

[96] Dai, J. J., Cheng, J. S., Liang, Y. Q., Jiang, T., Yuan, Y. J., Regulation of extracellular oxidoreduction potential enhanced (R, R)-2,3-butanediol production by *Paenibacillus polymyxa* CJX518. *Bioresour. Technol.* 2014, *167*, 433-440.

[97] Gao, J. A., Xu, H., Li, Q. J., Feng, X. H., Li, S., Optimization of medium for one-step fermentation of inulin extract from *Jerusalem artichoke* tubers using *Paenibacillus polymyxa* ZJ-9 to produce R,R-2,3-butanediol. *Bioresour. Technol.* 2010, *101*, 7076-7082.

[98] Moes, J., Griot, M., Keller, J., Heinzle, E., *et al.*, A microbial culture with oxygen-sensitive product distribution as a potential tool for characterizing bioreactor oxygen-transport. *Biotechnol. Bioeng.* 1985, *27*, 482-489.

[99] Biswas, R., Yamaoka, M., Nakayama, H., Kondo, T., *et al.*, Enhanced production of 2,3-butanediol by engineered *Bacillus subtilis*. *Appl. Microbiol. Biotechnol.* 2012, *94*, 651-658.

[100] Nilegaonkar, S., Bhosale, S. B., Kshirsagar, D. C., Kapadi, A. H., Production of 2,3-butanediol from glucose by *bacillus licheniformis*. *World J. Microbiol. Biotechnol.* 1992, *8*, 378-381.

[101] Xu, Y. Q., Chu, H. P., Gao, C., Tao, F., *et al.*, Systematic metabolic engineering of *Escherichia coli* for high-yield production of fuel bio-chemical 2,3-butanediol. *Metab. Eng.* 2014, *23*, 22-33.

[102] Alam, S., Capit, F., Weigand, W. A., Hong, J., Kinetics of 2,3-butanediol fermentation by *Bacillus amyloliquefaciens* - effect of initial substrate concentration and aeration. *J. Chem. Technol. Biotechnol.* 1990, *47*, 71-84.

[103] Ji, X. J., Huang, H., Ouyang, P. K., Microbial 2,3-butanediol production: A state-of-the-art review. *Biotechnol. Adv.* 2011, *29*, 351-364.

[104] Chen, G. C., Jordan, F., Brewers' yeast pyruvate decarboxylase produces acetoin from acetaldehyde: a novel tool to study the mechanism of steps subsequent to carbon dioxide loss. *Biochemistry* 1984, *23*, 3576-3582.

[105] Romano, P., Suzzi, G., Origin and production of acetoin during wine yeast fermentation. *Appl. Environ. Microbiol.* 1996, *62*, 309-315.

[106] Sergienko, E. A., Jordan, F., Catalytic acid-base groups in yeast pyruvate decarboxylase. 2. Insights into the specific roles of D28 and E477 from the rates and stereospecificity of formation of carboligase side products. *Biochemistry* 2001, *40*, 7369-7381.

[107] Ng, C. Y., Jung, M. Y., Lee, J., Oh, M. K., Production of 2,3-butanediol in *Saccharomyces cerevisiae* by *in silico* aided metabolic engineering. *Microb. Cell Fact.* 2012, *11*, 68.

[108] Kim, S. J., Seo, S. O., Jin, Y. S., Seo, J. H., Production of 2,3-butanediol by engineered *Saccharomyces cerevisiae*. *Bioresour. Technol.* 2013, *146*, 274-281.

[109] Flikweert, M. T., Van Der Zanden, L., Janssen, W. M., Steensma, H. Y., *et al.*, Pyruvate decarboxylase: an indispensable enzyme for growth of *Saccharomyces cerevisiae* on glucose. *Yeast* 1996, *12*, 247-257.

[110] Yan, D., Wang, C., Zhou, J., Liu, Y., *et al.*, Construction of reductive pathway in *Saccharomyces cerevisiae* for effective succinic acid fermentation at low pH value. *Bioresour. Technol.* 2014, *156*, 232-239.

[111] Lian, J., Chao, R., Zhao, H., Metabolic engineering of a *Saccharomyces cerevisiae* strain capable of simultaneously utilizing glucose and galactose to produce enantiopure (2R,3R)-butanediol. *Metab. Eng.* 2014, *23*, 92-99.

[112] van Maris, A. J., Geertman, J. M., Vermeulen, A., Groothuizen, M. K., *et al.*, Directed evolution of pyruvate decarboxylase-negative *Saccharomyces cerevisiae*, yielding a C2-independent, glucose-tolerant, and pyruvate-hyperproducing yeast. *Appl. Environ. Microbiol.* 2004, *70*, 159-166.

[113] Kim, S. J., Seo, S. O., Park, Y. C., Jin, Y. S., Seo, J. H., Production of 2,3-butanediol from xylose by engineered *Saccharomyces cerevisiae*. *J. Biotechnol.* 2014, *192*, 376-382.

[114] Nan, H., Seo, S. O., Oh, E. J., Seo, J. H., *et al.*, 2,3-butanediol production from cellobiose by engineered *Saccharomyces cerevisiae*. *Appl. Microbiol. Biotechnol.* 2014, *98*, 5757-5764.

[115] Ehsani, M., Fernandez, M. R., Biosca, J. A., Julien, A., Dequin, S., Engineering of 2,3-butanediol dehydrogenase to reduce acetoin formation by glycerol-overproducing, low-alcohol *Saccharomyces cerevisiae*. *Appl. Environ. Microbiol.* 2009, *75*, 3196-3205.

[116] Kim, J. W., Seo, S. O., Zhang, G. C., Jin, Y. S., Seo, J. H., Expression of *Lactococcus lactis* NADH oxidase increases 2,3-butanediol production in Pdc-deficient *Saccharomyces cerevisiae*. *Bioresour. Technol.* 2015.

[117] Gueldener, U., Heinisch, J., Koehler, G. J., Voss, D., Hegemann, J. H., A second set of *loxP* marker cassettes for Cre-mediated multiple gene knockouts in budding yeast. *Nucleic Acids Res.* 2002, *30*.

[118] Colby, D. W., Kellogg, B. A., Graff, C. P., Yeung, Y. A., *et al.*, Engineering antibody affinity by yeast surface display. *Protein Eng.* 2004, *388*, 348-358.

[119] Baek, S. H., Kim, S., Lee, K., Lee, J. K., Hahn, J. S., Cellulosic ethanol production by combination of cellulase-displaying yeast cells. *Enzyme Microb. Technol.* 2012, *51*, 366-372.

[120] Sung, M. K., Huh, W. K., Bimolecular fluorescence complementation low analysis system for *in vivo* detection of protein-protein interaction in *Saccharomyces cerevisiae*. *Yeast* 2007, *24*, 767-775.

[121] Kim, S., Hahn, J. S., Synthetic scaffold based on a cohesin-dockerin interaction for improved production of 2,3-butanediol in *Saccharomyces cerevisiae*. *J. Biotechnol.* 2014, *192*, 192-196.

[122] Li, L., Eom, H. J., Park, J. M., Seo, E., *et al.*, Characterization of the major dehydrogenase related to D-lactic acid synthesis in *Leuconostoc mesenteroides subsp mesenteroides* ATCC 8293. *Enzyme Microb. Technol.* 2012, *51*, 274-279.

[123] Ghose, T. K., Measurement of cellulase activities. *Pure Appl. Chem.* 1987, *59*, 257-268.

[124] Lee, K., Hahn, J. S., Interplay of Aro80 and GATA activators in regulation of genes for catabolism of aromatic amino acids in *Saccharomyces cerevisiae*. *Mol. Microbiol.* 2013, *88*, 1120-1134.

[125] Demain, A. L., Newcomb, M., Wu, J. H., Cellulase, clostridia, and ethanol. *Microbiology and molecular biology reviews : MMBR* 2005, *69*, 124-154.

[126] Hahn-Hagerdal, B., Galbe, M., Gorwa-Grauslund, M. F., Liden, G., Zacchi, G., Bio-ethanol - the fuel of tomorrow from the residues of today. *Trends Biotechnol.* 2006, *24*, 549-556.

[127] Fortman, J. L., Chhabra, S., Mukhopadhyay, A., Chou, H., *et al.*, Biofuel alternatives to ethanol: pumping the microbial well. *Trends Biotechnol.* 2008, *26*, 375-381.

[128] Gallezot, P., Catalytic Conversion of Biomass: Challenges and Issues. *Chemsuschem* 2008, *1*, 734-737.

[129] Sims, R. E. H., Mabee, W., Saddler, J. N., Taylor, M., An overview of second generation biofuel technologies. *Bioresour. Technol.* 2010, *101*, 1570-1580.

[130] Himmel, M. E., Ding, S. Y., Johnson, D. K., Adney, W. S., *et al.*, Biomass recalcitrance: engineering plants and enzymes for biofuels production. *Science* 2007, *315*, 804-807.

[131] Lynd, L. R., Laser, M. S., Brandsby, D., Dale, B. E., *et al.*, How biotech can transform biofuels. *Nat. Biotechnol.* 2008, *26*, 169-172.

[132] Ohara, H., Karita, S., Kimura, T., Sakka, K., Ohmiya, K., Characterization of the cellulolytic complex (cellulosome) from *Ruminococcus albus*. *Biosci., Biotechnol., Biochem.* 2000, *64*, 254-260.

[133] Bayer, E. A., Belaich, J. P., Shoham, Y., Lamed, R., The cellulosomes: Multienzyme machines for degradation of plant cell wall polysaccharides. *Annu. Rev. Microbiol.* 2004, *58*, 521-554.

[134] Fontes, C. M., Gilbert, H. J., Cellulosomes: Highly efficient nanomachines designed to deconstruct plant cell wall complex carbohydrates. *Annu. Rev. Biochem.* 2010, *79*, 655-681.

[135] Iwashita, K., Nagahara, T., Kimura, H., Takano, M., *et al.*, The bglA gene of *Aspergillus kawachii* encodes both extracellular and cell wall-bound beta-glucosidases. *Appl. Environ. Microbiol.* 1999, *65*, 5546-5553.

[136] Horikoshi, K., Ikeda, Y., Studies on the spore coats of *aspergillus oryzae*. II. Conidia coat-bound beta-glucosidase. *Biochim. Biophys. Acta Biochim Biophys Acta* 1965, *101*, 352-357.

[137] Eberhart, B. M., Beck, R. S., Localization of the beta-glucosidases in *Neurospora crassa*. *J. Bacteriol.* 1970, *101*, 408-417.

[138] Shah, M. A., Chaudhuri, T. K., Mishra, S., Strategy for purification of aggregation prone beta-glucosidases from the cell wall of yeast: a preparative scale approach. *New Biotechnology* 2012, *29*, 311-320.

[139] Messner, R., Hagspiel, K., Kubicek, C. P., Isolation of a beta-glucosidase binding and activating polysaccharide from cell-walls of *Trichoderma reesei*. *Arch. Microbiol.* 1990, *154*, 150-155.

[140] Boisset, C., Petrequin, C., Chanzy, H., Henrissat, B., Schulein, M., Optimized mixtures of recombinant *Humicola insolens* cellulases for the biodegradation of crystalline cellulose. *Biotechnol. Bioeng.* 2001, *72*, 339-345.

[141] Berger, E., Zhang, D., Zverlov, V. V., Schwarz, W. H., Two noncellulosomal cellulases of *Clostridium thermocellum*, Cel9I and Cel48Y, hydrolyse crystalline cellulose synergistically. *FEMS Microbiol. Lett.* 2007, *268*, 194-201.

[142] Morais, S., Heyman, A., Barak, Y., Caspi, J., *et al.*, Enhanced cellulose degradation by nano-complexed enzymes: Synergism between a scaffold-linked exoglucanase and a free endoglucanase. *J. Biotechnol.* 2010, *147*, 205-211.

[143] Yamada, R., Taniguchi, N., Tanaka, T., Ogino, C., *et al.*, Direct ethanol production from cellulosic materials using a diploid strain of *Saccharomyces cerevisiae* with optimized cellulase expression. *Biotechnology for Biofuels* 2011, *4*.

[144] Zhang, Y. H. P., Substrate channeling and enzyme complexes for biotechnological applications. *Biotechnol. Adv.* 2011, *29*, 715-725.

[145] Stahl, S. W., Nash, M. A., Fried, D. B., Slutzki, M., *et al.*, Single-molecule dissection of the high-affinity cohesin-dockerin complex. *Proc. Natl. Acad. Sci. USA* 2012, *109*, 20431-20436.

[146] Mechaly, A., Fierobe, H. P., Belaich, A., Belaich, J. P., *et al.*, Cohesin-dockerin interaction in cellulosome assembly - A single hydroxyl group of a dockerin domain distinguishes between nonrecognition and high affinity recognition. *J. Biol. Chem.* 2001, *276*, 9883-9888.

[147] Fontes, C. M., Gilbert, H. J., Cellulosomes: Highly efficient nanomachines designed to deconstruct plant cell wall complex carbohydrates. *Annu Rev Biochem* 2010, *79*, 655-681.

[148] Anderson, T. D., Miller, J. I., Fierobe, H. P., Clubb, R. T., Recombinant *Bacillus subtilis* that grows on untreated plant biomass. *Appl. Environ. Microbiol.* 2013, *79*, 867-876.

[149] Kim, S., Baek, S. H., Lee, K., Hahn, J. S., Cellulosic ethanol production using a yeast consortium displaying a minicellulosome and beta-glucosidase. *Microb. Cell Fact.* 2013, *12*.

[150] Craig, S. J., Foong, F. C., Nordon, R., Engineered proteins containing the cohesin and dockerin domains from *Clostridium thermocellum* provides a reversible, high affinity interaction for biotechnology applications. *J. Biotechnol.* 2006, *121*, 165-173.

[151] Demishtein, A., Karpol, A., Barak, Y., Lamed, R., Bayer, E. A., Characterization of a dockerin-based affinity tag: Application for purification of a broad variety of target proteins. *Journal of Molecular Recognition* 2010, *23*, 525-535.

[152] Jeon, S. D., Lee, J. E., Kim, S. J., Kim, S. W., Han, S. O., Analysis of selective, high protein-protein binding interaction of cohesin-dockerin complex using biosensing methods. *Biosensors & Bioelectronics* 2012, *35*, 382-389.

[153] You, C., Myung, S., Zhang, Y. H. P., Facilitated substrate channeling in a self-assembled trifunctional enzyme complex. *Angewandte Chemie-International Edition* 2012, *51*, 8787-8790.

[154] Liu, F., Banta, S., Chen, W., Functional assembly of a multi-enzyme methanol oxidation cascade on a surface-displayed trifunctional scaffold for enhanced NADH production. *Chem. Commun.* 2013, *49*, 3766-3768.

[155] Kerppola, T. K., Bimolecular fluorescence complementation (BiFC) analysis as a probe of protein interactions in living cells. *Annual Review of Biophysics* 2008, *37*, 465-487.

[156] Zeng, A. P., Sabra, W., Microbial production of diols as platform chemicals: Recent progresses. *Curr. Opin. Biotechnol.* 2011, *22*, 749-757.

[157] You, C., Zhang, Y. H. P., Annexation of a high-activity enzyme in a synthetic three-enzyme complex greatly decreases the degree of substrate channeling. *Acs Synthetic Biology* 2014, *3*, 380-386.

[158] Boles, E., Schulte, F., Miosga, T., Freidel, K., *et al.*, Characterization of a glucose-repressed pyruvate kinase (Pyk2p) in *Saccharomyces cerevisiae* that is catalytically insensitive to fructose-1,6-bisphosphate. *J. Bacteriol.* 1997, *179*, 2987-2993.

[159] Nielsen, J., Larsson, C., van Maris, A., Pronk, J., Metabolic engineering of yeast for production of fuels and chemicals. *Curr. Opin. Biotechnol.* 2013, *24*, 398-404.

[160] Cartwright, C. P., Li, Y., Zhu, Y. S., Kang, Y. S., Tipper, D. J., Use of beta-lactamase as a secreted reporter of promoter function in yeast. *Yeast* 1994, *10*, 497-508.

[161] Mumberg, D., Muller, R., Funk, M., Regulatable promoters of *Saccharomyces cerevisiae*: comparison of transcriptional activity and their use for heterologous expression. *Nucleic Acids Res.* 1994, *22*, 5767-5768.

[162] Macreadie, I. G., Horaitis, O., Verkuylen, A. J., Savin, K. W., Improved shuttle vectors for cloning and high-level Cu^{2+}-mediated expression of foreign genes in yeast. *Gene* 1991, *104*, 107-111.

[163] Rudolph, H., Hinnen, A., The yeast *PHO5* promoter: phosphate-control elements and sequences mediating mRNA start-site selection. *Proc. Natl. Acad. Sci. USA* 1987, *84*, 1340-1344.

[164] Hottiger, T., Kuhla, J., Pohlig, G., Furst, P., *et al.*, 2-micron vectors containing the *Saccharomyces cerevisiae* metallothionein gene as a selectable marker: excellent stability in complex media, and high-level expression of a recombinant protein from a *CUP1*-promoter-controlled expression cassette in cis. *Yeast* 1995, *11*, 1-14.

[165] Adams, B. G., Induction of galactokinase in *Saccharomyces cerevisiae*: kinetics of induction and glucose effects. *J. Bacteriol.* 1972, *111*, 308-315.

[166] Lohr, D., Venkov, P., Zlatanova, J., Transcriptional regulation in the yeast *GAL* gene family: a complex genetic network. *FASEB J.* 1995, *9*, 777-787.

[167] Johnston, M., A model fungal gene regulatory mechanism: the *GAL* genes of *Saccharomyces cerevisiae*. *Microbiological Reviews* 1987, *51*, 458-476.

[168] Lee, K. M., DaSilva, N. A., Evaluation of the *Saccharomyces cerevisiae ADH2* promoter for protein synthesis. *Yeast* 2005, *22*, 431-440.

[169] MacPherson, S., Larochelle, M., Turcotte, B., A fungal family of transcriptional regulators: the zinc cluster proteins. *Microbiol. Mol. Biol. Rev.* 2006, *70*, 583-604.

[170] Todd, R. B., Andrianopoulos, A., Evolution of a fungal regulatory gene family: the $Zn(II)_2Cys_6$ binuclear cluster DNA binding motif. *Fungal Genet. Biol.* 1997, *21*, 388-405.

[171] Des Etages, S. A., Falvey, D. A., Reece, R. J., Brandriss, M. C., Functional analysis of the *PUT3* transcriptional activator of the proline utilization pathway in *Saccharomyces cerevisiae*. *Genetics* 1996, *142*, 1069-1082.

[172] Sze, J. Y., Woontner, M., Jaehning, J. A., Kohlhaw, G. B., *In vitro* transcriptional activation by a metabolic intermediate: activation by Leu3 depends on alpha-isopropylmalate. *Science* 1992, *258*, 1143-1145.

[173] Hahn, S., Young, E. T., Transcriptional regulation in *Saccharomyces cerevisiae*: transcription factor regulation and function, mechanisms of initiation, and roles of activators and coactivators. *Genetics* 2011, *189*, 705-736.

[174] Nevoigt, E., Fischer, C., Mucha, O., Matthaus, F., *et al.*, Engineering promoter regulation. *Biotechnol. Bioeng.* 2007, *96*, 550-558.

[175] Iraqui, I., Vissers, S., Andre, B., Urrestarazu, A., Transcriptional induction by aromatic amino acids in *Saccharomyces cerevisiae*. *Mol. Cell. Biol.* 1999, *19*, 3360-3371.

[176] Hazelwood, L. A., Daran, J. M., van Maris, A. J., Pronk, J. T., Dickinson, J. R., The Ehrlich pathway for fusel alcohol production: a century of research on *Saccharomyces cerevisiae* metabolism. *Appl. Environ. Microbiol.* 2008, *74*, 2259-2266.

[177] Eden, E., Lipson, D., Yogev, S., Yakhini, Z., Discovering motifs in ranked lists of DNA sequences. *PLoS Comp. Biol.* 2007, *3*, e39.

[178] Xiao, Z., Lu, J. R., Strategies for enhancing fermentative production of acetoin: a review. *Biotechnol. Adv.* 2014, *32*, 492-503.

[179] Andre, B., The *UGA3* gene regulating the GABA catabolic pathway in *Saccharomyces cerevisiae* codes for a putative zinc-finger protein acting on RNA amount. *Molecular & general genetics : MGG* 1990, *220*, 269-276.

[180] Talibi, D., Grenson, M., Andre, B., Cis- and trans-acting elements determining induction of the genes of the gamma-aminobutyrate (GABA) utilization pathway in *Saccharomyces cerevisiae*. *Nucleic Acids Res.* 1995, *23*, 550-557.

[181] Cardillo, S. B., Correa Garcia, S., Bermudez Moretti, M., Common features and differences in the expression of the three genes forming the *UGA* regulon in *Saccharomyces cerevisiae*. *Biochem. Biophys. Res. Commun.* 2011, *410*, 885-889.

[182] Idicula, A. M., Blatch, G. L., Cooper, T. G., Dorrington, R. A., Binding and activation by the zinc cluster transcription factors of *Saccharomyces cerevisiae*. Redefining the UAS_{GABA} and its interaction with Uga3p. *J. Biol. Chem.* 2002, *277*, 45977-45983.

[183] Garcia, S. C., Moretti, M. B., Batlle, A., Constitutive expression of the *UGA4* gene in *Saccharomyces cerevisiae* depends on two positive-acting proteins, Uga3p and Uga35p. *FEMS Microbiol. Lett.* 2000, *184*, 219-224.

[184] Ida, Y., Furusawa, C., Hirasawa, T., Shimizu, H., Stable disruption of ethanol production by deletion of the genes encoding alcohol dehydrogenase isozymes in *Saccharomyces cerevisiae*. *J. Biosci. Bioeng.* 2012, *113*, 192-195.

[185] Albertyn, J., Hohmann, S., Thevelein, J. M., Prior, B. A., Gpd1, which encodes glycerol-3-phosphate dehydrogenase, is essential for growth under osmotic-stress in *Saccharomyces cerevisiae*, and its expression is regulated by the high-osmolarity glycerol response pathway. *Mol. Cell. Biol.* 1994, *14*, 4135-4144.

[186] Eriksson, P., Andre, L., Ansell, R., Blomberg, A., Adler, L., Cloning and characterization of *GPD2*, a second gene encoding sn-glycerol 3-phosphate dehydrogenase (NAD^+) in *Saccharomyces cerevisiae*, and its comparison with *GPD1*. *Mol. Microbiol.* 1995, *17*, 95-107.

[187] Yan, D., Wang, C., Zhou, J., Liu, Y., *et al.*, Construction of reductive pathway in *Saccharomyces cerevisiae* for effective succinic acid fermentation at low pH value. *Bioresour. Technol.* 2014, *156*, 232-239.

[188] Ding, W. T., Zhang, G. C., Liu, J. J., 3 ' Truncation of the *GPD1* promoter in *Saccharomyces cerevisiae* for improved ethanol yield and productivity. *Appl. Environ. Microbiol.* 2013, *79*, 3273-3281.

[189] Ida, Y., Hirasawa, T., Furusawa, C., Shimizu, H., Utilization of *Saccharomyces cerevisiae* recombinant strain incapable of both ethanol and glycerol biosynthesis for anaerobic bioproduction. *Appl. Microbiol. Biotechnol.* 2013, *97*, 4811-4819.

[190] Kong, Q. X., Gu, J. G., Cao, L. M., Zhang, A. L., *et al.*, Improved production of ethanol by deleting *FPS1* and over-expressing *GLT1* in *Saccharomyces cerevisiae*. *Biotechnol. Lett.* 2006, *28*, 2033-2038.

[191] Chen, X. L., Li, S. B., Liu, L. M., Engineering redox balance through cofactor systerms. *Trends Biotechnol.* 2014, *32*, 337-343.

[192] Forster, J., Famili, I., Fu, P., Palsson, B. O., Nielsen, J., Genome-scale reconstruction of the Saccharomyces cerevisiae metabolic network. *Genome Res.* 2003, *13*, 244-253.

[193] Heux, S., Cachon, R., Dequin, S., Cofactor engineering in *Saccharomyces cerevisiae*: Expression of a H_2O-forming NADH oxidase and impact on redox metabolism. *Metab. Eng.* 2006, *8*, 303-314.

[194] Bastian, S., Liu, X., Meyerowitz, J. T., Snow, C. D., *et al.*, Engineered ketol-acid reductoisomerase and alcohol dehydrogenase enable anaerobic 2-methylpropan-1-ol production at theoretical yield in *Escherichia coli*. *Metab. Eng.* 2011, *13*, 345-352.

[195] Hou, J., Vemuri, G. N., Bao, X., Olsson, L., Impact of overexpressing NADH kinase on glucose and xylose metabolism in recombinant xylose-utilizing *Saccharomyces cerevisiae*. *Appl. Microbiol. Biotechnol.* 2009, *82*, 909-919.

[196] Zhang, X., Zhang, R. Z., Bao, T., Rao, Z. M., *et al.*, The rebalanced pathway significantly enhances acetoin production by disruption of acetoin reductase gene and moderate-expression of a new water-forming NADH oxidase in *Bacillus subtilis*. *Metab. Eng.* 2014, *23*, 34-41.

[197] Leskovac, V., Trivic, S., Pericin, D., The three zinc-containing alcohol dehydrogenases from baker's yeast, *Saccharomyces cerevisiae*. *FEMS Yeast Res.* 2002, *2*, 481-494.

[198] de Smidt, O., du Preez, J. C., Albertyn, J., The alcohol dehydrogenases of *Saccharomyces cerevisiae*: a comprehensive review. *FEMS Yeast Res.* 2008, *8*, 967-978.

[199] Drewke, C., Thielen, J., Ciriacy, M., Ethanol formation in *adh*^{0} mutants reveals the existence of a novel acetaldehyde-reducing activity in *Saccharomyces cerevisiae*. *J. Bacteriol.* 1990, *172*, 3909-3917.

[200] Bakker, B. M., Overkamp, K. M., van Maris, A. J., Kotter, P., *et al.*, Stoichiometry and compartmentation of NADH metabolism in *Saccharomyces cerevisiae*. *FEMS Microbiol. Rev.* 2001, *25*, 15-37.

[201] Cronwright, G. R., Rohwer, J. M., Prior, B. A., Metabolic control analysis of glycerol synthesis in *Saccharomyces cerevisiae*. *Appl. Environ. Microbiol.* 2002, *68*, 4448-4456.

[202] Guadalupe Medina, V., Almering, M. J., van Maris, A. J., Pronk, J. T., Elimination of glycerol production in anaerobic cultures of a *Saccharomyces cerevisiae* strain engineered to use acetic acid as an electron acceptor. *Appl. Environ. Microbiol.* 2010, *76*, 190-195.

[203] Vemuri, G. N., Eiteman, M. A., McEwen, J. E., Olsson, L., Nielsen, J., Increasing NADH oxidation reduces overflow metabolism in *Saccharomyces cerevisiae*. *Proc. Natl. Acad. Sci. USA* 2007, *104*, 2402-2407.

[204] Zhang, G. C., Liu, J. J., Ding, W. T., Decreased xylitol formation during xylose fermentation in *Saccharomyces cerevisiae* due to overexpression of water-forming NADH oxidase. *Appl. Environ. Microbiol.* 2012, *78*, 1081-1086.

[205] Sun, J. A., Zhang, L. Y., Rao, B., Shen, Y. L., Wei, D. Z., Enhanced acetoin production by *Serratia marcescens* H32 with expression of a water-forming NADH oxidase. *Bioresour. Technol.* 2012, *119*, 94-98.

[206] Ji, X. J., Xia, Z. F., Fu, N. H., Nie, Z. K., *et al.*, Cofactor engineering through heterologous expression of an NADH oxidase and its impact on metabolic flux redistribution in *Klebsiella pneumoniae*. *Biotechnology for Biofuels* 2013, *6*.

[207] Sudar, M., Findrik, Z., Domanovac, M. V., Vasic-Racki, D., Coenzyme regeneration catalyzed by NADH oxidase from *Lactococcus lactis*. *Biochem. Eng. J.* 2014, *88*, 12-18.

[208] Price, V. L., Taylor, W. E., Clevenger, W., Worthington, M., Young, E. T., Expression of heterologous proteins in *Saccharomyces cerevisiae* using the *ADH2* promoter. *Methods Enzymol.* 1990, *185*, 308-318.

[209] Curran, K. A., Karim, A. S., Gupta, A., Alper, H. S., Use of expression-enhancing terminators in *Saccharomyces cerevisiae* to increase mRNA half-life and improve gene expression control for metabolic engineering applications. *Metab. Eng.* 2013, *19*, 88-97.

[210] Raveh-Sadka, T., Levo, M., Shabi, U., Shany, B., *et al.*, Manipulating nucleosome disfavoring sequences allows fine-tune regulation of gene expression in yeast. *Nat. Genet.* 2012, *44*, 743-750.

Abstract in Korean

국 문 초 록

Saccharomyces cerevisiae 는 연구가 활발히 진행된 진핵 모델 시스템으로서, 연료 및 화학 물질 생산을 위한 미생물 세포 공장으로써의 높은 가능성을 지닌다. 본 연구에서는, 다양한 대사 공학적 전략을 섬유소 유래 에탄올의 생산 및 2,3-부탄다이올의 생산에 적용하여 그 가능성을 확인하였다.

첫 번째로, 통합적 단일 생물 공정용 효모 균주를 개발하기 위하여 *Clostridium thermocellum* 의 셀룰로좀 구조를 *S. cerevisiae* 세포 표면에 모사하였다. 셀룰로좀은 구조 단백질인 scaffoldin 을 구성하는 cohesin 도메인과 효소에 포함되어 있는 dockerin 도메인의 친화력 높은 상호 결합에 의해 이루어진다. Scaffoldin (mini CipA)를 표면에 고정화하는 세포와 CelA, CBHII, BGLI 을 분비하는 세 종류의 세포로 '세포 컨소시엄'을 구성하였고, 셀룰로좀의 기능 및 에탄올 생산을 극대화 할 수 있는 최적 비율을 탐색하였다. 그 결과, mini CipA:CelA:CBHII:BGL1 비율이 2:3:3:0.53 일 때 가장 효율적이었으며, 94 시간 발효 후 1.80 g/L 의 에탄올을 생산하였다. 이는 동일한 비율로 구성된 컨소시엄 (1.48 g/L) 에 비하여 약 20% 향상된 결과이다.

두 번째로, 높은 친화력을 지니는 cohesin-dockerin 상호 결합을 이용하여 기질 채널링 모듈을 설계하였다. 기질 채널링이란 효소 작용으로 생성된 중간 대사 물질이 외부로 확산되지 않고 다음 효소로 전달되는 현상으로, 반응 속도를 향상시킬 수 있는 방법이다. 2, 3, 7 개의 cohesin 도메인으로 구성된 합성 scaffold 를 구축하였고, dockerin-융합

단백질과의 상호 결합을 pull-down 기법과 이분자 형광 상보 기법을 이용하여 확인하였다. Dockerin 이 융합된 AlsS, AlsD, Bdh1 을 사용하여 2,3-부탄다이올 생산에 적용하였으며, 그 결과 scaffold 를 구성하는 cohesin 도메인의 개수가 증가함에 따라 2,3-부탄다이올의 생산이 증가함을 확인하였다.

세 번째로, 물질대사 분기점에서의 기질 채널링의 효과를 확인하기 위하여 피루브산의 물질대사에 기질 채널링을 도입하였다. Cohesin-dockerin 상호 결합을 사용하여 피루브산-전환 효소가 피루브산 키나아제(Pyk1)에 결합 할 수 있게 하였다. 피루브산 키나아제는 해당 과정의 마지막 단계에서 포스포에놀피루브산을 피루브산으로 전환한다. 피루브산 채널링의 기반 균주로서 PYK1-Coh-Myc 을 제작하였고, dockerin-융합 단백질과 cohesin-융합 Pyk1 의 상호 결합을 면역 침강 기법을 이용하여 확인하였다. 젖산 생산과 2,3-부탄다이올 생산에 적용한 결과, 목적 대사 산물의 생산이 증가하였고 에탄올의 생산은 감소하였다.

네 번째로, Aro80 전사 조절 인자의 결합 위치를 기반으로 방향족 아미노산-유도성 프로모터를 제작하였다. Aro80 결합 위치의 수, 플라스미드 카피 수, 트립토판 처리 농도를 조절함으로써 다양한 발현 세기를 프로모터를 얻을 수 있었다. *ARO9* 코어 프로모터에 4 개의 Aro80 결합 위치를 지니는 합성 프로모터인 U_4C_{ARO9} 를 AlsS 와 AlsD 의 발현에 도입한 결과, 트립토판 처리 농도에 따라 아세토인 생성이 증가함을 확인하였다. 또한 γ-아미노부틸릭산-유도성 *UGA4* 프로모터 또한 유도 물질의 농도에 의존적으로 전사가 유도됨을 확인하였다.

마지막으로, 경쟁 경로의 제거 및 산화환원 보조인자의 불균형 해소를 통해 *S. cerevisiae* 에서의 2,3-부탄다이올 생산을 단계적으로 향상시켰다. *B. subtilis* 유래의 2,3-부탄다이올 생합성 경로를 도입하고

에탄올과 글리세롤 생산 경로를 제거함으로써 포도당이 2,3-부탄다이올로 성공적으로 전환됨을 확인하였다. 또한, *L. lactis* 유래의 NADH 산화효소 (noxE)를 과발현시킴으로써 2,3-부탄다이올 생산 경로의 도입으로 유발된 산화-환원 보조인자의 불균형을 해소시켰다. AlsS, AlsD, Bdh1, NoxE 가 단일 벡터에서 과발현된 최종 균주 *adh1-5Δgpd1Δgpd2Δ* 는 최종적으로 72.9 g/L 의 2,3-부탄다이올을 생산하였으며, 높은 수율 (0.41 g/g 포도당)과 생산성 (1.43 g/(L·h))을 나타내었다.

주요어 : 대사공학, 기질 채널링, 프로모터 엔지니어링, 2,3-부탄다이올, 섬유소 유래 에탄올, *Saccharomyces cerevisiae*

학 번 : 2009-20983